Journal Pre-proof

Chemically modified biochar for enhanced heavy metals adsorption in aqueous solutions

Fatma Abdelrhman , Shri Ram , Jingmo Zhou , Ziad Ahmed , Noor-ul Huda Altaf , Ehab Mostafa , Yaning Zhang

PII: S2772-4433(26)00036-X
DOI: https://doi.org/10.1016/j.recm.2026.100205
Reference: RECM 100205

To appear in: *Resources Chemicals and Materials*

Received date: 14 February 2026
Revised date: 26 April 2026
Accepted date: 18 May 2026

Please cite this article as: Fatma Abdelrhman , Shri Ram , Jingmo Zhou , Ziad Ahmed , Noor-ul Huda Altaf , Ehab Mostafa , Yaning Zhang , Chemically modified biochar for enhanced heavy metals adsorption in aqueous solutions, *Resources Chemicals and Materials* (2026), doi: https://doi.org/10.1016/j.recm.2026.100205

Highlights

- Chemical modification enhances biochar properties (surface area, pore volume & size).
- Cationic/anionic metal adsorption mechanisms on modified biochar are presented.
- Regeneration & reuse of spent modified biochar via desorption cycles was explored.
- Field validation, green synthesis, and spent adsorbent management are key priorities.

Chemically modified biochar for enhanced heavy metals adsorption in aqueous solutions

Fatma Abdelrhman[a, b], Shri Ram[a], Jingmo Zhou[a], Ziad Ahmed[a, c], Noor-ul Huda Altaf[a], Ehab Mostafa[b,*], Yaning Zhang[a,*]

[a] *School of Energy Science and Engineering, Harbin Institute of Technology, Harbin, 150001, China.*

[b] *Agricultural Engineering Department, Faculty of Agriculture, Cairo University, Giza, 12613, Egypt.*

[c] *Agricultural Engineering Department, Faculty of Agriculture, Ain Shams University, Cairo, 11241, Egypt.*

[*]Corresponding authors: emostafa@agr.cu.edu.eg (E. Mostafa); ynzhang@hit.edu.cn (Y. Zhang).

Abstract

Widespread discharge of heavy metals (HMs) into aquatic environments due to industrial and agricultural practices poses a significant risk to the ecosystem and public health. Biochar is a kind of carbon-rich porous materials derived from pyrolyzing biomass, which is recognized as a promising and cost-effective adsorbent. However, the limited adsorption capacities of pristine biochar, especially towards anionic metal species, restrict its practical usage. Strategies of chemical modification, including the use of acids, alkalis, oxidants, and metal impregnation, have been extensively explored to enhance the physicochemical properties of pristine biochar and improve its adsorption performance. This review provides a comprehensive analysis of these modification techniques and systematically compares heavy metal adsorption performance of pristine and modified biochar for both cationic (e.g., Pb^{2+}, Cd^{2+}, Cu^{2+}, Ni^{2+}, Hg^{0}) and anionic (e.g., Cr(VI), As(V), Sb(III)) species, elucidating fundamental mechanisms such as precipitation, complexation, ion exchange, and redox reactions. The review also addresses the environmental risks and secondary pollution

potential of chemical modification processes, including waste liquid discharge containing residual modifiers and leaching of toxic substances from modified biochar. Reported data indicate that the modified biochar has excellent regeneration capabilities, maintaining 80-100% recovery in repeated cycles with diverse regeneration agents. Consequently, the review also outlined the regeneration potential and reusability of the spent modified biochar, as well as its various disposal and resource utilization pathways. Economic analysis and life cycle assessment were included, and the critical challenges, including variabilities, lack of real-life and long-term studies, and scaling difficulties, were addressed. Future perspectives include standardization, field validation, green modification strategies, advanced characterization with in-situ techniques, and multifunctional biochars to translate laboratory research into sustainable field-level applications.

Keywords: Adsorption; biochar; chemical modification; heavy metal; disposal; regeneration.

Content

1. Introduction

Due to recent progress in industrialization and urbanization, various harmful heavy metals are being released into the aquatic environment through industrial wastes, the use of heavy metal-containing fertilizers and pesticides in agriculture, and improper waste disposal [1, 2]. Contamination of water by heavy metals is a major concern for the ecosystem and human health, as their toxicity arises from their ability to bioaccumulate in the food chain, and the likelihood of causing serious diseases, such as organ damage and neurological disorders [3-5]. Heavy metals (HM) include both cationic species viz., cadmium (Cd), lead (Pb), copper (Cu), mercury (Hg), nickel (Ni), zinc (Zn), and cobalt (Co), and anionic metalloids such as arsenic (As), chromium (Cr), and antimony (Sb).

To address heavy metal contamination in aqueous media, numerous studies have focused on various remediation approaches, including chemical, physical, and biological techniques [6, 7]. However, each technique has distinct advantages, but many are characterized by high costs, inefficiency in large-scale operations, elevated energy usage, non-selectivity, and the generation of toxic chemical waste, which requires proper disposal. Among various heavy metal removal techniques, chemical methods are the most prevalent because they are highly efficient, easy to use, simple in design, and cost-effective [8, 9]. Further, adsorption is recognized as a dependable chemical technology and is favored by numerous industries [10]. Numerous materials such as biochar, activated carbon, zeolites, sludge ash, fly ash, sewage, and woody biomass possess effective adsorption performance towards removing heavy metals from aqueous media [2, 6, 11].

Biochar (BC), also referred as "pyro-char," is a carbon-rich byproduct derived from agricultural wastes, forestry residues, municipal sludge, and animal waste [12-16]. Biochar can be produced through various techniques, including pyrolysis, gasification, hydrothermal carbonization, and torrefaction [17, 18]. Further, BC exhibits greater stability compared to

naturally occurring carbonaceous compounds, making it a more effective agent for carbon sequestration to mitigate climate change [19, 20]. Also, BC serves as an economical and sustainable adsorbent material due to its chemical stability, surface structure, and functional groups [21-24]. Heavy metals adsorption by biochar involves various mechanisms, including surface complexation, precipitation, cation exchange, electrostatic interactions, physical adsorption, and redox reaction [25, 26].

However, the heavy metal adsorption efficiency of pristine biochar is limited, especially for anionic metal species, where its adsorption capacity is lower [27]. Therefore, modification techniques (i.e., physical, chemical, and biological) are used to improve characteristics of fresh biochar such as surface area, pore volume, and functional groups [28]. Researchers have shown a lot of interest in modified biochar research in recent years, as illustrated in **Fig. 1**. The application of biochar in heavy metal remediation has evolved significantly over the past decade, shifting from a basic adsorbent to an engineered material. Historically, the versatility of biocar was initially recognized for its effectiveness in agriculture and soil science as a soil amendment for carbon sequestration and nutrient retention [29]. Nonetheless, when the drawbacks of pristine biochar, such as its non-specific surface chemistry and limited ion-exchange capacity, became apparent, the late twentieth century witnessed a significant shift towards the modification of biochar [2]. This shift used chemical treatments to enhance pore size distribution and surface chemistry for environmental remediation, particularly in aquatic systems [30].

The historical evolution of modified biochar is carefully illustrated in the bibliometric trends shown in **Fig. 1**. As depicted in **Fig. 1 (a)**, publications concerning modified biochar remained modest until around 2018, after which a significant surge was observed. This increase reflects that researchers recognize modification strategies can overcome the intrinsic limitations of pristine biochar, particularly its restricted affinity for anionic heavy metals like

As(V) and Cr(VI). The rapid increase from 2018 to 2021 suggests the widespread adoption of a variety of modification strategies. By 2025, annual publications reached 5922, illustrating that modified biochar has matured into a mainstream research area within environmental remediation. The predominant types of these publications are research papers (64.2%) and review articles (25%). The disciplinary distribution in **Fig. 1 (b)** highlights the evolution of biochar research, with Environmental Science as the leading field (34.6%), the substantial contributions from Chemical Engineering (25.1%) and Materials Science (8.3%) demonstrate that the modified biochar is now treated as an engineered material rather than a simple waste-derived adsorbent. This interdisciplinary approach has facilitated the development of biochars with controlled surface chemistry, tailored pore structures, and specific binding sites aimed at targeted heavy metal removal.

Among the aforementioned techniques, chemical modification methods are frequently employed due to their effectiveness in controlling and enhancing heavy metal adsorption capacity through the introduction of specific functional groups, increased surface area, and targeted contaminant binding. Therefore, the current review focuses exclusively on chemically modified biochar. Despite the growing body of literature on modified biochar, there are still numerous critical gaps. To the best of our knowledge, the majority of the extant reviews on modified biochar for heavy metal adsorption have concentrated on specific modification methods or individual metals [2, 30-32]. Further, regeneration of spent chemically modified biochar is important to extend the service life and economic viability. Although chemical and thermal regeneration techniques are known for carbon-based materials, a comprehensive understanding of the effective methods, optimal conditions, and regeneration mechanisms for chemically modified biochar remains lacking. A review that systematically compares chemically modified biochar performance across both cationic and anionic heavy metals, while also providing a comprehensive analysis of regeneration

methods, safe disposal of spent modified biochar and associated risks, and economic and life cycle considerations, has not yet been published.

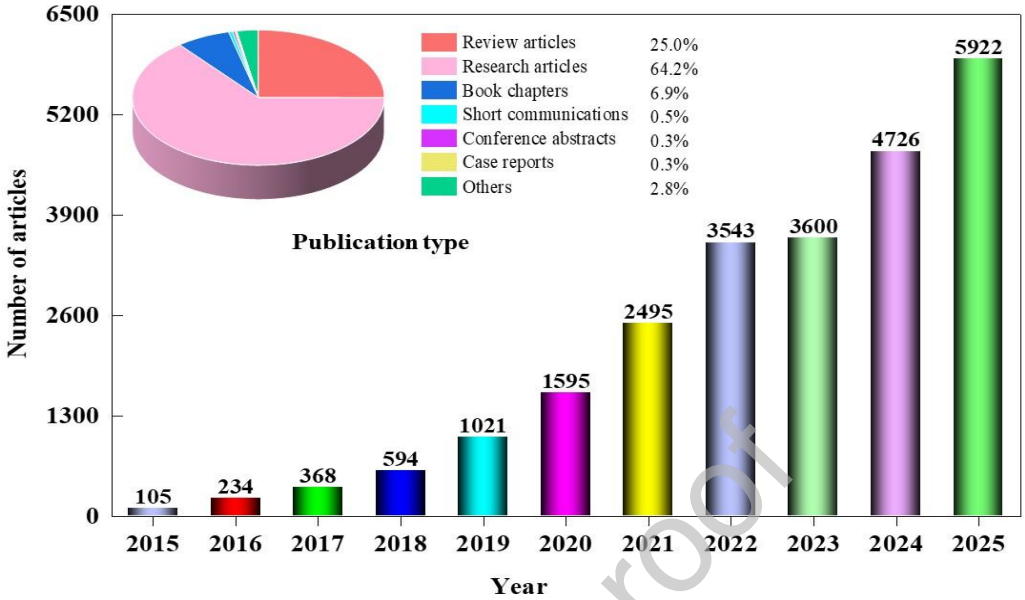

(a) Number of articles published with the topic of "modified biochar"

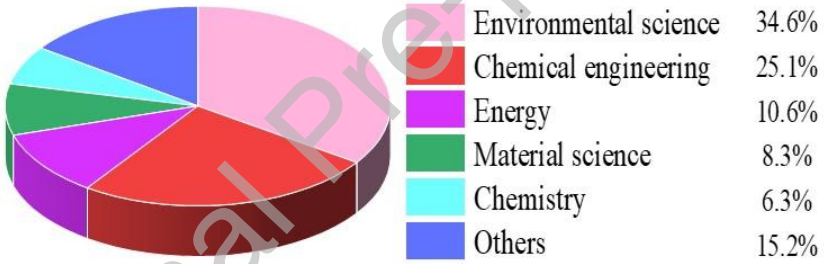

(b) Subject area

Fig. 1. Number of articles published with the topic of "modified biochar" in the recent ten years from (2015-2025) (source: data was obtained from Scopus on 2 December 2025).

Therefore, the present review provides a comprehensive overview of chemical modification methods (acids, alkalis, oxidants, and metal impregnation) of biochar and their impact on the physicochemical characteristics of pristine biochar. Additionally, it assesses the efficiencies of modified biochar for the adsorption of both cationic and anionic heavy metals and attempts to understand the primary mechanisms. In addition, the review also studies methods of regenerating saturated adsorbents and their efficiency in reuse, which increases their lifespan, evaluates safe disposal options for spent modified biochar, assesses economic

feasibility and life cycle considerations, and discusses the challenges and future perspectives of this topic.

2. Chemical modification of biochar

Biochar is one of the carbon-rich materials that has gained considerable attention for its applications in environmental remediation, soil amendments, and carbon sequestration. However, the unmodified (pristine) biochar often shows limited functionality. Thus, to make it suitable for different applications, it is necessary to modify its characteristics, such as porous structure, surface area, functional groups, and nutrient content. The modification of BC can be divided into physical, biological, and chemical methods [33-36], as shown in **Fig. 2**. Physical modification methods are generally used because of their simplicity. However, they are less effective, require considerable energy, and need long activation times [37]. Meanwhile, biological modifications classified as microbial and enzymatic modifications are capable of reducing heavy metal concentrations via adsorption and ion exchange [1]. Also, the process is environmentally friendly as it improves nutrient cycling. But, it takes more time, has less predictability and control, and poses the risk of generating pathogenic or unwanted organisms. In addition, chemical methods require lower activation temperatures, can be easily controlled, and help in the production of high-performance products. Though, managing the waste generated during chemical modifications poses a significant challenge that can be mitigated using advanced wastewater treatment technologies.

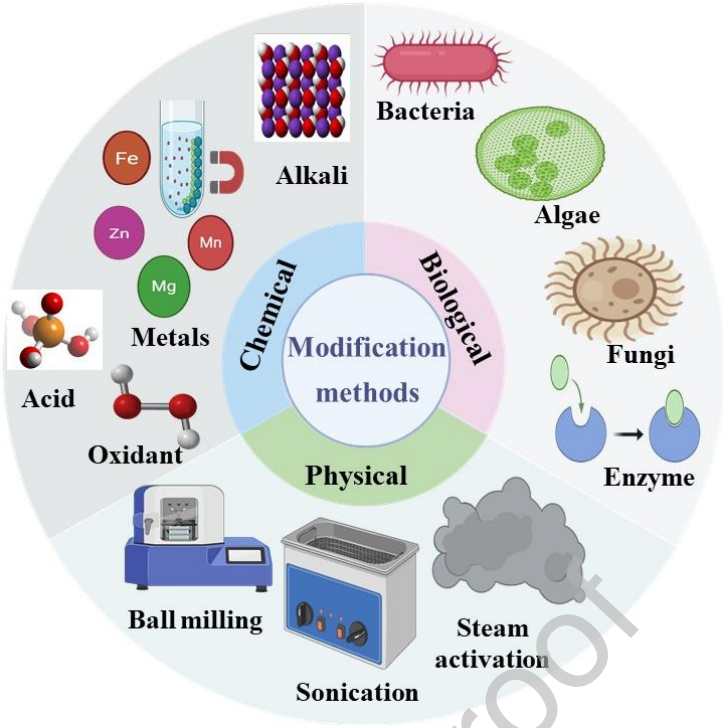

Fig. 2. Biochar modification methods.

Considering the scientific advantages and widespread use of chemically modified biochar, this review focuses on the chemical modification methods and their effects on the physicochemical properties of pristine biochar. Chemical modification involves the modification of pristine biochar using chemical reagents to change the surface chemistry and properties. It generally involves a one-step or a two-step modification process. In a single-step process, both pyrolysis and modification are accomplished concurrently in the presence of the chemical agent. Conversely, in a two-step process, the biomass is initially pyrolyzed, followed by modification with an appropriate chemical agent [38]. Chemical modification includes acid treatment, alkali treatment, oxidation, and metal impregnation. Structural and compositional changes in modified biochar can be characterized using X-ray diffraction (XRD) for crystal morphology, Fourier-transform infrared spectroscopy (FTIR) for functional groups, and X-ray photoelectron spectroscopy (XPS) for elemental surface states. A field emission scanning electron microscope instrument equipped with an energy dispersive

spectroscopy (SEM-EDS) was utilized to analyze surface morphology and elemental distribution of different biochars [39, 40], as shown in **Fig. 3**.

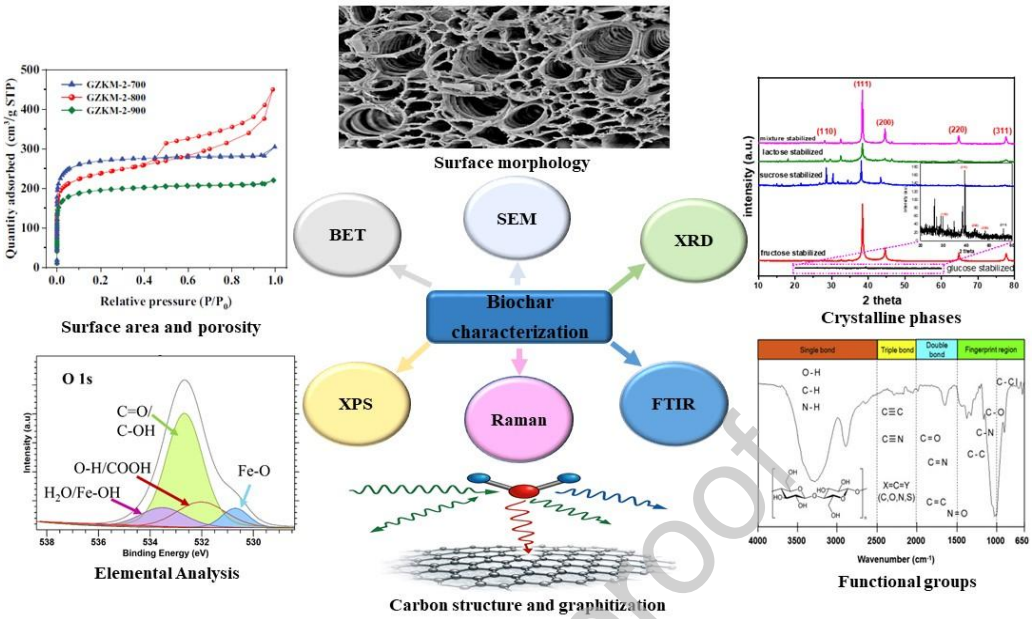

Fig. 3. Biochar characterization techniques.

2.1 Acid modification

Acid modification usually eliminates the impurities (e.g., metals and ash), enhances the hydrophilic properties, and provides new acidic functional groups into the pristine biochar [41]. Additionally, acid modification can change the biochar surface area [42]. The biochar can be soaked at an acid/biochar ratio up to 10:1 in the temperature range of 25-120 °C [41]. The most appropriate acid modifiers include phosphoric acid (H_3PO_4), sulfuric acid (H_2SO_4), nitric acid (HNO_3), and hydrochloric acid (HCl), which can be applied before or after carbonization pyrolysis [43]. Through acid modifications, various functional groups can be introduced, such as carbonyl (C=O), hydroxyl (-OH), carboxyl (-COOH), while other specific functional groups, such as phosphate esters (P-O-C) and additional nitro ($-NO_2$) can be provided from H_3PO_4 and HNO_3, respectively. In addition, H_3PO_4 stands out as an exceptional chemical modification agent due to its affordability, reduced environmental pollution and equipment corrosion, enhanced safety, and superior chemical recovery [44, 45].

In this regard, H_3PO_4-modified tea branch biochar exhibited a decrease in the N, H, and C compared with the pristine biochar, while an increase in oxygen content was reported [46], as presented in **Table 1**. Simultaneously, the O/C and (O+N)/C ratios of H_3PO_4-modified tea branch biochar exceeded those of pristine biochar, suggesting that H_3PO_4 modification effectively enhanced the hydrophilicity of the pristine biochar. A decrease in H/C ratio of modified biochar suggests that H_3PO_4 modification enhanced the aromaticity of pristine biochar by facilitating the transformation of aliphatic carbon structures into aromatic carbon structures within the biochar.

Additionally, H_3PO_4-modified tea branch biochar increased the specific surface area (SSA) by 1.9-fold compared to pristine biochar. Also, H_3PO_4 modification oxidizes and carbonizes biochar by fixing the oxygen-containing functional groups onto the pore walls, resulting in pore size reduction, while supporting new pore formation and transforming mesopores to micropores [45].

Table 1 Physicochemical characterization of pristine and acid-modified biochar.

Feedstock	Temperature (°C)	Modifier	Type	SSA ($m^2 g^{-1}$)	TPV ($cm^3 g^{-1}$)	APS (nm)	Ash%	C %	O%	H%	N%	Ref.
Hay (pellets)	550	No	Pristine	-	-	-	5.3	47.4	45.3	5.80	1.40	[47]
		H_3PO_4	Modified	271.00	0.158	2.34	32.3	79.1	16.9	1.70	2.20	
Aspergillus oryzae-Microcystis aeruginosa	750	No	Pristine	114.55	0.08240	5.23	-	34.20	49.50	-	1.07	[48]
		HCl	Modified	338.58	0.265	4.92	-	76.56	11.47	-	11.57	
Tobacco	600	No	Pristine	23.90	0.041	6.70	-	42.3	15.0	0.90	1.50	[49]
		HCl	Modified	353.40	0.245	2.70	-	68.3	19.8	1.30	2.60	
Corn		No	Pristine	29.00	0.041	5.60	-	47.9	25.7	1.00	2.20	
		HCl	Modified	93.30	0.163	2.2	-	70.3	11.2	0.90	2.60	
Wheat		No	Pristine	23.40	0.071	5.70	-	65.3	10.0	0.90	0.50	
		HCl	Modified	88.60	0.070	3.10	-	73.4	10.8	0.6	0.20	
Black bean		No	Pristine	4.50	0.026	19.80	-	59.5	8.4	0.90	2.10	
		HCl	Modified	60.70	0.064	4.20	-	70.8	9.7	1.10	2.10	
Yunnan pine powder	550	No	Pristine	194.77	0.162	3.45	-	79.41	15.81	-	-	[50]
		H_2SO_4	Modified	114.38	0.046	4.34	-	90.34	9.53	-	-	
		H_3PO_4	Modified	117.64	0.093	3.19	-	90	9.74	-	-	
Walnut shell	550	No	Pristine	116.63	0.093	2.67	-	87.82	11.92	-	-	
		H_2SO_4	Modified	198.77	0.086	3.26	-	86.84	12.99	-	-	
		H_3PO_4	Modified	736.62	0.290	2.43	-	86.54	13.36	-	-	
Tea branch	600	No	Pristine	176.00	0.090	4.58	10.74	71.37	12.89	3.56	1.44	[46]
		H_3PO_4	Modified	336.00	0.150	3.53	9.17	68.22	14.2	2.67	1.04	
Swine manure	700	No	Pristine	227.56	0.140	-	60.73	31.96	4.77	0.66	1.60	[51]
		H_3PO_4	Modified	319.04	0.250	-	43.98	48.35	4.41	0.66	2.23	
Rice straw		No	Pristine	369.26	0.230	-	58.97	31.77	7.23	0.98	0.96	
		H_3PO_4	Modified	372.21	0.230	-	55.27	37.77	5.31	0.43	1.05	
Tea waste	500	No	Pristine	-	-	-	11.40	56.57	24.82	2.96	2.55	[52]
		HNO_3	Modified	-	-	-	3.10	71.03	33.78	4.39	5.26	
Wheat straw	700	No	Pristine	57.18	0.053	3.70	-	-	-	-	-	[53]
		HCl	Modified	197.19	0.141	2.86	-	-	-	-	-	

Rice straw	500	No	Pristine	71.35	-	-	-	25.50	73.13	0.37	-	[54]
		HNO_3	Modified	87.20	-	-	-	17.24	81.39	0.79	0.58	

Similarly, the SSA of H_3PO_4-modified pine tree sawdust biochar increased from 9.36 to 930 m^2 g^{-1}. In addition, H_3PO_4-modified biochar exhibits intermediate porosity at high impregnation ratios, resulting in a hierarchically porous structure suitable for various applications [55]. Conversely, Taha et al. [56] reported that paddy straw biochar treated with 1 M of H_3PO_4 slightly decreases the SSA from 522.5 to 517.1 m^2 g^{-1}. Similar results were observed for H_3PO_4 modification of Yunnan pine powder, as SSA reduced from 194.77 to 117.64 m^2 g^{-1} with a corresponding decline in total pore volume (TPV) from 0.1623 to 0.0926 cm^{-3} g^{-1} [50]. Accordingly, the variation in SSA generally relies on the acid concentration, type of acid, feedstock type, and composition of raw feedstock.

Like strong acids, modification of biochar using weak acid (i.e., HNO_3) facilitates functional group fixation via nitration and oxidation, resulting into introduction of nitro (NO_2) and carboxylic acid (-COOH) groups. Though HNO_3 treatment may deteriorate micropore walls at high concentrations due to its corrosive properties, limiting its usage. However, HNO_3 oxidation enhances the presence of oxygen-containing functional groups on activated carbon surface. Also, it results into reduced SSA and TPV as opposed to pristine biochar [57]. It was observed that the N_2 saturation adsorption capacity of HNO_3 modified samples increased with higher concentrations up to 6 mol L^{-1}, while it reduced at 8 mol L^{-1}, indicating the detrimental impacts on surface area and microporous structure [58].

Meanwhile, Liu et al. [50] also studied the effect of 30 % H_3PO_4 or H_2SO_4 on walnut shell biochar and revealed that both acid treatments increased the SSA and TPV as compared to pristine biochar. Also, H_2SO_4 slightly raised the SSA from 195 to 199 m^2 g^{-1}, and TPV from 0.09 to 0.10 cm^3 g^{-1}. However, H_3PO_4 led to a more substantial increase in SSA (737 m^2 g^{-1}) and TPV (0.29 cm^3 g^{-1}). Further, interaction between carbon atoms in biochar and H_2SO_4 was explained by Tomczyk et al. [2]. Consequently, H_3PO_4 acid established ester linkages

with the -OH groups, incorporated phosphorus atoms into the carbon matrix, as shown in the following reactions:

$$2H_2SO_4+C \rightarrow 2SO_2+CO_2+2H_2O \quad (1)$$

$$2ROH+H_3PO_4 \rightarrow RO\text{-}PO_2H\text{-}OS+2H_2O \quad (2)$$

In addition, it was observed that HCl eliminates salts from the pores, expands both inorganic and organic components, and imparts positive charges to the biochar surface during HCl modification [59]. Also, it increased SSA of rice straw from 71.35 to 87.2 $m^2\ g^{-1}$ [54]. Similarly, HCl-modification of corn straw biochar pyrolyzed at 700 °C increased the SSA from 33.3 to 40.24 $m^2\ g^{-1}$. However, this modification did not alter the chemical composition [60]. The comparative efficiency of sulfuric acid (SM), hydrochloric acid (HM), and nitric acid (NM) in modifying tea waste biochar was evaluated across a temperature range from 300-700 °C [52]. The authors discussed the effect of the three acids on the surface functional groups as illustrated in **Fig. 4**. In BC300, carboxylic groups contributed 17% of the total surface acidity; in BC500, this percentage dropped to 8%. The maximum enrichment of total surface acidity for both BC300 and BC500 was achieved upon NM (1.6-1.8 times), attributed exclusively to the introduction of carboxylic groups.

Consequently, acid modifications generally enhanced the surface area, increased pore volume, and enhanced the presence of hydrophobic and acidic groups, which results into enhanced heavy metals adsorption. The enhancement is achieved through two main mechanisms. Firstly, enhancing the SSA and pore structure of the adsorbent, which influences the physical adsorption capacity. Secondly, by introducing the acidic functional groups, which participate in the chemical adsorption by influencing the overall removal efficiency of the treated adsorbent [61].

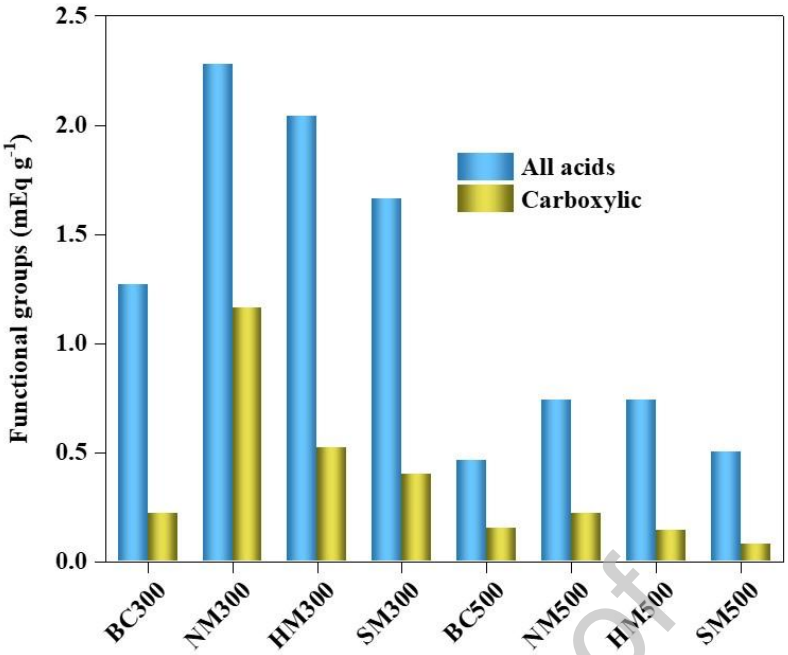

Fig. 4. Surface functional groups comparison for raw and modified biochar: Sulfuric acid modification (SM), Hydrochloric acid modification (HM), Nitric acid modification (NM). Adapted from [52].

In conclusion, different acid types modify biochar via different chemical pathways. The selection of a suitable acid, its concentration, and temperature can affect the resulting modified biochar characteristics and adsorption performance. For instance, H_2SO_4 catalyzes the decarboxylation of functional groups and induces sulfonation [50], while HNO_3 facilitates the introduction of nitrogen groups over biochar surface through electrophilic substitution. Subsequently, HCl significantly reduced graphitic and aromatic groups, while increasing the concentration of oxygenated groups [52], and H_3PO_4 modification reduced the oxygen-containing functional groups, leading to the production of porous and structurally disordered carbon. This process facilitated lignin-derived structure degradation and enriched the biochar by incorporating phosphorus-oxygen groups (e.g., P-O-C and P=O) into its carbon network [2].

2.2 Alkali modification

Alkali modification is generally used to enhance the SSA and TPV, and also introduces oxygen-containing functional groups, viz., ether, carbonyl, carboxyl, and hydroxyl groups. For this, potassium hydroxide (KOH) and sodium hydroxide (NaOH) are commonly used as reagents. Therefore, a full understanding of the link between surface structure and pore assessment is essential to maximize biochar synthesis from biomass. Surface area and pore size are the common indicators for biochar analysis because they are simple and allow for quick assessments to evaluate adsorption performance. For instance, Tang et al. [53] observed variations in textural properties of wheat straw using NaOH modification. Also, SSA and TPV increased from 57.18 to 254.95 m^2 g^{-1} and 0.053 to 0.123 cm^3 g^{-1}, respectively, while average pore size (APS) reduced from 3.697 to 1.925 nm as compared to pristine biochar, as shown in **Table 2**. In principle, an increased proportion of microporosity corresponds to a larger SSA. Furthermore, elevated ash content in agricultural residue (i.e., palm kernel shell and coconut shell) constitutes a significant obstacle to producing high-quality biochar [62]. However, the NaOH modification has the potential to reduce the ash content by up to 24%, since NaOH is anticipated to remove the mineral constituents as per reactions (3) and (4) [63].

$$2NaOH+SiO_2 \rightarrow Na_2SiO_3+H_2O \quad (3)$$

$$2NaOH+AlO_2O_3 \rightarrow 2NaAlO_2+H_2O \quad (4)$$

In addition to the texture parameters, Chen et al. [64] found that KOH-modified waste chicken feathers had a lower H/C ratio (2.80) than pristine biochar (2.91), suggesting greater aromaticity. In addition, KOH modification enhanced O/C and (N+O)/C ratios, indicating greater polarity and hydrophilicity. Subsequently, it also increased the adsorption capacities for polar compounds. After KOH modification, there was a reduction in surface area, pore volume, and pore size, likely due to KOH-induced degradation and collapse of micropore walls. On the other hand, KOH-modification of rice straw biogas residue significantly

increased the SSA and TPV from 273.26 to 2372.51 m^2 g^{-1} and 0.24 to 1.20 cm^3 g^{-1}, respectively, indicating the presence of high adsorption sites [65]. Although the process of BC modification with KOH is complicated, it also improves the porosity and surface area. Additionally, KOH decomposes into metallic potassium and potassium carbonate during thermal treatment, and these resulting substances mix with the carbon matrix while separating the graphitic layers and creating micropores and mesopores. The simultaneous oxidative reactions and gas release (CO, CO_2, H_2) during KOH modification further highlight the porosity characteristics [59].

The KOH/BC ratios alongside process temperature have a significant effect on the activation process. Generally, a higher ratio leads to enhanced surface area and pore volume. Also, it tends to shift the pore size distribution toward narrower micropores. Elevated temperatures, particularly those exceeding potassium's boiling point (760 °C), facilitate the intercalation of metallic potassium, resulting in the formation of new pores [66]. This process is facilitated by the reactions between potassium carbonate and carbon, resulting in the increased porosity and simultaneous enhanced carbon burn-off [67].

Table 2 Physicochemical characterization of pristine and alkali-modified biochar.

Feedstock	Temperature (°C)	Modifier	Type	SSA ($m^2 g^{-1}$)	TPV ($cm^3 g^{-1}$)	APS (nm)	Ash%	C %	O%	H%	N%	Ref.
Aspergillus oryzae-Microcystis aeruginosa	750	No	Pristine	114.55	0.083	5.230	-	34.20	49.50	-	1.07	[48]
		NaOH	Modified	283.91	0.217	5.11	-	58.18	31.43	-	9.70	
Corn straw	500	No	Pristine	232.72	0.098	1.27		77.30	11.26	2.35	0.87	[68]
		NaOH	Modified	279.64	0.115	1.201		67.37	18.32	2.51	1.32	
Sewage sludge	650	No	Pristine	19.81	0.063	13.54	-	10.00	10.31	1.04	0.49	[69]
		K_2CO_3	Modified	23.29	0.069	19.80		3.83	10.70	1.36	1.55	
Rice husk	450-500	No	Pristine	34.40	0.028	-	42.2	42.10	0.50	2.20	12.10	[70]
		KOH	Modified	117.80	0.073	-	3.50	76.40	0.90	3.30	16.90	
Yunnan pine powder	550	No	Pristine	195.00	0.160	3.45	-	79.41	15.81	-	-	[50]
		KOH	Modified	713.00	0.410	2.41	-	89.80	9.65	-	-	
Walnut shell	550	No	Pristine	116.63	0.093	2.67	-	87.82	11.92	-	-	
		KOH	Modified	983.75	0.265	2.11	-	85.87	13.61	-	-	
Wheat straw	700	No	Pristine	57.18	0.053	3.70	-	-	-	-	-	[53]
		NaOH	Modified	254.95	0.123	1.93	-	-	-	-	-	
Douglas fir green wood chips	900-1000	No	Pristine	535.00	0.249	1.86	2.89	80.36	13.78	2.00	0.97	[71]
		KOH	Modified	1050.00	0.672	25.6	16.9	52.21	27.98	2.63	0.28	
Rice straw	550	No	Pristine	71.35	-	-		25.50	73.13	0.37	-	[54]
		KOH	Modified	143.30	-	-	-	20.10	76.38	3.15	0.37	

Beyond NaOH and KOH, other alkali agents can also modify biochar through enhancing its functional groups, SSA, and porosity. For instance, K_2CO_3 and K_2O have the potential to expand the existing pores and create new ones [72]. In this regard, corn straw, spent mushroom substrate, and hardwood sawdust were modified using K_2CO_3 [73]. Their results revealed that a reduction in O content post-pyrolysis can be attributed to the cleavage of chemical bonds and volatilization of materials during the process [74]. The modified biochar showed lower O/C and H/C molar ratios than their corresponding raw materials, suggesting that the dehydration and aromatic ring polycondensation reactions occurred during the pyrolysis [75]. Additionally, lower (O + N)/C ratios of corn straw, spent mushroom substrate, and hardwood sawdust modified BC as compared to raw materials indicate the effective removal of numerous polar functional groups during the pyrolysis [76]. The SSA values were 184.47, 105.29, and 16.36 $m^2\ g^{-1}$, and TPV were 0.158, 0.080, and 0.036 $cm^3\ g^{-1}$, respectively, for spent mushroom substrate, hardwood sawdust, and corn straw-modified BC samples. This indicates that the varieties of feedstocks also influence the characteristics of modified biochar. The study conducted by Chen et al. [77] compared the modification of Jute fibers using acid (H_3PO_4) or alkali (KOH). According to SEM results, H_3PO_4-modified biochar sticks of raw Jute fibers possess a lotus root-like axial porous structure [78, 79]. Also, H_3PO_4 activation may yield -C-P-C- linkages and pyrophosphate, thereby enhancing the stability of the carbon structure [80, 81].

The microwave-assisted H_3PO_4/KOH dual modification was used to examine the impact of H_3PO_4-to-biomass impregnation ratio on the biochar characteristics [39]. In this study, a modified two-step modification was performed: first, biomass was impregnated with different ratios of H_3PO_4:biomass (0:1, 1:1, 2:1, 3:1, and 4:1) and pyrolyzed at 450 °C, followed by microwave-KOH modification at 750 °C. As the impregnation ratio increased from KBC (0:1) to PKBC-3(3:1), the SSA increased from 1,340 to 3,040 $m^2\ g^{-1}$, indicating a 127% rise

as shown in **Fig. 5**, while TPV increased from 0.6 to 1.9 $cm^3 g^{-1}$ (a 217% rise). The fraction of mesopores exceeded 30% at 1:1, identifying the hierarchical pore development. At the ratio of 2:1 to 3:1, the mesopore fraction stabilizes at 40%, while volume of micropores stayed below 1 $cm^3 g^{-1}$. All modified samples showed a combination of Type I and Type IV isotherms, including the existence of both micropores and mesopores, and PKBC-3 (3:1) showed H4-type hysteresis loop at P/P_0>0.4, describing a lamellar mesoporous structure as illustrated in **Fig. 6**. However, PKBC-4 showed a decrease in the hysteresis area, suggesting pore collapse due to the over-modification. Results indicated that H_3PO_4: biomass ratio of 3:1 is optimal, highlighting the critical role of impregnation ratio on the characteristics of chemically modified biochar.

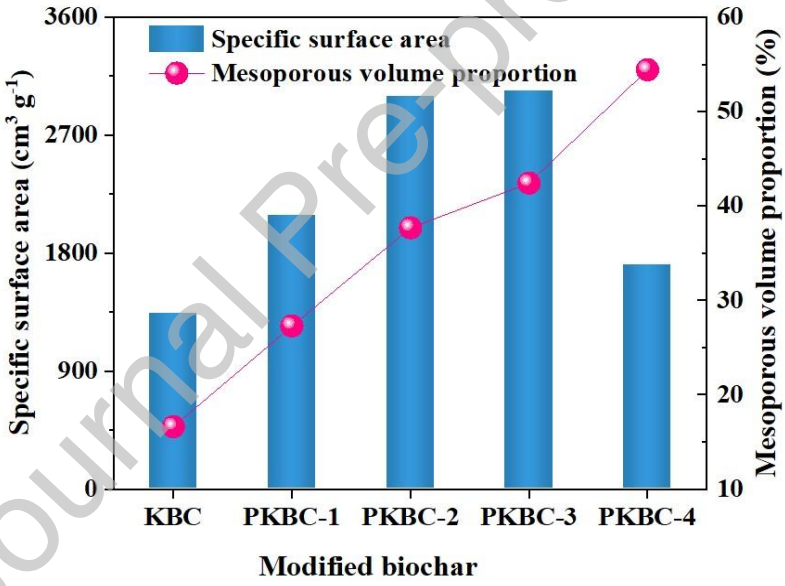

Fig. 5. Specific surface area and mesoporous volume proportions of different biochar [39].

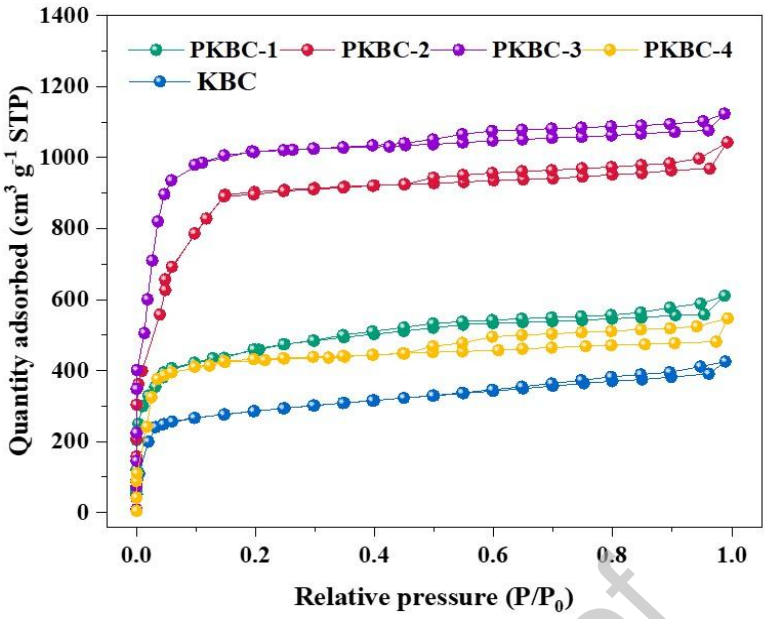

Fig. 6. N_2 adsorption and desorption of different biochars [39].

2.3 Oxidants modification

Oxidants such as hydrogen peroxide (H_2O_2), potassium permanganate **(**$KMnO_4$), and ozone (O_3) can be used to functionalize the biochar surface [82, 83]. Due to their powerful oxidative properties, these agents generate additional oxygen-containing functional groups (i.e., carbonyl, carboxyl, and phenolic hydroxyl groups) to improve the surface chemistry of BC.

H_2O_2-modified biochar is frequently used to improve the adsorption characteristics of biochar due to its purity and economic viability [84]. Generally, modification of BC using H_2O_2 involves submerging the biochar in a solution of H_2O_2 ranging from 1 to 30% and agitating it for 2-3 hours, then filtering, washing, and drying. For instance, Murtaza et al. [61] found that H_2O_2 modification of manure biochar increased the carboxyl content by 101% and oxygen content by 63%, whereas the ash content decreased by 42%. FTIR results of H_2O_2-pinewood-modified biochar showed a reduction in the peak (C=C) at 1585 cm^{-1} compared to the untreated sample, suggesting a partial alteration of the aromatic carbon structure [82]. Authors noted that the enhanced intensity of peaks at 1315 cm^{-1} and 1700 cm^{-1} related to carboxylic acid functionality after H_2O_2 treatment. In another study, H_2O_2 modification led to

an increased peak intensity at 775 cm^{-1}, indicating increased C–H stretching probably due to transformation of aromatic C=C ring structures [85].

Depending on the chemical composition and physical integrity of the biomass, H_2O_2 treatment can either increase the surface area by creating new pores through the oxidation of blocking components or reduce it by destroying the pore structure, as shown in **Table 3**.

The introduction of H_2O_2 to the peanut hull resulted in a significant increase in the SSA from 1.30 to 96.9 $m^2\ g^{-1}$ [84]. In contrast, the modification of residual coffee wastes using H_2O_2 significantly decreased the SSA from 6.6 to 4.8 $m^2\ g^{-1}$after the modification [86]. When BC is modified with H_2O_2 and then thermally treated, H_2O_2 is deposited on its surface, and mesopores decompose into H_2O and O_2. Further, H_2O_2 reacts with carbonaceous structures to produce gases such as CO, CO_2, and H_2, as presented in reactions (5-7) [59].

$$2H_2O_2 \rightarrow H_2O + O_2 \quad (5)$$

$$H_2O_2 + C \rightarrow H_2O + CO_2 \quad (6)$$

$$H_2O_2 + 2C \rightarrow H_2 + 2CO \quad (7)$$

Besides H_2O_2 modification, $KMnO_4$ has also been used as an oxidant in modifying biochar. In this regard, $KMnO_4$-treated hickory wood BC produced through slow pyrolysis (600 °C) showed a reduction in C, H, and N contents (66.10%, 1.49%, and 0.03%, respectively) as compared to pristine biochar (81.81%, 2.17%, and 0.73%, respectively) [87]. This CHN reduction could be attributed to $KMnO_4$'s significant oxidative action on the feedstock. On the other hand, the surface O content significantly increased, likely due to the introduction of new oxygen-containing groups and/or MnO_x particles via $KMnO_4$ modification. Additionally, $KMnO_4$-modified biochar increased the SSA (205 $m^2\ g^{-1}$) as opposed to pristine biochar (101 $m^2\ g^{-1}$). Thus, $KMnO_4$ modification enhanced the biochar surface characteristics by improving its suitability as an environmental remediation adsorbent.

Table 3 Physicochemical characterization of pristine and oxidant-modified biochar.

Feedstock	Temperature (°C)	Modifier	Type	SSA ($m^2 g^{-1}$)	TPV ($cm^3 g^{-1}$)	APS (nm)	Ash%	C %	O%	H%	N%	Ref.
Durian shell	300	No	Pristine	2.19	0.005	10.25	-	64.08	25.75	4.71	1.49	[88]
		H_2O_2	Modified	1.95	0.005	11.00	-	64.81	26.81	5.03	1.48	
		$KMnO_4$	Modified	2.11	0.006	11.89	-	62.68	26.10	5.19	1.40	
		$KMnO_4/H_2O_2$	Modified	3.01	0.008	11.50	-	59.96	28.93	5.19	1.18	
Miscanthus giganteus	350	No	Pristine	0.71	0.001	5.78		64.48	14.82	3.85	0.77	[89]
		H_2O_2	Modified	6.50	0.002	6.43		62.40	20.19	3.74	1.07	
	600	No	Pristine	0.72	0.0003	11.48		73.99	6.91	2.23	0.30	
		H_2O_2	Modified	.95	0.001	5.40		77.79	6.01	2.40	0.38	
Residual coffee wastes	500	No	Pristine	6.60	0.008	7.40	8.26	78.17	5.94	3.19	4.03	[86]
		H_2O_2	Modified	4.80	0.005	4.20	11.28	74.69	6.51	3.36	3.96	
Eucalyptus wood	550	No	Pristine	249.00	-	-	-	75.50	21.50	2.90	0.10	[90]
		H_2O_2	Modified	261.00	-	-	-	64.80	32.60	2.30	0.30	
Rice straw	650	No	Pristine	-	-	-	-	31.92	66.87	1.21	-	[54]
		$KMnO_4$	Modified	-	-	-	-	10.97	88.47	0.555	-	
Peanut hull	300	No	Pristine	1.30	-	-	-	56.30	36.60	5.60	0.90	[84]
		H_2O_2	Modified	96.90	-	-	-	48.30	43.80	5.80	0.80	
Platanus orientalis L leaves	750	No	Pristine	3.42	0.020	19.58	21.83	68.29	5.86	2.66	1.37	[91]
		$KMnO_4$	Modified	41.58	0.080	8.13	32.70	51.72	12.22	2.16	1.20	
		H_2O_2	Modified	5.11	0.020	14.22	16.37	69.76	8.85	3.43	1.59	
		K_2CrO_7	Modified	8.36	0.030	13.57	15.56	71.43	8.50	3.03	1.48	

The comparative efficiency of H_2O_2 and $KMnO_4$ as oxidant modifiers was reported by Ali et al. [92] for orange-shell and pea-shell BC. The pristine orange shell and pea shell BC showed SSAs of 68 and 115 $m^2\ g^{-1}$, respectively. Following modification, H_2O_2- increased SSA to 135 $m^2\ g^{-1}$ for orange-shell, and 176 $m^2\ g^{-1}$ for pea-shell. $KMnO_4$ modification showed a further increase in the SSA, reaching 198 $m^2\ g^{-1}$ for orange-shell and 245 $m^2\ g^{-1}$ for pea-shell. This study confirmed that both H_2O_2 and $KMnO_4$ enhanced the porosity of biochar, with $KMnO_4$ showing a pronounced impact under the reported experiment conditions.

Additionally, Ozone (O_3) is another effective oxidant for biochar modification. For instance, a study explored the modification of *Pisum sativum* peels by ozone, followed by ammonium hydroxide and FTIR results revealed an enhanced peak intensity at 1701 $cm^{-1,}$ corresponding to C=O stretching, reflecting the role of O_3 in the introduction of oxygenated functional groups [93]. However, the SSA and TPV decreased, likely due to clogging of pores by the newly formed functional groups.

2.4 Impregnation with metal

Metal impregnation of biochar can improve its adsorption efficiency by introducing various active sites. Impregnation with metals involving metal oxides and salts resulted in a significant enhancement of the average oxygen-carbon molar ratio of the raw materials. Biochar is loaded with metal oxides primarily through methods such as chemical impregnation, precipitation, and chemical vapor deposition. In chemical impregnation, the biochar is soaked in a metal salt solution and then calcined, resulting in the precipitation of metal oxide nanoparticles that enhance porosity, surface area, and functional groups [94]. Precipitation involves adjusting the pH of the solution to uniformly precipitate metal ions such as (Fe, Mg, or Al) hydroxides or oxides onto the biochar surface, producing atomically distributed nanoparticles of uniform size and high stability, which result from the formation of Metal-O-C chemical bonds [83, 95, 96]. Chemical vapor deposition is an advanced

technique that converts metal precursors into a gaseous form to create high-purity and versatile products [97]. Overall, these metal loading techniques greatly enhance the capability of biochar to adsorb targeted pollutants via various mechanisms such as surface complexation, ion exchange, and surface precipitation.

The importance of metal oxides and salts lies in their efficiency to alter the surface charge of the biochar, thus improving their adsorption ability for specific pollutants. They can also improve the magnetic properties of biochar, usually through iron-based modifications, which facilitate the recovery and reutilization of the modified biochar from water and improve the biochar's catalytic potential in the advanced oxidation processes (viz. persulfate activation) [98]. There are two main ways to synthesize these metal-biochar composites [99, 100], as shown in **Fig. 7**. The first method is to mix metal salts or oxides directly with the raw feedstock before pyrolysis. Another option is to synthesize the biochar, then impregnate it in metal solutions.

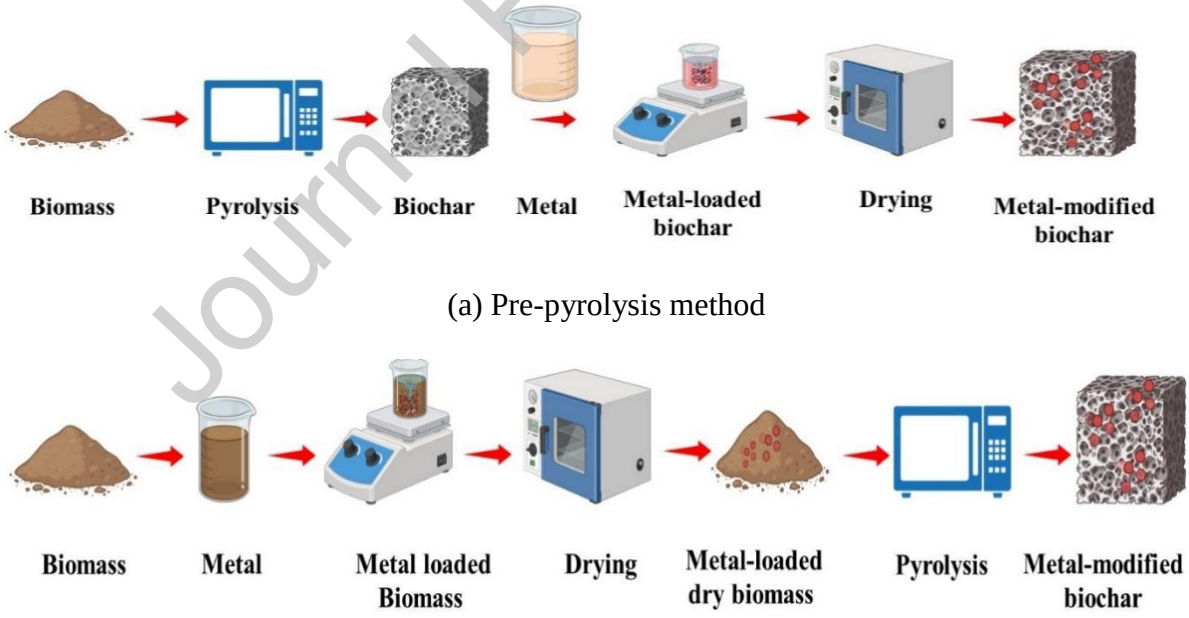

(a) Pre-pyrolysis method

(b) Post-pyrolysis method

Fig. 7. Pre-pyrolysis and post-pyrolysis processes employed for modifying biochar with metal to synthesize metal oxide biochar-based composites. Adapted from Sizmur et al. [99].

The iron (Fe), manganese (Mn), magnesium (Mg), zinc (Zn), and aluminium (Al) are most commonly used for metal modification [101-106]. In comparison to various metal oxides/ salts, Fe stands out as the most prevalent element on earth, offering greater cost-effectiveness and posing reduced environmental risks [107]. Consequently, Fe-modified biochar is advocated for wastewater remediation due to its numerous benefits. Fe-modification represents a highly developed and practical approach for environmental contaminants remediation using BC, particularly in large-scale applications. A method for BC modification via Fe is proposed with two primary objectives: i) enhancing the separation efficiency to facilitate biochar recycling and reuse [108]; ii) augmenting the decontamination efficacy through the interaction between Fe and targeted contaminants [109].

Fe-modified biochar has been synthesized using iron oxides such as goethite, hematite, iron sulfide (FeS), and nano zero-valent iron (nZVI) [110-113]. In one study, Zhu et al. [114] modified wheat straw biochar using α-FeOOH to produce a composite (α-FeOOH@BC). Compared to pristine biochar, TPV and SSA of α-FeOOH@BC increased 4.75 and 6.14 times, respectively, while APS decreased 2.65 times. FTIR analysis confirmed the existence of the Fe-O group, indicating the deposition of well-crystallized α-FeOOH over biochar surface via co-precipitation. Similar results were reported by Khan et al. [115], who used ferric nitrate to modify the corn straw for producing magnetic iron-modified corn straw. The magnetic iron-modified corn straw biochar significantly increased SSA from 93.7 to 313.9 m^2 g^{-1} and also increased TPV compared to the pristine biochar, as shown in **Table 4.** These results confirmed that the iron impregnation affected the pore activation and altered the pore structure of the pristine biochar [116]. In addition to the enhancement in the SSA characteristics, magnetic hysteresis loops were utilized to examine the magnetic properties of the magnetic biochar. The curve exhibited characteristic super-paramagnetic behavior, with magnetization values of 9.75 emu g^{-1}. The magnetically modified BC could be separated

easily when subjected to an external magnetic field. This phenomenon can explain the practical benefits of magnetic biochar for easy separation, thereby facilitating its recycling and reuse.

Besides the importance of Fe-based materials, Mn has been extensively utilized owing to its numerous advantages, such as the abundance of terrestrial resources, operational simplicity, and environmental considerations [102]. For example, a series of Mn-coated BC samples, characterized by varying manganese-to-biochar mass ratios was synthesized using $MnSO_4 \cdot H_2O$ as a modifier [117]. Authors found that the SSA decreased from 54.9 to 24.2 m^2 g^1 with an increase in Mn-coated concentration, while the APS of biochar increased from 55.8 to 69.4 μm, which indicated that manganese oxides (MnO_x) and oxygen-containing functional groups occupied the most medium and micropores in Mn-coated biochar. Similarly, Loblolly pine (*Pinus taeda*) was impregnated with $MnCl_2 \cdot H_2O$, then pyrolyzed at 600 °C, producing MnO-loaded biochar with a carbon content 6.7% lower than that of pristine biochar [118]. Nonetheless, BET analysis indicated two-times increase in SSA and a nearly seven-times increase in TPV.

Table 4 Physicochemical characterization of pristine and metal impregnation-modified biochar.

Feedstock	Temperature (°C)	Modifier	Type	SSA ($m^2 g^{-1}$)	TPV ($cm^3 g^{-1}$)	APS (nm)	Ash%	C%	O%	H%	N%	Ref.
Wheat straw	600	No	Pristine	227.12	-	-	-	79.67	13.77	1.98	1.15	[119]
		$MgCl_2$	Modified	292.21	-	-	-	54.55	15.49	2.34	0.55	
		$MgCl_2$-$AlCl_3$	Modified	268.51	-	-	-	43.08	12.94	2.03	0.41	
Green waste	650	No	Pristine	110.7	-	-	6.6	69.30	-	2.70	1.10	[120]
		$FeCl_3 \cdot 6H_2O$	Modified	74.5	-	-	15.8	59.90	-	2.20	0.90	
Pig carcass	650	No	Pristine	18.4	-	-	60.0	30.80	-	1.30	2.10	
		$FeCl_3 \cdot 6H_2O$	Modified	43.6	-	-	76.3	40.40	-	1.50	1.80	
Platanus orientalis branches	650	No	Pristine	110.7	-	-	-	69.30	-	2.70	1.10	[121]
		$FeCl_3 \cdot 6H_2O$	Modified	74.5	-	-	-	59.90	-	2.20	0.90	
Corn straw	600	No	Pristine	61.0	-	-	16.77	75.50	-	2.95	1.91	[122]
		$KMnO_4$ + $Fe(NO_3)_3$	Modified	208.0	-	-	27.53	67.30	-	2.38	1.83	
Pine powder	550	No	Pristine	194.77	0.162	3.45	-	79.41	15.81	-	-	[50]
		$ZnCl_2$	Modified	534.40	0.309	2.35	-	86.91	11.91	-	-	
Walnut shell	550	No	Pristine	116.63	0.093	2.67	-	87.82	11.92	-	-	
		$ZnCl_2$	Modified	209.18	0.190	2.85	-	79.07	16.79	-	-	
Coconut shell	400	No	Pristine	2.38	0.006	11.55	2.15	76.63	-	3.11	0.00	[28]
		$MgCl_2$	Modified	2.66	0.009	14.86	16.02	52.38	-	3.60	0.00	
Pine cones	500	No	Pristine	6.60	0.016	-	2.13	67.88	22.07	3.89	0.55	[123]
		$Zn(NO_3)_2$	Modified	11.50	0.028	-	2.14	71.21	20.43	3.03	0.51	
Corn straw	800	No	Pristine	93.70	0.050	2.28	10.79	86.14	8.25	1.34	1.11	[115]
		Ferric nitrate	Modified	313.9	0.220	2.86	17.66	48.65	29.40	1.01	1.42	

In addition to Fe and Mn, the addition of other metals like Mg and Zn demonstrated their important roles in providing more functionality to biochar, thus improving its application in wastewater treatment. Li et al. [103] synthesized Mg-loaded biochar samples from different biomass by impregnating the biomass with $MgCl_2$ solution, followed by pyrolysis. The SEM analysis identified the presence of spherical to irregularly shaped Mg particles in the forms of $Mg_2(OH)_3Cl{\cdot}4H_2O$ and MgO on the biochar surface, indicating the potential for ion exchange and surface-mediated processes. Similarly, an identical approach was employed for the manufacture of a MgO hybrid carbonaceous composite generated from sugar cane leaf waste [124]. The existence of Mg compounds on the composite surface was confirmed using SEM- energy-dispersive X-ray spectroscopy (EDX). MgO improved the formation of the nanotube-like carbon sponge structure, highlighting its importance in heavy metal adsorption. XRD analysis confirmed the generation of MgO with diffraction peaks observed at 2θ of 37.1°, 43.1°, 62.5°, 74.7°, and 78.6°.

ZnO/ZnS-modified biochar (BC) was created through the pyrolysis of corn stover and zinc [101]. The ZnO/ZnS-BC had a much greater SSA (397.4 $m^2\ g^{-1}$) in contrast to pristine biochar (102.9 $m^2\ g^{-1}$). According to some researchers, increasing the impregnation ratio of $ZnCl_2$ leads to increased surface area and pore volume. These cavities may represent the areas formerly occupied by $ZnCl_2$, which was later evaporated during the carbonization process. Thus, in addition to the impregnation ratio, an increase in temperature (600–900°C) promotes the evaporation of additional $ZnCl_2$ crystals and the formation of more cavities [59].

2.5 Comparative analysis of chemical modification methods

To enable a direct quantitative comparison of chemical modification techniques under unified experimental conditions, three modifications (HNO_3, KOH, H_2O_2) were tested using five feedstocks (sewage sludge, rice husk, oilseed rape, wheat straw, willow) at 500-700 °C [125]. The results showed that HNO_3 most effectively increased O and N contents for wheat

straw and dramatically raised SSA for sewage sludge, but reduced SSA for willow at 500 °C. KOH modification excelled for rice husk (SSA: 3.88 to 115.50 $m^2 \cdot g^{-1}$; ash: 40% to 20.20%) but decreased SSA for willow under N_2 (2.98 to 0.84 $m^2 \cdot g^{-1}$). H_2O_2 was least effective, causing minimal changes. Willow produced under CO_2 at 700 °C showed exceptionally high pristine SSA, largely retained after all modifications. Overall, no single modification method was universally optimal; effectiveness depended strongly on feedstock, temperature, and carrier gas. HNO_3 modification is the most aggressive, maximizing O and N incorporation and ash removal but often reducing SSA; KOH modification excels at porosity development and carbon retention but is highly feedstock-dependent; H_2O_2 modification is the mildest, causing minimal changes to most properties [125]. Additionally, under unified experimental conditions, the effects of different chemical modifications on the pore structure [126]. Their results found that NaOH modification achieved the highest surface area and smallest pore size, followed by HCl, and then the pristine biochar. $FeCl_3$ significantly reduced the surface area and increased pore size due to pore blockage.

According to the collected data in sections 2.1-2.5, alkali modification (KOH, NaOH) achieves the highest specific surface area enhancement, followed by acid modification and metal impregnation. Oxidant modification showed the smallest SSA increase but effectively introduced oxygen-containing functional groups. A comparison of the textural properties of biochars modified by acid, alkali, oxidant, and metal impregnation methods is provided in **Table 5**.

Table 5 Effect of chemical modification on the textural properties of biochars

Feedstock	Temperature (°C)	Modifier	SSA ($m^2 g^{-1}$)	TPV ($cm^3 g^{-1}$)	APS (nm)	Ref.
Corn straw	500	No	1215.62	-	2.27	[126]
		HCL	1505.92	-	2.14	
		NaOH	1716.76	-	2.13	
		$FeCl_3$	600.36	-	3.82	
Rice straw	300-400	No	25.76	0.025	3.90	[22]
		HCL	20.70	0.025	4.75	
		NaOH	89.08	0.109	4.89	
		H_2O_2	11.94	0.017	5.79	
		MnO_x	34.20	0.044	5.20	
		FeO_x	10.26	0.021	8.12	
Wood chips	300-400	No	0.31	0.002	28.26	
		HCL	0.42	0.003	30.21	
		NaOH	0.38	0.005	53.73	
		H_2O_2	0.38	0.003	33.87	
		MnO_x	9.32	0.020	8.76	
		FeO_x	2.04	0.018	35.06	
Mixture waste	300-400	No	1.40	0.011	31.04	
		HCL	34.04	0.032	3.70	
		NaOH	10.31	0.016	6.25	
		H_2O_2	44.54	0.040	3.56	
		MnO_x	17.49	0.064	14.72	
		FeO_x	85.75	0.229	10.73	

*Mixture waste: comprising 70% wood chip, 10% dolomite, 10% treacle, 5% zeolite, and 5% peat.

Therefore, the overall impact of various modification techniques on the physicochemical characteristics of modified biochar [127] is illustrated in **Fig. 8**. However, the extensive range

of modification techniques requires the assessment of factors such as cost, environmental impact, and raw material properties [128, 129]. To address the need, **Table 6** provides a horizontal comparison of four major biochar modification techniques across different dimensions: modification mechanism, enhanced properties, advantages, limitations, applicable conditions, economic benefits, and engineering practicability. This comparison enables the selection of the most appropriate modification strategy based on specific contaminant type, water chemistry, scale of operation, and budget.

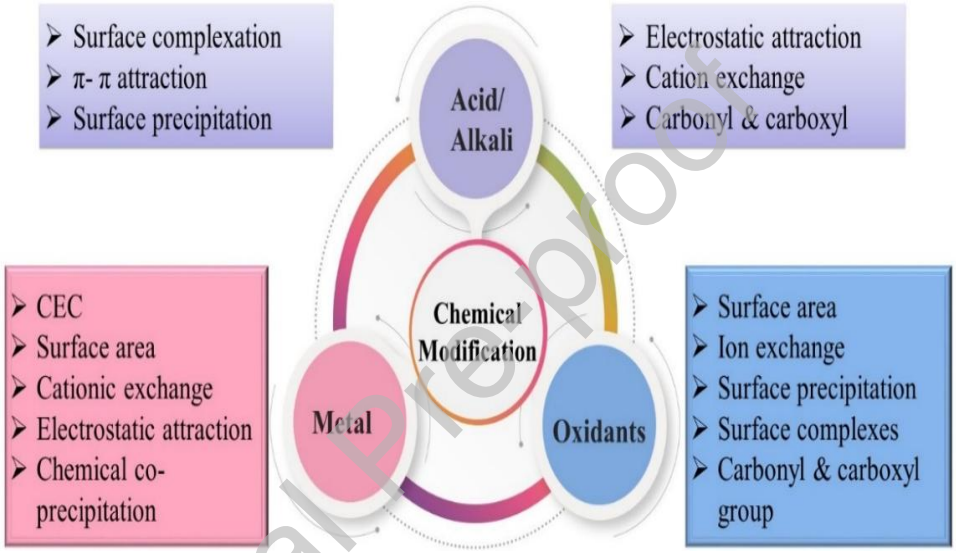

Fig. 8. Summary of the physicochemical characteristics of the chemically modified biochar.

Table 6 Systematic horizontal comparison of acid, alkali, metal impregnation, and oxidants modification techniques for biochar.

Modification technique	Acid modification	Alkali modification	Metal impregnation	Oxidants modification
Mechanism	Introduction of surface functional groups, enhanced surface complexation, hydrogen bonding, and π–π interactions.	Provide oxygen- groups; surface precipitation of metal hydroxides; enhanced cation exchange and electrostatic interaction.	Enable ion exchange, coordination, surface complexation, electrostatic interactions, promotion of microbial activity, and electron transfer.	Provide oxygen groups, enhanced ion exchange, and surface complexation.
Enhanced properties	Increased surface functional groups; improved surface charge; enhanced adsorption capacity for heavy metals and organic pollutants.	Increased specific surface area and porosity; improved heavy metal adsorption; enhanced microbial colonization potential.	High selectivity for specific contaminants (such as arsenic); magnetic separability in case of using iron; increased surface area and porosity; enhanced redox reactivity and microbial stimulation	Increased specific surface area, porosity, and oxygen groups; improved affinity for heavy metals.
Advantages	Enhances chemical activity by adding oxygen groups and removing surface impurities; slightly increases pore structure.	Increases surface area and adds functional groups, enhancing complexation and cation exchange; improves Cd, Pb, and Zn adsorption under single-metal conditions and is effective across different biochar types.	Provides strong specific adsorption (e.g., for anions like AsO_4^{3-}, $Cr_2O_7^{2-}$); allows magnetic recovery and reuse; can simultaneously adsorb and catalytically degrade pollutants.	$KMnO_4$ modification increases the specific surface area of biochar and introduces manganese oxide groups, enhancing heavy metal adsorption performances.
Limitations	May reduce specific surface area, limiting adsorption	May show unstable performance in competitive	**Reduced adsorption efficiency in competitive**	May reduce surface negative charge,

	capacity, sometimes lower than pristine biochar, decreases surface negative charge, reducing electrostatic adsorption of cationic metals.	adsorption, with reduced capacity for Cd and Zn due to Pb preference; limited effectiveness for certain biochars; can partially dissolve silica structures.	**environments; complex and costly modification process; excessive iron loading may block pores or cause agglomeration, limiting reactivity and stability.**	weakening cation exchange; excessive treatment can damage pore structure and cause secondary pollution via manganese leaching.

Continued Table 6

Modification technique	**Acid modification**	**Alkali modification**	**Metal impregnation**	**Oxidants modification**
Applicable conditions	Best for removing cationic heavy metals (Pb, Cu) from acidic wastewater; biochar with low initial ash content.	Best for removing Cd, Pb, Zn from neutral to slightly acidic waters. Avoid treating anionic pollutants. Effective in conditions requiring high surface area and high cation exchange capacity.	Best for the selective removal of oxyanions from wastewater; applications requiring magnetic separation. Avoid acidic conditions (metal leaching).	Best for removing some heavy metals (Hg^{2+}, Pb^{2+}) from water; suitable for H_2O_2 oxidation at moderate temperatures (60-90 °C).
Economic benefits	Low cost (common acids: HCl, H_2SO_4, HNO_3); acid can be recycled partially; suitable for small-scale operations. Disadvantage: corrosion-resistant equipment needed; neutralisation cost for acidic waste.	Low to medium cost (KOH, NaOH are cheap); high yield increase per unit biochar; KOH can be partially recovered. Disadvantage: high alkali consumption; wastewater neutralisation cost.	High cost (Metal impregnation can be costly), particularly for precious metals, but it offers long-term stability.	Very low cost if using H_2O_2; moderate cost for $KMnO_4$ (but Mn residue reduces reusability). Best economic return for high-volume organic wastewater treatment.
Engineering practicability	High: well-established equipment; easy scale-up. Challenge: acid handling safety; neutralisation step	Medium to high: simple soaking or mixing process, but strong alkali requires careful handling and reactor	Low to medium: requires multi-step synthesis with controlled metal impregnation; post-recovery	High: very simple setup; mild conditions; no special reactor needed. Easily

	required before discharge. Common in industrial fixed-bed reactors.	materials (stainless steel or lined). A large-scale application is feasible.	magnetic separation adds capital cost. Best suited for high-value, low-volume applications.	integrated into existing water treatment plants as a pre-treatment or polishing step.
Ref.	[22, 130]	[22, 68]	[131-133]	[132, 134]

3. Heavy metals adsorption in aqueous solutions

3.1 Factors affecting the heavy metals adsorption

The adsorption capacity of heavy metals is influenced by several factors, such as biochar characterization, adsorption conditions, and coexisting substances, as summarized in **Fig. 9**. Modified biochar properties significantly affect heavy metal adsorption. For example, the high SSA provides more active sites and contact between pollutants and modified biochar, leading to improved interaction and adsorption capability [135, 136]. Consequently, the SSA should be integrated with a suitable pore structure to optimize adsorption ability. Pore structures are generally categorized into micropores (<2 nm), mesopores (2-50 nm), and macropores (>50 nm) [137, 138]. Micropores provide a high specific surface area, rendering them effective for adsorbing small molecules and ions. However, an excess micropore structure increases diffusion resistance, thereby hindering diffusion rate and reducing adsorption capacity. Mesopores are essential for the adsorption of larger molecules, as they decrease diffusion resistance, improve adsorption kinetics, and increase overall adsorption efficiency. As a result, materials engineered for the removal of heavy metals generally display mesoporous structures.

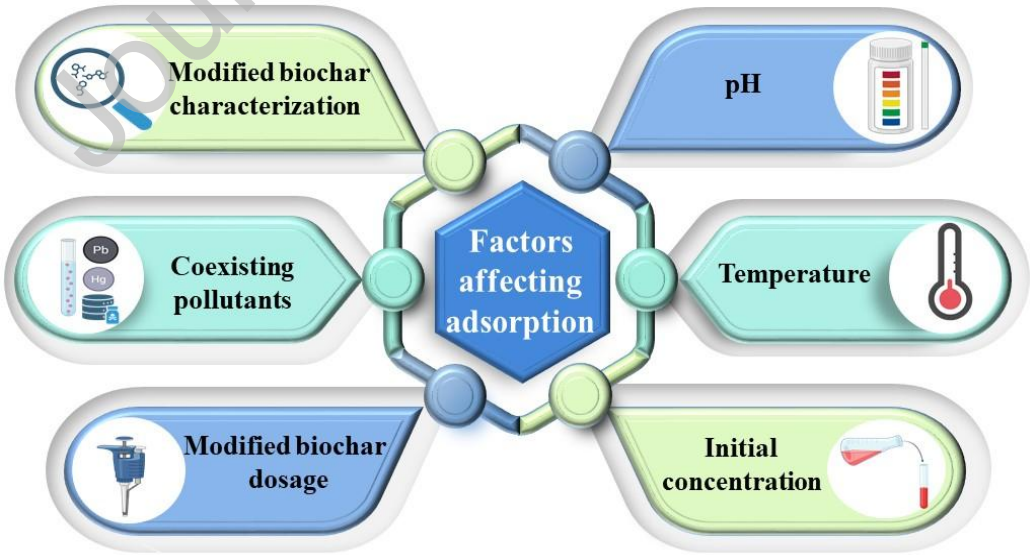

Fig. 9. Key factors influencing heavy metal(loid)s adsorption using modified biochar.

Additionally, surface functional groups govern the electrical characteristics of biochar and directly interact with heavy metals, such as through mechanisms like co-precipitation and complexation, thereby enhancing adsorption capacity [139]. Hydrophilic groups, including -OH and -COOH, effectively adsorb polar molecules or ions, while hydrophobic groups, such as $-CH_3$, can adsorb hydrophobic organic compounds. Positively charged amino groups (NH_2) are able to adsorb negatively charged substances [136]. In addition to biochar characterization, the adsorption conditions, including pH, modifier dosage, pollutant concentration, and temperature, significantly influence the adsorption capacity. Among these, pH is the most influential factor [140]; it affects both the solubility and speciation of heavy metal ions as well as the surface charge of the biochar. At low pH (acidic conditions), metal ions remain soluble in their free cationic form. Conversely, at elevated pH values, these ions may precipitate as hydroxide [136].

The temperature effect is associated with the thermodynamic characteristics of the adsorption process. In exothermic reactions, an increase in temperature typically inhibits adsorption, as the release of heat diminishes the driving force necessary for the adsorption process [141]. In contrast, in endothermic processes, elevated temperatures typically facilitate adsorption. The increase in temperature further speeds the diffusion of heavy metal ions within the solution, enhancing their access to biochar pores. This effect is especially significant in materials with abundant mesoporous and macroporous structures. The initial concentration of Heavy metals significantly impacts the adsorption behavior. When the concentration is low, the adsorption sites on the biochar surface remain unsaturated, facilitating a linear adsorption process. At elevated concentrations, these sites approach near saturation, leading to a progressive decline in the adsorption rate until the process ultimately approaches equilibrium [142, 143].

Coexisting pollutants in natural water affect the adsorption of heavy metals by biochar through competitive adsorption at active sites. Typically, ions with greater charges (e.g., trivalent compared to divalent) or smaller hydrated radii exhibit favorable adsorption [136]. Furthermore, biochar surfaces may possess diverse adsorption sites capable of selectively binding distinct metal ions. Interactions between multiple ion species and organic co-contaminants may lead to synergistic effects. Therefore, overall adsorption efficiency is governed by biochar characteristics, aqueous environment conditions, and coexisting substances [136].

3.2 Cationic heavy metals adsorption

Cationic heavy metals are positively charged metal ions in aqueous solutions, including Cd, Pb, Cu, Zn, Hg, and Ni. These metals generally form cations by losing electrons, resulting in a net positive charge that allows them to bind to negatively charged sites on adsorbents like biochar. Cationic heavy metals are extremely harmful to aquatic organisms and humans, frequently causing poisoning and organ damage even at minimal concentrations. Recent research on the adsorption efficiency of modified biochar for cationic heavy metals, including the possible mechanisms, is summarized in **Table 7**.

Regarding the alkali modification, the KOH-modified biochar from waste chicken feathers (KNB) exhibits 2.8 times higher surface alkalinity than the pristine biochar [64]. The enhanced surface functionality provided abundant adsorption sites, allowing KNB to achieve adsorption capacities of 143.00 mg g^{-1} for Cd^{2+} and 62.14 mg g^{-1} for Pb^{2+}; however, the surface area decreased after modification. Therefore, the adsorption capabilities of KNB for Cd and Pb indicate that the enhancement is attributable to the chemical surface properties rather than physical factors such as SSA.

Moreover, K_2CO_3 was used to chemically modify spent mushroom substrate (SMS), hardwood sawdust, and corn straw [73]. Compared to the other biochars, SMS-modified

biochar demonstrated enhanced adsorption performance for Pb^{2+} and Cd^{2+}, achieving maximum adsorption amounts of 90.58 mg g^{-1} for Pb^{2+} and 25.35 mg g^{-1} for Cd^{2+}. The highest adsorption of Cd^{2+} and Pb^{2+} is linked with the existence of C-O and C-C functional groups on SMS-modified biochar [144]. Analyses using FTIR, XRD, XPS, and SEM-EDS indicated that the Cd^{2+} and Pb^{2+} adsorption mechanisms likely involve ion exchange, mineral precipitation, complexation, and cation π-π bond interactions.

Table 7 Adsorption performance of modified biochar for cationic heavy metals.

Feedstock	Modifier	Concentration (mg L^{-1})	Dose (g L^{-1})	Equilibrium time (h)	Heavy metal	Q_{max} (mg g^{-1})	Mechanism	Ref.
Peanut shell	$KHCO_3$/MgO	300	0.4	48	Cd(II)	1625.5	Ion-exchange.	[145]
Garden waste	HNO_3	50	1	24	Cd(II)	111.1	Pore filling, electrostatic attraction, ion-exchange, π-π EDA and complexation.	[146]
Eucalyptus	MgO	200	0.1-7	10	Cd(II)	829.11	Precipitation and ion exchange, cation-π interaction, and complexation.	[147]
Chicken feathers	KOH	0.1-20	0.2	24	Cd(II)	62.14	Electrostatic interactions, complexation, cation-π interactions, and precipitation.	[64]
wood chips	KOH	100	1	24	Pb(II)	140.0	Chelation, electrostatic attraction, and ion exchange.	[71]
Tea branch	H_3PO_4	300	2	1.5	Cd(II)	98.25	Cation exchange, precipitation, complexation, and π electron interactions.	[46]
		400	2	1	Pb(II)	127.5		
Coconut shell	$MgCl_2$	300	0.5	24	Cd (II)	205.14	Precipitation, ion exchange, oxygen-containing functional groups interaction, and coordination with π-electrons.	[28]
		300	0.5	24	Pb (II)	532.28		
Rice husk	MgO	500	2.5	4	Zn(II)	1.3	Complexation, ion exchange, and precipitation.	[148]
Orange peel	Fe	20	1	6	Ni(II)	37.4	Adsorption via pore diffusion through carbon pores.	[149]
Peanut shell	$KMnO_4$/KOH	0-150	0.1-0.3	24	Ni(II)	87.2	Co-precipitation and complexation.	[150]
Rice husk	MgAl	200	2.5	24	Cu(II)	104.34	Precipitation and ion exchange.	[151]
Peanut shell	Magnetic Fe_3O_4	200	1	6	Cu(II)	234.1	Complexation, ion exchange, and the Van der Waals force.	[152]

Corn straw biogas residue	KOH	80	0.3	3	Hg(II)	269.08	Surface complexation, intraparticle diffusion, interaction and electrostatic attraction.	[153]

Acid modification significantly affects the adsorption of heavy metals onto biochar surfaces. For instance, H_3PO_4-modified tea branch biochar (PTBB) exhibited maximal adsorption capabilities of 98.25 mg g^{-1} for Cd^{2+} and 127.5 mg g^{-1} for Pb^{2+} at pH 6 and a dosage of 2 g L^{-1}, representing increases of 1.5 times for Cd^{2+} and 1.3 times for Pb^{2+} compared to the pristine biochar [46], as illustrated in **Table 7**. The primary adsorption mechanisms of PTBB were precipitation (accounting for 36.7-42.18% of removal) and complexation (accounting for 50.52-50.56% of removal). The improved adsorption is related to the formation of phosphorus-biochar composite, where the crosslinking of P-O-P and C bonds enhances biomass carbon retention in biochar. The composite exhibited significantly greater Pb^{2+} adsorption capacity compared to the pristine biochar, likely due to phosphate precipitation and surface adsorption mechanisms [55]. Reactions (8)-(13) describe this process [46].

$$Cd^{2+}+CO_3^{2-}\rightarrow CdCO_3\downarrow \quad (8)$$

$$Pb^{2+}+CO_3^{2-}\rightarrow PbCO_3\downarrow \quad (9)$$

$$Cd^{2+}+PO_4^{3-}\rightarrow Cd_3(PO_4)_2\downarrow \quad (10)$$

$$Pb^{2+}+PO_4^{3-}\rightarrow Pb_3(PO_4)_2\downarrow \quad (11)$$

$$2Cd^{2+}+P_2O_7^{4-}\rightarrow Cd_2P_2O_7\downarrow \quad (12)$$

$$2Pb^{2+}+P_2O_7^{4-}\rightarrow Pb_2P_2O_7\downarrow \quad (13)$$

In addition to acid and alkali modification, the oxidant-modified biochar enhances heavy metal adsorption in several studies. Oxidant-modified biochar effectively adsorbed Zn, Cu, Cd, and Pb, attributed to the transition of the mechanism from precipitation to complexation [61]. For example, Wang and Liu [141] investigated H_2O_2-modification of yak manure biochar. Their results also indicated that after modification, the oxygen content of manure biochar increased by 63.4% and carboxyl group content increased by 101%, while the ash content decreased by 42%. Consequently, the maximum adsorption capacity of Pb^{2+} reached

169.57 mg g^{-1} by the modified biochar compared to 76.41 mg g^{-1} for the pristine biochar. Moreover, H_2O_2 modification increased oxygen-containing functional groups, particularly carboxyl groups [84]. Consequently, the modified biochar exhibited a Pb^{2+} sorption capacity of 22.82 mg g^{-1}, over 20 times higher than pristine biochar (0.88 mg g^{-1}). In packed column tests, the modified biochar was approximately 20 times more effective in filtering Pb^{2+}. In a multi-metal system, the modified biochar column still effectively removed lead, as well as other heavy metals (i.e., Cu^{2+}, Ni^{2+}, and Cd^{2+}) from water flow. Model results indicated that the heavy metal removal ability of the modified biochar follows the order of Pb^{2+} > Cu^{2+} >Cd^{2+} > Ni^{2+}. $KMnO_4$-modified hickory wood showed superior adsorption capacity for Pb(II), Cd(II), and Cu(II), with maximum capacities of 153.1, 28.1, and 34.2 mg g^{-1}, respectively, all higher than the pristine biochar [87]. The authors demonstrated that dosage, initial solution pH, and ionic strength in the batch experiments influenced the removal efficiency. They concluded that the adsorption by $KMnO_4$-modified biochar primarily occurred via a surface adsorption mechanism, involving interaction with both surface MnO_x particles and oxygen-containing functional groups.

In another study, the effect of Cd^{2+} adsorption using $KMnO_4$ or H_2O_2 modification of pea shells and orange shells was investigated by Ali et al. [92]. The maximum Cd^{2+} removal efficiency was 57.25% for orange shell biochar, 68.95% for pea shell biochar, 82.45% for H_2O_2 orange shell biochar, 82.25% for H_2O_2 pea shell biochar, 86.85% for $KMnO_4$ orange shell biochar and 93.10% for $KMnO_4$-pea shell biochar. These results indicated that the removal efficiency of Cd was taken in the following order: $KMnO_4$-pea shell biochar> $KMnO_4$-orange shell biochar> H_2O_2-pea shell biochar> H_2O_2-orange shell biochar> pea shell biochar> orange shell biochar. Complexation was the main mechanism for Cd^{2+} removal, and the removal efficiency of cadmium increased from 63.1% to 93.2% as the biochar dosage was elevated from 0.1 to 2 g L^{-1}.

Besides H_2O_2 and $KMnO_4$, ozone is used to modify biochar for enhancing the adsorption of heavy metals. For example, the modification of *Pisum sativum* peels using ozone followed by ammonium hydroxide indicated its efficacy in Cu^{2+} adsorption; the maximum adsorptions were 126.25 to 156.25 mg g^{-1} for ozone-modified biochar and ozone followed by ammonium hydroxide, respectively [93]. The main mechanisms were the physical adsorption and the electrostatic attraction between the amino groups introduced by the modification and Cu^{2+} ions.

Biochar modification using metals is another effective strategy. For instance, hydrate manganeseoxide (HMO) nanoparticles were impregnated into a peanut shell-derived biochar to obtain a remarkable nanocomposite adsorbent (HMO-BC) [154]. The HMO-BC exhibited Pb(II) and Cd(II) adsorption capacities of 67.9 and 22.3 mg g^{-1}, respectively, with superior selectivity over pristine biochar in the presence of competing cations (Ca^{2+}, Mg^{2+}, Na^{+}): capacity declines were 8-23% (Pb) and 38-58% (Cd) for HMO-BC, compared to 40-84% (Pb) and 60-87% (Cd) for pristine biochar. XPS analysis revealed a dual mechanism: negatively charged oxygen-containing groups on modified biochar facilitated pre-concentration of metal cations via the Donnan membrane effect, while HMO nanoparticles provided specific inner-sphere complexation. Besides the batch experiment, the practical applicability of HMO-BC was evaluated in a fixed-bed column. Using synthetic wastewater, HMO-BC treated 1910 bed volumes (BV) of Pb(II) solution before breakthrough at 1 mg L^{-1}, compared to only 280 BV for pristine biochar; a 6.8-fold improvement. For Cd(II) (breakthrough at 0.1 mg L^{-1}), HMO-BC treated 100 BV versus 20 BV for pristine biochar. Under stricter electroplating industry standards (0.2 mg L^{-1} for Pb, 0.05 mg L^{-1} for Cd), HMO-BC treated 1410 BV (Pb) and 70 BV (Cd), while pristine biochar treated only 260 BV and 20 BV, respectively. When applied to real contaminated electroplating wastewater from Ningbo, China, the HMO-BC treated 525 BV before Pb(II) breakthrough (0.2 mg L^{-1}),

compared to only 60 BV for pristine biochar; an 8.75-fold improvement. The authors also observed that intentional flow interruption caused sudden drops in Pb concentration, indicating that previously adsorbed metals diffused into interior pores, freeing external binding sites for continued adsorption. The possible mechanisms for Pb(II) and Cd(II) adsorption were through both nonspecific outer-sphere surface complexation provided by oxygen-containing groups in BC and specific inner-sphere complexation offered by the impregnated HMO.

Similarly, Mn-Zn ferrite/biochar (MZF-BC) was tested in authentic wastewater from Shaanxi Lingyun Electronics Ltd to evaluate its practical applicability [155]. The wastewater was filtered (0.45 μm), adjusted to pH 5.0, and treated with 0.05 g of MZF-BC per 100 mL at 298 K for 240 min. The presence of coexisting ions (Mg^{2+}, Ca^{2+}, Fe^{3+}, SO_4^{2-}, Cl^-) did not significantly affect adsorption. Removal efficiencies for Pb^{2+} and Cd^{2+} were 97.4-98.5% and 97.3-97.8%, respectively, and wastewater pH increased from 6.1-6.4. The effluent meets China's battery industry emission standards (pH: 6-9; Pb: 0.7 mg L^{-1}; Cd: 0.05 mg L^{-1}), indicating that Mn-Zn ferrite/biochar is a promising adsorbent for lead-acid battery wastewater treatment. The primary mechanisms for Pb^{2+} adsorption involve ion exchange, electrostatic attraction and precipitation interactions.

Wu et al. [28] modified coconut shell with $MgCl_2$ and found that the modified biochar enhanced the removal efficiency for Pb and Cd. The maximum adsorption capacities of Pb and Cd were 532.28 and 205.14 mg g^{-1}, respectively, representing an increase of approximately 20 and 30 times over the pristine biochar **(Table 7)**. This improvement was attributed to enhanced ion exchange and mineral precipitation, as the modification did not significantly change the SSA and pore structure, indicating that the chemical adsorption played a more significant role than physical adsorption. In another study, α-FeOOH modified wheat straw biochar composite (α-FeOOH@BC) was investigated [114]. The composite

exhibited Cd(II) adsorption capacity that was 2.67 and 6.74 times higher than that of BC and α-FeOOH, respectively, with the main removal mechanism related to surface complexation. Furthermore, carrageenan gum biochar surface (BC CA300) was grafted with olivine mineral $(Mg, Fe)_2 SiO_4$ via the hydrothermal carbonization (HTC) method to synthesize engineered biochar (BC CAOL) [156], as shown in **Fig. 10 (a)**. The synergistic existence of K(I), Mg(II), Fe(II), Fe(III), and Si(IV) during the HTC promotes the formation of a more porous structure, as depicted in **Fig. 10 (b-e)**. The engineered biochar demonstrated an adsorption capacity of 340.98 mg g^{-1}, which is 4.7 times higher than that of pure biochar (72.51 mg g^{-1}). After the adsorption, (BC CAOL) exhibited a relatively obstructed structure, as illustrated in **Fig. 10 (f-i)**, exhibited a relatively obstructed structure. The primary adsorption mechanisms for Cu (II) are included precipitation, complexation, chelation, ion exchange, and pore-filling, as found in **Fig. 11**.

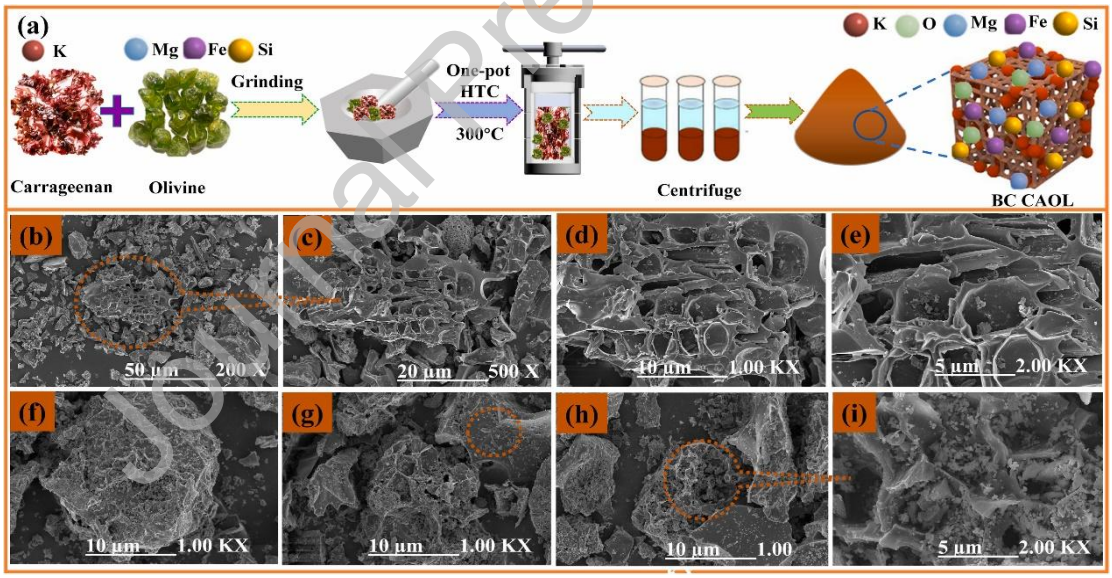

Fig. 10. Schematic of the preparation (a), SEM images of carrageenan gum and Olivine engineered biochar before (b)-(e), and after Cu (II) adsorption(f)-(i) [142].

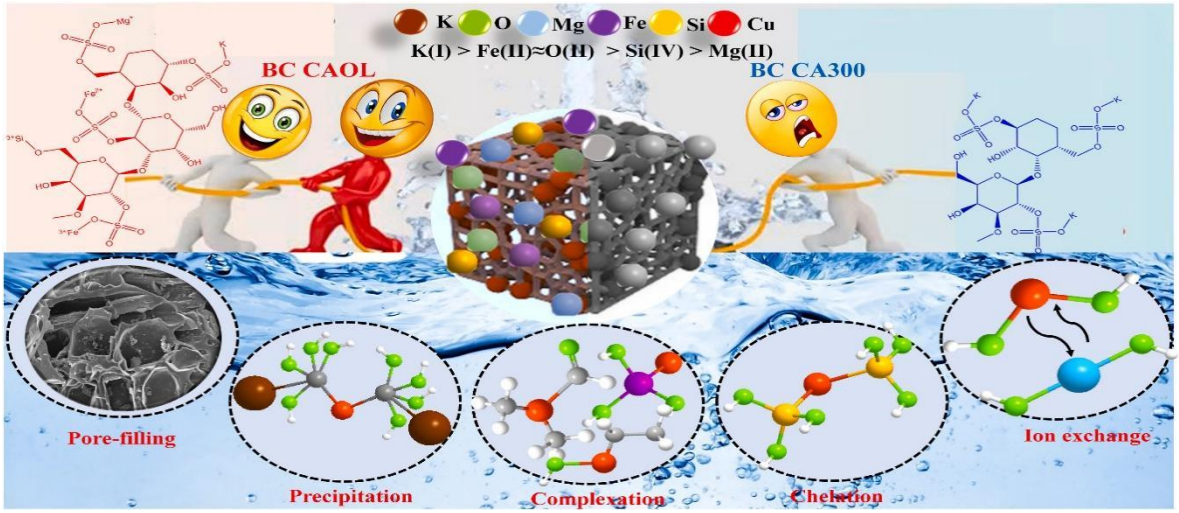

Fig. 11. The possible adsorption mechanism of Cu (II) using engineered biochar (BC CAOL) [156].

A meta-analysis by Ghorbani and Amirahmadi [157] evaluated modification strategies for cationic heavy metals (Cd, Pb, Cu), highlighting that metal oxide-modified biochar had the highest adsorption efficiencies with effect sizes of 63.8% (Cd), 66.7% (Pb), and 58.1% (Cu). Base modification showed moderate enhancements (21.1% for Cd, 22.5% for Pb, and 42.1% for Cu). Strong acid modifications improved Cd and Cu adsorption by 37.8% and 31.7%, respectively, while Pb showed no significant change. The enhanced efficiency results from physicochemical improvements by metal oxides, including increased surface area, greater porosity, and more active sites. These features foster stronger interactions with metal ions via complexation and electrostatic attraction [95].

Cationic heavy metal adsorption is a complex process governed by several factors. For instance, the adsorption is highly dependent on solution pH, which influences both metal specification and the surface charge of adsorbents. For instance, in alkaline conditions, Cd(II) and Pb(II) are precipitated as hydroxides [158-160]. The surface charge of biochar is shifted with pH, as at low pH levels, the surface becomes positively charged, leading to electrostatic repulsion with cations. In contrast, at higher pH, the surface acquires a negative charge, promoting the electrostatic attraction and improving adsorption capacity [145, 161]. The

effect of pH was reported in the study on Cd(II) and Pb(II) adsorption using banana stem and leaf biochar. When the pH increased from 2.0 to 3.5, the equilibrium adsorption capacity (Q_e) for Pb(II) increased significantly from 2 to 200 mg L^{-1}, and for Cd(II) rose gradually from 3 to 35 mg L^{-1} [162].

Temperature can affect the adsorption process depending on the thermodynamic nature of the process. For example, Pb(II) adsorption onto a particular biochar was reported to be exothermic. The Q_e decreased from 65 mg g^{-1} to 30 mg g^{-1} as the temperature increased from 15 °C to 45 °C with an initial Pb(II) concentration of 400 mg L^{-1} [163]. However, in the endothermic processes, adsorption increased with temperature. For instance, magnetically modified biochar enhanced Q_e and adsorption rates for Pb(II) at elevated temperature, particularly at high concentrations (>100 mg L^{-1}) [164]. Furthermore, temperature may alter the reactivity of surface functional groups (such as -OH and -COOH) on biochar, thereby enhancing adsorption ability.

Regarding adsorbate concentration, the adsorption of Cd (II) by coconut shell biochar exhibits linear behavior below 5 mg L^{-1}, whereas at higher concentrations, the adsorption capacity gradually approaches saturation (>20 mg g^{-1}) [165]. Additionally, coexisting pollutants influence the adsorption of heavy metals. For instance, the study on the influence of Na^+, K^+, Ca^{2+}, and Al^{3+} on Pb(II) adsorption found that Al^{3+} exerts the most significant impact because of the competitive binding [166].

3.3 Anionic heavy metals adsorption

Anionic heavy metals, including chromium (Cr), arsenic (As), and antimony (Sb), are negatively charged ions or oxyanions in aqueous environments. These anionic forms are associated with higher valence states, enhancing their mobility in the environment and necessitating specialized adsorbents with positively charged or exchangeable sites for effective adsorption. While modified biochar can adsorb different elements, it generally

exhibits superior adsorption of cationic heavy metals compared to anionic forms due to their distinct chemical properties and aqueous speciation.

The inorganic arsenic occurs primarily in two forms: the highly toxic arsenite As(III) (AsO_3^{3-}), and the less-toxic arsenate As(V) (AsO_4^{3-}) [167]. Cr ranks as the seventh most prevalent element within the Earth's crust, with two stable valence states: highly toxic Cr(VI) and less toxic Cr(III) [168-170]. Furthermore, the toxicity of trivalent Sb(III) species is approximately tenfold higher than that of Sb(V) [171]. Chemical modification using alkali, such as KOH and NaOH, significantly enhanced the adsorption capacity of anions, as shown in **Table 8**. For instance, KOH addition to municipal solid waste increased the SSA from 29.1 to 49.1 $m^2\ g^{-1}$, and the TPV from 0.039 to 0.357 $cm^3\ g^{-1}$, resulting in As (V) adsorption capacity of 30.98 mg g^{-1}, which is 1.3 times more than the pristine biochar (24.49 mg g^{-1}) [172]. Similarly, KOH-modified corn straw increased the SSA from 14.70 m^2g^{-1} (raw corn straw) to 2183.79 $m^2\ g^{-1}$, achieving an adsorption capacity of 116.97 mg for Cr(VI) [80]. The improved adsorption of both As (V) and Cr(VI) is attributed to the physical adsorption, as increased SSA and the TPV facilitate the rapid mass transfer and offer more active binding sites for metal ions.

Acid modification also improves the adsorption of anionic metals. H_3PO_4-modified *Lagerstroemia speciosa* seed hull achieved 99.97% removal efficiency for Cr (VI) under experimental conditions of (pH 2, adsorbent dosage 2 g L^{-1}, and Cr concentration 50 mg L^{-1} [173]. The high efficiency was due to the high SSA (246.23 $m^2\ g^{-1}$) and low APS (2.36 nm). Similarly, H_3PO_4-modified tea waste biochar showed a maximum As (V) adsorption capacity of 33 mg g^{-1}, with possible mechanisms including weak van der Waals forces of attraction and physisorption [174]. The existence of mesoporous structures and acidic functional groups improved the adsorption for both As(V) and Cr(VI).

Table 8 Adsorption performance of modified biochar for anionic metalloids.

Feedstock	Modifier	Concentration (mg L^{-1})	Dose (g L^{-1})	Equilibrium time (h)	Heavy metal	Q_{max} (mg g^{-1})	Mechanism	Ref.
Peanut shell	$KMnO_4$/KOH	0.05-1	0.3-3	4	As(III)	1.5	Physical adsorption, ion exchange, electrostatic attraction, surface complexation.	[175]
		0.05-1	0.3-3	4	As (V)	1.5		
Rice residue	Zirconium hydroxide	50	2	1	As(III)	107.6	Inner-sphere complexation and electrostatic adsorption.	[176]
		50	2	1	As (V)	40.8		
Bamboo	$Fe(NO_3)_3$/$FeSO_4$	60	1	5	As(III)	265.3	Inner-sphere complexation and electrostatic attraction.	[177]
Pine wood	nZVI	0-400	2	1	As(V)	124.5	Surface complexation and a reduction reaction	[178]
Tea waste	H_3PO_4	1-5	0.8	8	As(V)	33	Weak Van der Waals forces of attraction via physisorption.	[174]
Municipal solid waste	KOH	5-400	2	10	As(V)	30.98	Surface complexation and ion exchange.	[172]
Corn stem	Fe-Mn oxide	20	2.5	2	As(III)	8.8	Surface adsorption/oxidation.	[179]
Wheat straw	Bi_2O_3	5-200	2	24	As (III)	16.2	Lewis acid-base reaction between the bismuth atom and arsenite.	[180]
Pinecone	Zn-Ni-Fe_4O_3	10-150	1-20	2	Cr(VI)	29.7	H-bonding or electrostatic interactions.	[181]
Digestion residue	KOH	150	0.1-0.5	3	Cr(VI)	209.65	Pore adsorption, electrostatic interaction and surface complexation.	[65]
Seed hull	H_3PO_4	50	2	2.3	Cr(VI)	41.92	electrostatic attraction, reduction phenomenon and mass transfer mechanism.	[173]
Wood chips	KOH	100	1	24	Cr(VI)	127.2	Electrostatic interactions.	[71]

The investigation of metal-based modification, such as Fe-based (nZVI, FeS, and FeOOH), offers reductive species such as Fe^0, S(II), and Fe(II) that improve the removal efficiency. For instance, α-FeOOH modified wheat straw biochar (α-FeOOH@BC) exhibited an adsorption capacity for As(III) that was 6.74 times higher than that of the pristine biochar [114]. In another study, Zhou et al. [182] demonstrated that the nZVI modified biochar achieved 99.7% removal of Cr(VI), with a removal rate of 199.46 mg g^{-1} within 60 min, transforming the toxic Cr(VI) to the less toxic Cr(III) due to the action with Fe^0.

Manganese also showed effectiveness in heavy metal(loid) adsorption. In this context, manganese-modified biochar increased the As(III) and As(V) adsorption from 387 to 7236 μg g^{-1} and from 110 to 1469 μg g^{-1}, as the initial concentration of As raised from 500 to 40,000 μg L^{-1} [183]. Redox reactions between As(III), Mn(III), and Mn(IV) oxidize As(V) to As(III), as illustrated in reactions (14) and (15) [184, 185]. Similarly, Mn-coated biochar adsorbed Sb(III) and Sb(V) with a capacity of 0.9 and 0.7 mg g^{-1}, respectively, through mechanisms involving inner-sphere complexation and oxidation [117].

$$2MnO_{2(s)}+H_3AsO_{3(aq)} \leftrightarrow 2MnOOH^*_{(s)}+H_3AsO_{4(aq)} \quad (14)$$

$$2MnOOH^*_{(s)}+H_3AsO_{4(aq)} \leftrightarrow 2MnO_{(s)}+H_3AsO_4(aq)+H_2O_{(I)} \quad (15)$$

The study by Zuo et al. [126] compared various modification strategies for Cr(VI) adsorption using biochar derived from corn straw pyrolyzed at 500 °C. Three modification methods: acid (HCl), alkali (NaOH), and metal salt ($FeCl_3$), were utilized, resulting in biochar variants (HMB, NaMB, FeMB). At 25 °C and pH=2 with an initial concentration of 50 mg L^{-1}, the adsorption followed the Langmuir isotherm and quasi-secondary kinetic models. Among all materials, Fe-modified biochar (FeMB) exhibited the highest experimental adsorption capacity (Qe = 23.40 mg·g^{-1}), followed closely by NaMB (22.36 mg·g^{-1}), while pristine biochar (14.39 mg·g^{-1}) and HMB (11.92 mg·g^{-1}) showed substantially lower capacities. The adsorption mechanism involves monolayer chemical adsorption via

electrostatic interactions, surface functional group complexation, and reduction, influenced by biochar's polarity and hydrophilicity.

Different mechanisms are responsible for the adsorption of anionic heavy metals. One primary mechanism is redox reactions, enabled by surface functional groups and redox-active components of the modified biochar. For instance, the interaction between oxygen-containing functional groups on the biochar surface can reduce Cr(VI) to Cr(III) [186]. Hydrogen bonding between metal ions and hydroxyl and carboxyl groups on the modified biochar can also improve the adsorption. For example, ferrate-modified biochar removed over 91% of arsenic, representing a 34% increase compared to using ferrate alone [187]. These improvements were achieved through the oxidation of As(III) to As(V), followed by adsorption via hydrogen bonding, electrostatic attraction, and As-O-Fe bonding.

3.4. Cationic/anionic interaction in single and mixed systems

In real wastewater, multiple heavy metals compete for limited adsorption sites on modified biochar, making adsorption behavior more complex than in single-metal systems [188, 189]. In a comparative study, three types of biochar (RBC: rice husk, WBC: wood chip, MBC: mixture) were modified using five methods: acidic, alkaline, oxidic, manganese oxide (MnO_x), and iron oxide (FeO_x) impregnation [22]. All biochars were produced under consistent pyrolysis conditions (300-400°C), under identical experimental conditions (10 mg L^{-1} initial metal concentration, 1 g L^{-1} adsorbent dose, 24 h contact time, 25°C). The adsorption characteristics of three heavy metals (Cd, Pb, and Zn) under single and mixed conditions were compared and evaluated. The adsorbed amount of the pristine biochar decreased in the order of MBC > RBC > WBC, with more Pb being absorbed (5.28-8.24 mg g^{-1}) than Cd (3.01-6.08 mg g^{-1}) and Zn (1.47-4.72 mg g^{-1}). Only MnO_x-impregnated biochars demonstrated exceptional adsorption regardless of biochar type (Cd > 9.15 mg g^{-1}; Pb > 9.98 mg g^{-1}; Zn > 6.58 mg g^{-1}) under mixed conditions, while other modifications showed lower

efficiency than pristine biochar. The distribution coefficient (Kd) followed Pb > Cd > Zn, indicating that Pb replaced Zn in competitive adsorption due to higher surface affinity.

In binary Pb(II)/Cd(II) systems, modification type dictates selectivity. Zahedifar et al. [190] used multi-functional magnetic biochar (MMF-BC), achieving adsorption capacities of 61.25 mg g^{-1} for Pb(II) and 53.75 mg g^{-1} for Cd(II), with no significant selectivity. In contrast, Liang et al. [191] used MnO_2-biochar and achieved maximum capacities of 268.0 mg g^{-1} for Pb and 45.8 mg g^{-1} for Cd. Clearly, MnO_2-biochar has higher selectivity for Pb(II) and Cd(II) adsorption in Pb(II) and Cd(II) binary system. This result provides a possible path to preferentially separate Pb(II) from Pb(II) and Cd(II) binary system based on the larger difference in adsorption capacity. Ding et al. [192] used alkali-modified biochar to adsorb Pb^{2+}, Cd^{2+}, Cu^{2+}, Zn^{2+}, and Ni^{2+} from mixed multi-metal solutions. Langmuir capacities were 19.1 mg g^{-1} for Pb^{2+}, 17.9 mg g^{-1} for Cu^{2+}, 1.83 mg g^{-1} for Zn^{2+}, and below 1.0 mg/g for Cd^{2+} and Ni^{2+}. Compared to single-metal systems (Pb^{2+}: 53.6 mg g^{-1}), the 2.8-fold decline demonstrates large competing effects. In alkali-modified biochar fixed-bed columns, Pb^{2+} and Cu^{2+} were preferentially adsorbed, while Cd^{2+}, Zn^{2+}, and Ni^{2+} showed no adsorption.

Beyond competition among cationic metals, the coexistence of cationic and anionic species introduces additional complexity, ranging from competitive inhibition to synergistic enhancement depending on the specific metal pair and biochar modification. A critical meta-analysis addressed this significant gap by comprehensively evaluating the efficacy of metal oxide-loaded biochar in adsorbing both cationic (e.g., Cd^{2+}, Pb^{2+}) and anionic (e.g., AsO_4^{3-}, CrO_4^{2-}) heavy metals from contaminated environments [193]. For cationic metals, Cu- and Mn-loaded biochar were most effective (effect sizes: 1.51 and 1.22), primarily governed by ion exchange and surface complexation. Conversely, for anionic species, Zr- and Fe-modified biochar showed superior performance (effect sizes: 2.29 and 1.43), driven by electrostatic interactions and inner-sphere complexation. Key factors influencing adsorption included

acidic pH (enhancing protonation and electrostatic attraction), elevated temperatures (improving ion diffusion), and moderate contaminant concentrations (optimizing active site utilization).

Moreover, Ganie et al. [194] synthesized nano zero-valent iron-modified sugarcane bagasse biochar (nZVI-SBC); biochar was produced at a pyrolysis temperature of 750 °C. When evaluated in mixed solutions containing metal cations (Ni^{2+}, Cd^{2+}) and anions (CrO_4^{2-}, and AsO_4^{3-}) in a solution of 100 mg L^{-1} of each metal. It was observed that the maximum adsorption capacity of nZVI-SBC on Cd^{2+}, Ni^{2+}, CrO_4^{2-}, and AsO_4^{3-} exhibited the adsorption capacities of 44.0, 40.3, 87.8, and 47.6 mg g^{-1} with surface complexation and co-precipitation mechanisms. The adsorption performance of acetate-Fe/Mg-layered double hydroxides modified biochar was investigated under various heavy metals, pH values, and ionic strengths [195]. In binary systems, the presence of 25 mg L^{-1} Cu(II) reduced Pb(II) removal from 95.48% to 80.27%. Conversely, As(V) increased Cu(II) removal, and the presence of Pb(II) or Cu(II) enhanced As(V) adsorption. The coexistence of As(V) and Pb(II)/Cu(II) resulted in a concurrent enhancement of the adsorption capacity of modified biochar for both As(V) and Pb(II)/Cu(II), indicating synergistic interactions between these species, reflecting the synergistic electrostatic interactions and ternary surface complexes formation on the adsorbent surface [196].

3.5 Adsorption mechanism of modified biochar

The adsorption capacity of modified biochar for heavy metals is affected by several mechanisms, including physical adsorption, chemisorption, and electrostatic interactions. Physical adsorption involves pore filling, where metal ions occupy the porous structure of biochar, aided by Van der Waals forces that bind metal ions to the surface and internal pores. The optimized surface chemistry of biochar provides ample adsorption sites. Chemisorption, particularly through surface complexation, is also crucial, as metal ions like Pb^{2+} create stable

complexes with functional groups on the modified biochar surface, such as carboxyl and hydroxyl groups. Ion exchange mechanisms, where intrinsic cations like Ca^{2+} and Mg^{2+} in modified biochar exchange with heavy metal ions, play an important role in removing metals from aqueous solutions. This ion exchange efficiency was demonstrated by Yu et al. [197], who found that iron-modified biochar effectively removed Ni^{2+} from contaminated water.

Electrostatic adsorption is crucial for biochar's interactions with metals, dependent on the surface charge, which varies with the system's pH. Cr(VI) removal by biochar occurs in two steps: adsorption via electrostatic forces and subsequent reduction to Cr(III), which is released into water. The reduction process consumes H^+, leading to a negatively charged biochar surface, which facilitates the re-adsorption of cationic Cr(III) through electrostatic interactions [1]. Precipitation and redox reactions further enhance heavy metal removal on modified biochar. In some cases, modified biochar can also promote sedimentation, where precipitation reactions form insoluble compounds with heavy metals, further enhancing biochar's adsorption capacity. For example, SEM images reveal a uniform distribution of nanoscale CdS particles on modified biochar, with XRD confirming CdS formation at $2\theta = 26.8°$. This indicates that replacing iron sulfide with Cd^{2+} to form CdS is crucial for capturing Cd^{2+}, thereby improving heavy metal removal efficiency [198]. Additionally, redox cycling between Fe^{3+} and Fe^{2+} is significant for heavy metal adsorption on iron-modified materials [113].

Density Functional Theory (DFT) and Molecular Dynamics (MD) simulations enhance experimental studies by providing atomic-level insights into the interactions between modified biochar and heavy metals [199]. DFT simulations predict stable conformations and binding sites by evaluating the electronic structure, binding energies, and chemical interactions between the biochar and heavy metals. These calculations demonstrate the influence of hydroxyl, carboxyl, and phenolic groups on binding affinity. For instance, DFT

calculations showed that carboxyl groups have a high affinity for Pb(II) and Cu(II) due to significant electrostatic and ligand interactions [200]. Binding energy calculations provide quantitative data on the stability of biochar-heavy metal complexes and the efficacy of biochar in immobilizing heavy metals [201]. MD simulations offer dynamic insights into these interactions by modelling atomic movements over time, thereby elucidating adsorption kinetics, diffusive behaviours, and structural alterations in the biochar. MD has examined the effects of pH, temperature, and ionic strength on these interactions [199], demonstrating that the porous structure and extensive surface area of biochar enhance metal ion diffusion and adsorption, thus pinpointing optimal adsorption sites and pathways within the biochar matrix.

In summary, modified biochar demonstrates varied adsorption capacities for different heavy metal (loid)s. It generally exhibits a greater adsorption capacity for cations than for anions. This difference is attributed to variations in metal forms and physicochemical properties in water (forms and hydrated ionic radii), as well as the biochar surface (such as charge and functional groups). The main adsorption mechanisms for heavy metal(loid)s by chemically modified biochar are summarized in **Fig. 12**. Overall, the synergistic combination with the optimized pore structure, functional group diversity, and active component loading of the modified biochar enables it to efficiently remove a wide range of heavy metals through multi-pathway coupling to enhance the potential of water treatment applications.

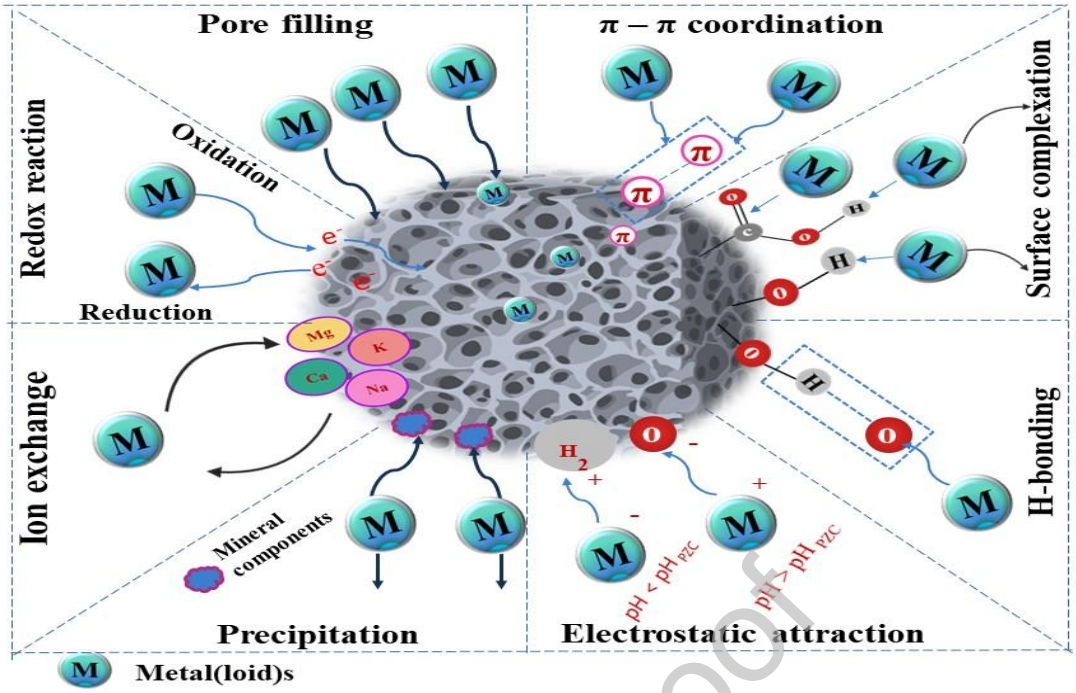

Fig. 12. Summary of main adsorption mechanisms for metal(loid)s by chemically modified biochar. Adapted from Chen et al. [107].

Understanding heavy metal removal by modified biochar necessitates advanced in-situ characterization techniques to monitor dynamic processes at various spatial scales. Traditional ex-situ methods like FTIR, XRD, and SEM provide useful structural data capture, only static snapshots after adsorption completion [202]. Moreover, these techniques necessitate complex and destructive sample preparation while limiting observations to two-dimensional (2D) morphological information and preventing real-time, three-dimensional (3D) visualization of heavy metal distribution during the adsorption process [203]. To address these limitations, non-destructive three-dimensional in-situ observation techniques are needed.

Advanced micro-computed tomography (micro-CT) solves this gap by facilitating real-time visualization and localization of heavy metals on biochar, offering volumetric structural information without sample destruction, and providing mechanistic insights that are not achievable by conventional methods [203]. Moreover, advanced imaging techniques like

micro-CT and high-resolution spatial analyses can elucidate microscale heterogeneity in contaminant distribution and establish specific reaction zones within the biochar matrix, information essential for enhancing material design and predicting long-term field efficacy [204]. For example, the micro-CT system was used to directly visualize and localize Pb(II) adsorption on wheat straw pellet biochar in real time [205]. Normalized digital images captured the dynamic adsorption process at initial Pb(II) concentrations of 100, 200, 300, and 400 mg L^{-1} over varying intervals. This micro-CT-guided approach provides visual, evidence-based insights into adsorption kinetics. Micro-CT was used to elucidate in-situ Cu(II) adsorption on corn cob biochar. At an initial concentration of 200 mg L^{-1}, adsorption kinetics were tracked over 10 time points (5 min-48 h). The results indicated that 80% of adsorption happened in the early stage by surface-preferential processes, subsequently followed by internal diffusion over time. The micro-CT findings correlated effectively with the FTIR analysis, indicating that micro-CT is a viable tool for 3D in-situ visualization of heavy metal adsorption on biochar [203].

Recent advancements in in situ analytical frameworks underscore the effectiveness of direct potentiometry with ion-selective electrodes (ISEs), enabling continuous in situ real-time monitoring of metal ion concentration during adsorption processes for monitoring heavy removal. Egorin et al. [206] demonstrated lead ion-selective potentiometry to track adsorption on birch biochar in real-time, achieving a sensitivity of 0.1 mg L^{-1}, revealing two-stage kinetic processes limited by intraparticle diffusion, and confirming ion exchange as the primary mechanism. This technique provides non-destructive, quantitative measurements without the need for sample withdrawal or complex instrumental setups.

Diffuse reflectance infrared Fourier transform spectroscopy (DRIFTS) has garnered increased attention as an optimal in-situ technology for the real-time assessment of the chemical characteristics of interfacial interactions [207]. Unlike traditional ex situ FTIR, in

situ DRIFTS allows for the observation of transient surface functionalities under varying thermal and oxidative conditions. Sun et al. [208] effectively illustrated the capability of in-situ DRIFTS for real-time observation of biochar surface functionality changes during thermal air oxidation. Employing corncob biochars produced at 300 °C, 500 °C, and 700 °C, they monitored the dynamic changes of C-OH, -CH_x, COOH, C=O, and C-O-C functional groups from ambient temperature to 500°C. The findings indicated that whereas surface functionality undergoes significant changes during initial low-temperature oxidation, the weight of biochar remains constant, implying the chemisorption of O_2 as intermediate oxygenated functional groups. Furthermore, in-situ DRIFTS was employed to observe the changes of functional groups on cellulose-derived biochar in relation to pyrolysis temperature and heating rates of 5, 10, 15, and 20 °C min^{-1} [209].

Attenuated total reflectance Fourier transform infrared (ATR-FTIR) spectroscopy is crucial for studying real-time interactions between heavy metals and biochar surfaces. Unlike ex-situ FTIR methods, in-situ ATR-FTIR allows for continuous monitoring of adsorption processes at the solid-liquid interface in aqueous environments without sample destruction. In-situ ATR-FTIR was used to examine the adsorption of Cr(VI) on the surfaces of hydrochar and pyrochar. The spectra exhibited distinct Cr-O stretching vibrations of CrO_4^{2-} and $HCrO_4^-$ at 884, 899, and 947 cm^{-1}, offering direct evidence of Cr(VI) speciation and surface complexation throughout the adsorption process [210].

Advanced in situ characterization techniques are pivotal for biochar research, allowing real-time monitoring of adsorption kinetics and performance without destructive sampling. However, their application, particularly with chemically modified biochar, is very limited, as most studies use conventional ex situ methods that only provide static data. This results in significant gaps in understanding real-time changes in surface functional groups, heavy metal speciation, and adsorption mechanisms. Incorporating machine learning and neural networks

with experimental data could enhance adsorbent design and performance predictions across varying conditions.

4. Regeneration and reusability of biochar

The disposal of spent biochar loaded with pollutants in landfills poses a risk to groundwater and soil, while the incineration can release harmful gases and generate hazardous ash [211]. Similarly, direct charge of spent biochar into aquatic ecosystems may cause secondary contamination. Furthermore, recovery processes such as high-speed centrifugation may induce metal desorption or the release of modifying agents, exacerbating pollution [212]. In addition, the pyrolysis process for biochar production can emit greenhouse gases and hazardous by-products, contributing to its environmental footprint [213]. The handling of spent biochar poses a contamination risk, as heavy metals and modifying agents may leach out [214]. Conversely, the regeneration and reuse of spent biochar can reduce both operational costs and waste volume, thereby improving its economic competitiveness and industrial applicability, while supporting environmental sustainability. Maintaining the long-term stability and reusability of biochar is critical, as its adsorption efficiency decreases over time. However, the recovery, regeneration, and recycling of adsorbents present challenges [215, 216].

The regeneration of any adsorbent depends on its type and quantity, the desorption process, and the used agents (e.g., acid, alkali, or salts). Basically, regeneration restores the functional characteristics of adsorption-saturated or reaction-inactivated modified biochar [1], thereby recovering its capacity for adsorption, catalysis, or energy storage. An effective desorption method enables a repeated adsorption-desorption cycle. The regeneration methods are commonly classified into chemical, thermal, and biological. Chemical regeneration employs reactive agents, whereas thermal regeneration relies on elevating temperatures. Biological regeneration utilizes microorganisms, such as heavy metal-tolerant *Pseudomonas*

bacteria, to immobilize or transform adsorbed metals to less toxic forms [217]. However, the biological regeneration is eco-friendly; it is time-consuming and limited by microbial activity. Given that the chemical and thermal methods are the most commonly used, the following section focuses on these approaches.

4.1 Chemical regeneration

Chemical regeneration restores the adsorbent by breaking the bond between the adsorbent and heavy metals using specific solvents or chemical agents or by chemically decomposing the adsorbed species [218], as shown in **Fig. 13**.

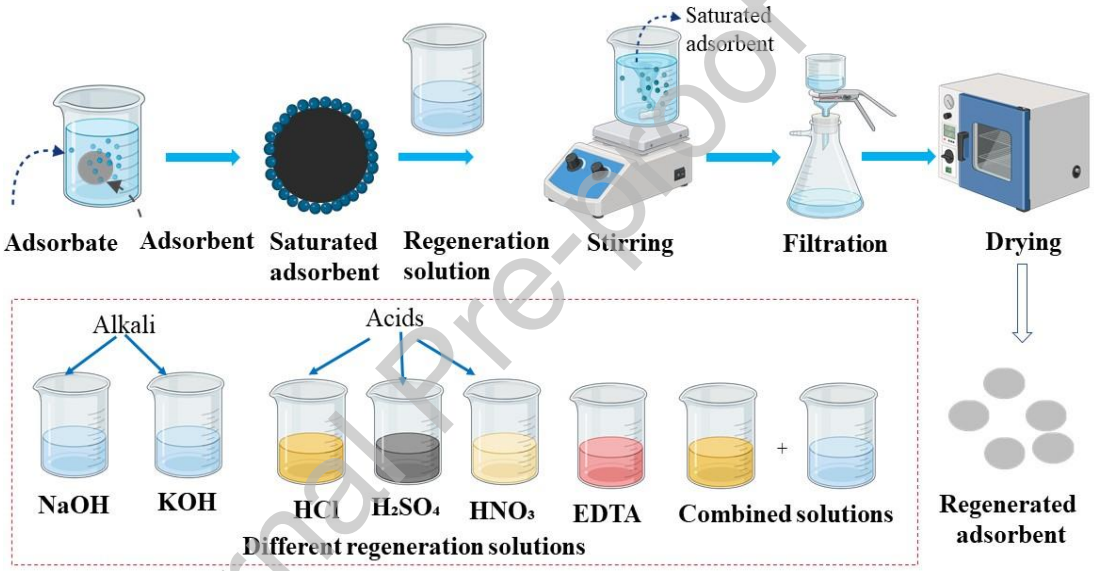

Fig. 13. Schematic of the chemical regeneration method.

The selection of reagents and their corresponding action mechanisms is critical. Commonly used reagents include acids (HCl, HNO_3, H_2SO_4), bases (NaOH, KOH), complexing agents such as ethylenediaminetetraacetic acid (EDTA), and salts (NaCl, KNO_3, $NaNO_3$, and $Ca(NO_3)_2$). Desorption experiments are an effective means to promote the reuse of adsorbent for heavy metal removal.

NaOH is widely used as a chemical agent. For instance, following Cd and Pb adsorption by Mg-modified biochar, the spent modified biochar was regenerated using 1 M NaOH under agitation for 24 hours at 100 rpm [28]. The regenerated biochar was rinsed, dried, and reused

in five consecutive adsorption-desorption recycle experiments. The results indicated that NaOH treatment could lead to the formation of Pb and Cd precipitates that remained on the biochar surface, thereby hindering subsequent adsorption. However, after five cycles, Pb and Cd adsorption capacities were 271.53 and 91.95 mg g^{-1}, respectively, demonstrating the efficient reusability. Additionally, NaOH solution effectively desorbed Cr(VI) via an ion-exchange mechanism under elevated pH levels, achieving removal efficiency higher than 60.35% after five reuse cycles [219].

In another study, the regeneration efficiency of *Opuntia ficus-indica* modified biochar contaminated with Ni(II) was examined over six consecutive cycles using 0.1M NaOH [220]. The removal efficiency declined from 92% to 87% after the first cycle and to approximately 80% after three cycles, mainly due to the loss of active sites and pore blockage. In a similar study, the nano zinc/bagasse BC regenerated with NaOH exhibited a decline in adsorption capacity but remained above 59.95 mg g^{-1} in the sixth cycle [221]. The observed decline can be attributed to the structural degradation and adverse changes in the physical and chemical properties of the materials, including a decrease in the SSA, TPV, and the integrity of functional groups.

Acids are another common approach that facilitates the desorption via a chemical reaction with metal ions. For example, Douglas fir biochar (NBC) and its magnetic counterpart (MBC) were regenerated using 0.1 M HCl [222]. During the first cycle, the Pb desorption from MBC exceeded 75%, while that from NBC was 41%. For Cd, desorption was 87% from MBC, compared to 41% from NBC. Similarly, the Mn-Zn ferrite/biochar composite was regenerated over six cycles using 0.2 M HCl, maintaining the removal efficiency of about 91.2% following the sixth cycle [155]. In a fixed-bed column adsorption/desorption experiment, 0.2 M HCl was utilized to regenerate hickory wood

alkaline modified biochar contaminated with Cu (II), achieving a regeneration efficiency of 85.1% [192].

HNO_3 is also utilized for chemical regeneration. Tea branch modified-biochar saturated with Cd^{2+} or Pb^{2+} was regenerated using 0.1 mol L^{-1} HNO_3 over five desorption-adsorption cycles [46]. Although regeneration efficiency decreased over these cycles, it remained above 80%; this decline was attributed to the partial saturation of surface-active sites and depletion of surface functional groups. In a comparative study of acids for regenerating Zn(II)-treated raw jujube seeds biochar, 0.1 M HNO_3, HCl, and H_2SO_4 achieved regeneration efficiencies of 90%, 93%, and 91%, respectively [223]. HCl was selected for five adsorption/desorption cycles and maintained an efficiency of approximately 87% after the final cycle, indicating stable regeneration performance. Similarly, Wan et al. [154] showed that HMO-BC can be regenerated using 0.2 M HCl and 4 wt% $CaCl_2$. The study achieved over 97% desorption of Pb(II) and Cd(II) from synthetic wastewater within 10 bed volumes. In real electroplating wastewater, the HMO-BC maintained full adsorption capacity over five cycles without a decline in desorption rate, indicating that modified biochars can be reused, thus lowering operational costs and reducing waste generation.

Complexing agents such as EDTA-2Na can also serve as effective desorbing agents. For Pb-loaded magnetic biochar, EDTA-2Na achieved a desorption efficiency of 91.1% [224]. Both SSA and pore volume increased during the regeneration cycles, as shown in **Fig. 14 (a),** which may be attributed to ash dissolution and partial loss of iron oxides. Meanwhile, the saturation magnetization decreased, as shown in **Fig. 14 (b)**. Therefore, the efficacy of chemical regeneration methods is influenced by factors such as surface functional groups, pore structure, and changes in active sites.

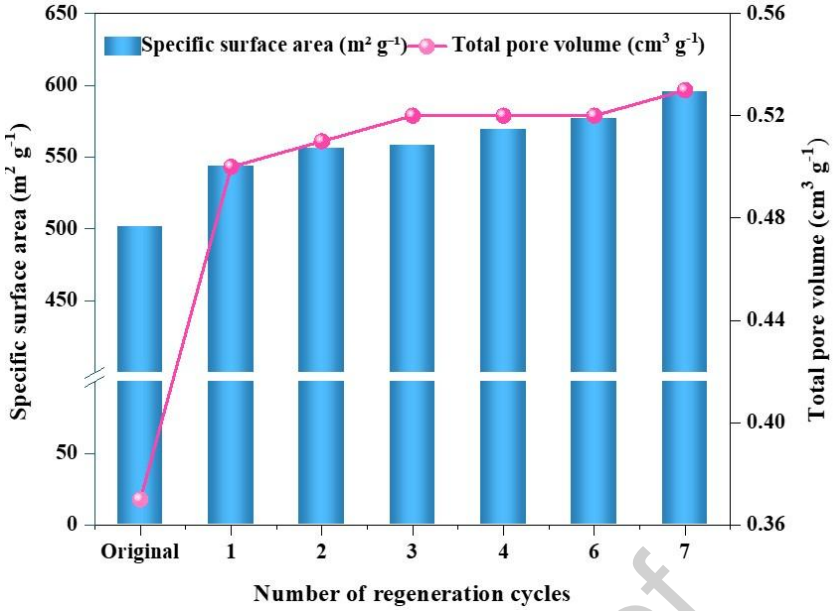

(a) Changes in SSA and TPV

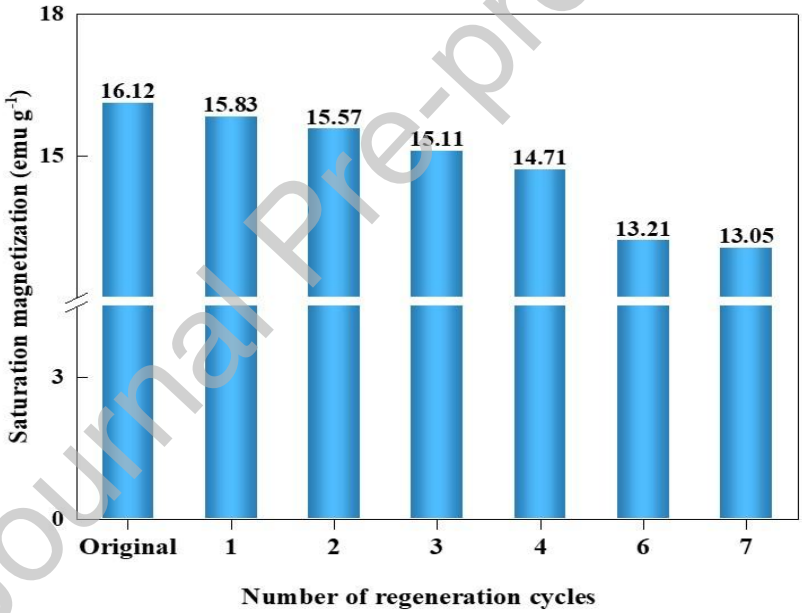

(b) Changes in the saturation magnetization

Fig. 14. Physicochemical characteristics of original and regenerated magnetic biochar. Adapted from Wang et al. [224].

The performance of chemical regeneration is affected by factors such as adsorption mechanisms, surface functional groups, and adsorbent pore structure. The long-term stability of modified biochar during regeneration cycles is critical, as metal oxides may dissolve at extreme pH or through ion exchange, while transition metals can lead to structural

degradation. Capacity loss during cycling arises from incomplete desorption, permanent coating of sites, and oxidation. Incorporating stabilizing elements like phosphorus, silica, or organic matter can significantly mitigate these degradation effects [225]. Biochar exhibits lower regeneration performance when pollutants are adsorbed through chemisorption compared to physisorption [226], as pollutants chemically react with the adsorbent, forming complex, sometimes irreversible compounds [227]. Consequently, biochar loses active sites over time due to blocked pores, which may result in a decline in its functionalities and mass after multiple adsorption/desorption cycles [71].

Additional factors influencing the regeneration include the type and concentration of desorbing agents, the biochar's surface functional groups, and its structural stability. Acidic desorbing agents (e.g., HNO_3, HCl, H_2SO_4) are more effective than alkaline agents for heavy metal desorption, as they dissolve metal complexes and precipitates. However, strong acids like HNO_3 can degrade biochar structure over cycles, reducing long-term reusability. HNO_3 is often more aggressive and can cause structural deterioration, while HCl is relatively benign [227]. The presence of oxygen-containing functional groups and minerals drives chemisorption mechanisms, which negatively impact regeneration performance [228]. Precipitation and complexation are particularly difficult to reverse, leading to a wide range of regeneration efficiencies in the last cycle, indicating instability in heavy metal regeneration **(Fig. 15)**. In contrast, cation exchange has a moderate impact on regeneration, as shown in **Table 9 and Fig. 15**.

Surface area and morphology of biochar also affect regeneration efficiency. Higher surface area enhances physisorption, but no correlation exists between desorption performance and surface area [229]. For strongly chemisorbed heavy metals, pore blockage and active site loss degrade biochar structure [230]. This degradation occurs abruptly after the

first cycle or gradually over subsequent cycles [28]. Thus, after the regeneration process, X-ray photoelectron spectroscopy and FTIR analysis could be used to characterize biochar.

Table 9 Functional groups and their corresponding removal mechanism and regeneration impact for heavy metals [227].

Functional group	Removal mechanism	Regeneration impact
Carbonyl	Precipitation	High
Hydroxyl (-OH)	Precipitation	High
Carboxyl (-COOH)	Complexation	High
Alcohol (R-OH)	Complexation	High
Carboxyl (-COOH)	Cation Exchange	Moderate
Minerals (Ca(II), Mg(II), K(I), Na(I))	Cation Exchange	Moderate
Aromatics (Carbon Rich)	Cation Exchange	Low
Phenols	Reduction	High
Amine group	Complexation	High

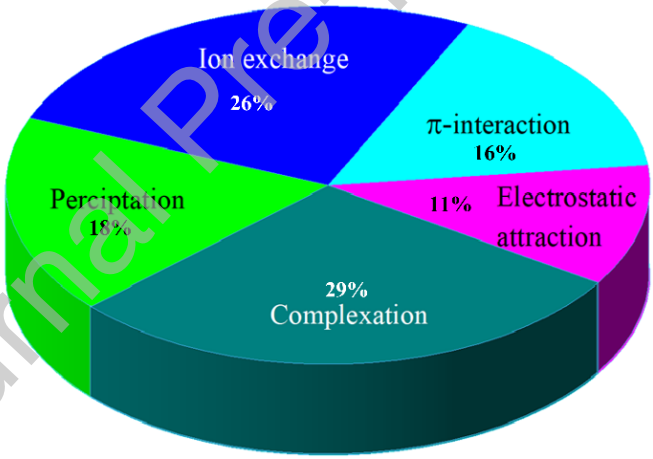

Fig. 15. Summary of heavy metal adsorption's removal mechanisms and regeneration efficiencies. Adapted from Alsawy et al. [227].

Table 10 summarizes the regeneration performance of various chemically modified biochars for heavy metal desorption, showing high recovery efficiencies (about 80–100%) over multiple regeneration cycles using HCl, NaOH, EDTA-2Na or mixed solutions. These results highlighted the strong reusability of chemically regenerated sorbents for heavy metal

removal. However, secondary contamination caused by the leaching of adsorbed contaminants should be carefully considered when applying chemical agents.

Table 10 Chemical regeneration, reusability, and removal efficiency of heavy metal(loid)s using modified biochar.

Adsorbent material	Pollutant	Type test	Eluent	First cycle efficiency(%)	No. of Cycles	Last cycle efficiency (%)	Ref.
Copper oxide-biochar	As(III)	Batch	HCl	96.77	4	93.60	[231]
Manganese oxide-biochar	As(III)	Batch	HCl	76.05	4	71.23	[231]
Fe-modified biochar	As(III)	Batch	NaOH	90.50	5	43.30	[149]
MgO-modified biochar	Cd(II)	Fixed-bed column	HCl + $CaCl_2$	93	5	85.00	[154]
KOH-modified biochar	Cd(II)	Batch	NaOH	35	3	13	[71]
Fe-modified biochar	Ni(II)	Batch	NaOH	100	5	100.00	[149]
NaOH-modified biochar	Ni(II)	Batch	NaOH	90	3	80	[220]
Mn-Zn ferrite/biochar	Pb(II)	Batch	HCl	~99	6	91.20	[155]
Si-Mn binary modified biochar	Cu(II)	Batch	EDTA-2Na	98.76	5	80.24	[230]
NaOH-modified biochar	Cu(II)	Batch	NaOH	92	3	79	[220]
Maghemite-modified biochar	Cr(VI)	Batch	NaOH	~97.3	6	87.7	[232]
KOH-activated biochar	Cr(VI)	Batch	NaOH	60	3	45	[71]

4.2 Thermal regeneration

Thermal regeneration involves heating biochar/modified biochar at elevated temperatures to facilitate the carbonization and decomposition of the adsorbed pollutants [233], as shown in **Fig. 16**. This process alters the binding interaction between adsorbents and heavy metals, facilitating their desorption or decomposition, and is particularly suitable for materials with high thermal stability. However, thermal regeneration may reduce the pore

size of the original biochar, which is attributed to the loss of organic carbon. For instance, following four desorption cycles, the adsorption capacity of Pb(II) by alumina-modified sludge biochar decreased from 475.850 mg g^{-1} to 392.575 mg g^{-1} [234]. Cui et al. [235] investigated the effect of temperature on the regeneration efficiency by treating the adsorption-saturated hydrochar at 700–900°C. Elevated temperatures effectively regenerated the biochar through the removal of Cd. The regenerated biochar exhibited increased ash and carbon content, reduced hydrogen and oxygen content, lower pH, and a greatly improved adsorption capacity for Cd (26.05–30.24 mg g^{-1}), compared to the pristine hydrochar (6.70 mg g^{-1}).

Fig. 16. Schematic of thermal regeneration.

Thermal regeneration efficiency depends on specific conditions. As demonstrated by Jia et al. [217], treatment under specific conditions (5% O_2, 600 °C) effectively regenerates multimetal-loaded biochars for Hg^0 adsorption via restoring active metal oxide sites. Hg^0 adsorption on the regenerated biochar followed a multilayer mechanism that involves both physical and chemical interactions, primarily governed by surface adsorption sites. However, regeneration performance initially increased and subsequently declined with increasing O_2 concentration and temperature. The regeneration performance over multiple cycles for Hg^0 adsorption was determined using eq. (16) [217].

$$E_R = \frac{E_{\text{Regenerated}}}{E_{\text{Fresh}}} \times 100\% \quad (16)$$

where $E_{Regenerated}$ and E_{Fresh} refer to the Hg^0 removal by regenerated and fresh biochar, respectively.

Both a simply synthesized magnetic sorbent ($TF_{0.46}$) and sonochemically synthesized magnetic biochar ($TUF_{0.46}$) were thermally regenerated after Hg^0 adsorption by heating at 450 °C for 1 hour under N_2 atmosphere [236]. The desorbed mercury was captured in NaOH solution. Over ten consecutive adsorption-regeneration cycles, the Hg^0 removal efficiency of ($TF_{0.46}$) and ($TUF_{0.46}$) dropped to proximiltely 72% and 91%, respectively, as shown in **Fig. 17**.

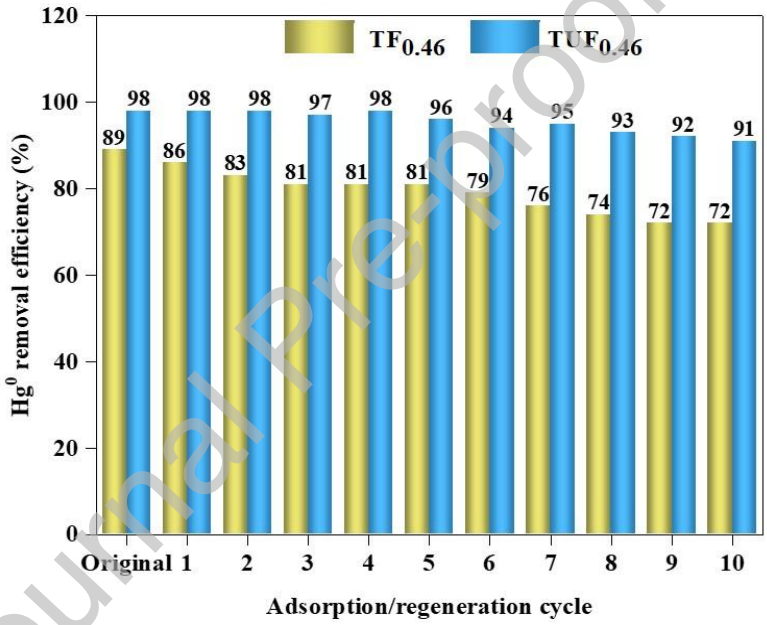

Fig. 17. Thermal regeneration and Hg^0 removal efficiency over 10 regenerated/adsorption cycles for sonochemically synthesized magnetic biochar ($TUF_{0.46}$) and magnetic tea biochar ($TF_{0.46}$) [236].

Overall, thermochemical processes represent an effective method for the safe disposal and regeneration of biochar/modified biochar adsorbents. Both chemical and thermal regeneration methods can effectively restore the modified biochar; however, the appropriate method should be chosen based on the type of pollutants, thermal stability, and the practical operating conditions. Although effective, the thermal regeneration method is more energy-

intensive and costly than other alternative techniques, which may explain the relatively limited published data on this subject [237]. Therefore, further investigation is needed.

5. End-of-life, environmental, and economic considerations

5.1 Disposal and end-of-life management of spent modified biochar

The disposal of modified biochar after the adsorption of heavy metals is a critical scientific problem that restricts its practical application. Improper management of heavy metals adsorbed within modified biochar may be released back into water or soil, causing secondary pollution [238]. Therefore, such biochar must be carefully handled to ensure that heavy metals are stably immobilized within the carbon matrix over the long term [239], thereby preventing their re-release into the environment. Following the remediation process, spent modified biochar is typically separated from the treated water via solid-liquid separation techniques, such as magnetic separation. The recovered biochar can subsequently undergo desorption through chemical elution, which concentrates heavy metals into a liquid fraction for recovery while regenerating the biochar for repeated use [240]. For instance, magnetic straw biochar functionalized with magnesium oxide and iron oxide displays pronounced magnetic characteristics, which facilitate the effective removal of Pb(II) from aqueous media. After four consecutive adsorption-desorption cycles, the material retains a regeneration efficiency for Pb(II) exceeding 82.01%, indicative of its outstanding cyclic stability [166].

However, few studies provide proper insight into the final disposal of spent biochar, which poses particular challenges in developing nations lacking furnaces and engineered landfills [241]. Five end-of-life pathways are generally considered for spent modified biochar: incineration, regeneration and reuse, landfill, fertilizer, and other safe disposal techniques [242, 243]. Incineration reduces volume and mass while enabling thermal energy recovery. Martín-Lara et al. [244] studied the pyrolysis of pinecone shell used for Cu^{2+} and

Pb^{2+} adsorption. The resulting biomass had higher carbon and lower oxygen, nitrogen, and sulfur than coal, indicating reduced corrosive/toxic gases and potential as a thermal energy source. Landfill disposal is simple and inexpensive but requires prior desorption of heavy metals to avoid secondary pollution [245]. Regeneration and reuse extend biochar lifespan; for example, EDTA-metal complexes have been successfully separated into different reagents, enabling stable performance over multiple cycles as described previously in section 4. Magnetic and centrifugal sedimentation can also be possible methods for the separation of iron/iron oxide modified biosorbent [246]. Spent biosorbent can be recycled to produce bricks and cement for the construction industry, but usage in large quantities can affect its mechanical strength. Also, heavy metals loaded on biochar-based sorbents can be used for the production of supercapacitors. For example, microwave oxidation carried out with Ni^{2+} loaded with biochar reduces the carbon content and increases oxygen content, which increases the capacitance, charge-discharge capacity, and power density [246, 247].

Research shows that biochar has a high potential for replacing expensive synthetic carbon nanoparticles for future supercapacitors [247]. Fertilizer application utilizes the organic content of spent biochar to improve soil quality, as demonstrated with marine algal biomass for Zn^{2+} removal and fishbone meat waste for lead removal [242]. Other safe disposal techniques include microwave sterilization of spent modified biochar followed by seal treatment in inert material. The fate of spent adsorbent must be considered once regeneration is no longer feasible. Energy recovery through incineration is a viable option. The calorific value of spent NaOH-modified biochar was measured at 20.37 MJ kg^{-1}, significantly higher than the minimum required for incineration [220]. Thus, NaOH-modified biochar can be utilized as an energy source in industries such as power plants, cement plants, and steel manufacturing.

5.2 Environmental risk of chemically modified biochar

Although chemical modification approaches significantly improve the heavy metal adsorption capability of biochar, a comprehensive evaluation must carefully consider the potential negative environmental externalities associated with these modification procedures. The current literature predominantly highlights enhanced performance metrics, including increased specific surface area, enhanced functional group density, and greater adsorption capacity [125], frequently neglecting the environmental impact of the modification processes. The primary environmental issues are: (1) the release of waste liquids, including residual chemical modifiers and reaction by-products, and (2) the potential leaching of toxic substances from the modified biochar during subsequent use or disposal.

Chemical modification techniques produce significant quantities of waste liquids that contain unreacted chemicals, reaction by-products, and leached pollutants from the biochar matrix. Acid/alkali treatment generates wastewater with severe pH levels (ranging from 1 to 13), significant salinity, and increased amounts of dissolved organic carbon leached from the biochar [98]. The resultant acidic or basic wastewater presents considerable treatment problems and potential hazards to aquatic habitats if inadequately managed. The research conducted by Hawryluk-Sidoruk et al. [125] showed that acid modification using HNO_3 was the most effective method for the removal of heavy metals from biochar, principally via the production of water-soluble salts. Nevertheless, significant dangers were identified: concentrated nitric acid induced passivation of Cr and Pb, obstructing their removal. KOH and H_2O_2 treatments were significantly less effective, particularly in biochars generated from sewage sludge, where heavy metal concentrations were elevated (10 to 1000 times higher). The reduction of heavy metals by these procedures was predominantly due to physical washing rather than chemical reaction, indicating less permanent immobilization. The efficacy is significantly influenced by the type of feedstock, the form of metal, and the conditions of modification, with no single method universally superior.

Metal salt impregnation poses a notable risk to environmental sustainability due to the process of soaking biochar in metal salt solutions, such as $ZnCl_2$ or $FeCl_3$. The remaining unadsorbed metal solutions constitute a significant waste stream with potentially ecotoxic concentrations of metals [248]. Proper treatment of these solutions is essential before discharge to prevent ecosystem contamination and long-term degradation of soil and water.

Chemically modified biochar can release toxic substances even after washing and purification, particularly in contaminated environments with variable pH, ionic strength, and dissolved organic matter. This poses a secondary contamination risk, raising concerns about its use in environmental remediation. Metal leaching, especially from biochars modified with metal salts, is a significant risk, with incomplete immobilization leading to remobilization under changing conditions. Metal leaching from impregnated biochars poses a documented risk, with studies indicating minimal leaching under optimized laboratory conditions. For instance, an Fe-modified biochar study reported only 38.13 μg L^{-1} iron release [248]. However, real environmental conditions with fluctuating pH and varying ionic strength can lead to significantly higher leaching rates. This variability underscores the need for comprehensive assessment methods to prevent modified biochars from becoming sources of contamination. Metal oxides may dissolve in natural waters by competitive ion exchange with abundant cations (e.g., Ca^{2+}, Mg^{2+}) or at very strong or very weak pH (especially acidic conditions), resulting in the release of toxic metals into the environment.

Standardised testing protocols have emerged as vital tools for the accurate and reliable evaluation of these hazards. The standard method for evaluating the potential for heavy metal leaching from biochar and other waste materials is the Toxicity Characteristic Leaching Procedure (TCLP) [249, 250]. This methodology is widely accepted and offers a standardized framework for comparing various biochar modification methods. Recent research has furthered the discipline by acknowledging the practical limitations of conventional TCLP

testing. An accelerated leaching protocol was developed by Zhao et al. [250] that significantly facilitated the routine leaching assessment of modified biochars prior to environmental application and accelerated the pace of biochar development research. This protocol strongly correlates with conventional TCLP results and reduces the analysis time from 18 hours to 30 minutes.

Beyond the chemical risk, the introduction of modified biochar may also alter indigenous microbial community structure and function in aquatic ecosystems. Modified biochar plays a dual role within these systems: as a physical adsorbent for contaminants and as a substrate for microbial communities [132]. Its high surface area, porous structure, and functional groups provide excellent attachment sites for microorganisms, facilitating biofilm formation on its surface and enhancing pollutants removal through biodegradation, reduction, and immobilization of heavy metals. Beneficial interaction has been demonstrated by iron-modified biochar, which promotes the growth of microbial genera such as *Bacillus*, *Geobacter*, and *Bradyrhizobium*, which are associated with denitrification, iron reduction, and nitrogen fixation processes, respectively [251]. Also, iron-modified biochar provides surface-bound Fe^{2+}/Fe^{3+} species, which function as electron shuttles in extracellular electron transfer, enhancing microbial metabolism and accelerating nitrate/nitrite reduction and anammox processes [252, 253]. Modified biochar generally enhances microbial diversity and richness by offering colonization surfaces and slow-release carbon sources, as demonstrated by increased community diversity indices such as Chao1, Shannon, and Simpson in constructed wetlands amended with composite modified biochar (e.g., $KMnO_4$- or $ZnCl_2$-MBC) [254, 255].

However, ecological risks accompany these benefits. For instance, manganese-modified biochar applied to sediments was found not only to adsorb heavy metals but also to shift the microbial community composition, increasing the relative abundance of certain taxonomic

groups, which suggests the potential for modified biochar to influence microbial ecology in contaminated systems [256]. Shifts in microbial community composition may lead to changes in the abundance of functional groups (e.g., nitrifiers, denitrifiers) that regulate nitrogen and phosphorus cycling, which could have cascading effects on water quality and ecosystem health [257]. Thus, biochar's capacity to alter the dynamics of microbial communities may have both positive and unintended ecological effects.

To mitigate pollution risks, targeted measures include neutralizing acid and alkaline waste streams before discharge, recycling recovered chemicals, and utilizing closed-loop recovery systems for concentrated reuse. Advanced treatments such as electrochemical neutralization help minimize waste discharge. Surface stabilization techniques, including metal oxide coatings and polymeric encapsulation, significantly reduce leaching of residual chemicals. For instance, Fe-Mn-bimetallic oxide-modified biochar decreased the leaching of metals from modified biochar over extended periods. pH-buffering modifications address leaching variability, with regular leachate monitoring being crucial. Selecting low-contaminant feedstocks (agricultural/forestry residues) reduces baseline leaching potential.

Green modification technologies like bio-assisted synthesis (e.g., phyto-synthesized copper oxide nanoparticles) reduce hazardous waste. Employing industrial waste as feedstock and modifiers fosters a circular economy. Silica-enhanced Fe/Mn decorated biochar composites have exhibited enhanced stability, as the silica acts as a protective coating that inhibits metal oxide leaching and degradation [225]. The incorporation of stabilising elements, such as phosphorus, silica, or organic matter, can significantly slow degradation processes, thereby reducing secondary contamination risks and extending the material's service life. The lifespan of material can be extended by recycling discarded biochar through thermal or chemical regeneration. However, it is crucial to carefully select the regeneration chemicals to prevent secondary contamination.

Stability and ecological factors must be incorporated into the design phase to guarantee ecologically safe and economically feasible closed-loop biochar applications. Further research must highlight long-term field studies to enhance understanding of the fate, transport, and ecological impacts of chemically modified biochar in real aquatic ecosystems.

5.3 Life cycle assessment and economic feasibility

5.3.1 Life cycle assessment

Modified biochar can efficiently remove heavy metals; however, its adsorption-release dynamics remain a concern [258]. Due to saturated adsorption sites, contaminants may be released, causing secondary pollution [259]. Moreover, pollutants loaded modified biochar may have toxic effects on exposed animals, plants, crops, microorganisms, and humans [260]. The underlying environmental risks of modified biochar require a comprehensive understanding and evaluation to support environmental governance [261]. Life cycle assessment (LCA) is a broadly applied tool for evaluating the environmental impacts of all the outputs and inputs of a product or process over its entire life cycle [262]. LCA encompasses raw material extraction, processing, manufacturing, distribution, usage, and final disposal, thereby offering a thorough sustainability analysis [263, 264].

The cycle begins with the extraction of raw materials, followed by transportation, pyrolysis, and manufacturing, and concludes with disposal [265]. ISO 14040 and ISO 14044 are the international standards that describe the principles and framework and provide the requirements and guidelines of the LCA [266]. The LCA comprises four key stages: 1) goal and scope definition, where objectives and boundaries are established; 2) inventory analysis (LCI), which assesses material and energy consumption and emissions; 3) life cycle impact assessment (LCIA), converting inventory data into environmental implications; and 4) interpretation of results, focusing on data validation and quality examination related to each stage [267]. The scope defines system boundaries: cradle-to-gate (raw material extraction to

factory gate) and cradle-to-grave (includes use and end-of-life stages) are the most common approaches in biochar LCA [268-270], as shown in **Fig. 18**. For automatic LCIA calculation, SimaPro, GaBi, and OpenLCA are among the most commonly used tools. SimaPro and GaBi offer extensive databases suited to expert-level modelling, while OpenLCA provides a flexible, open-source platform accessible to a broad range of users [271].

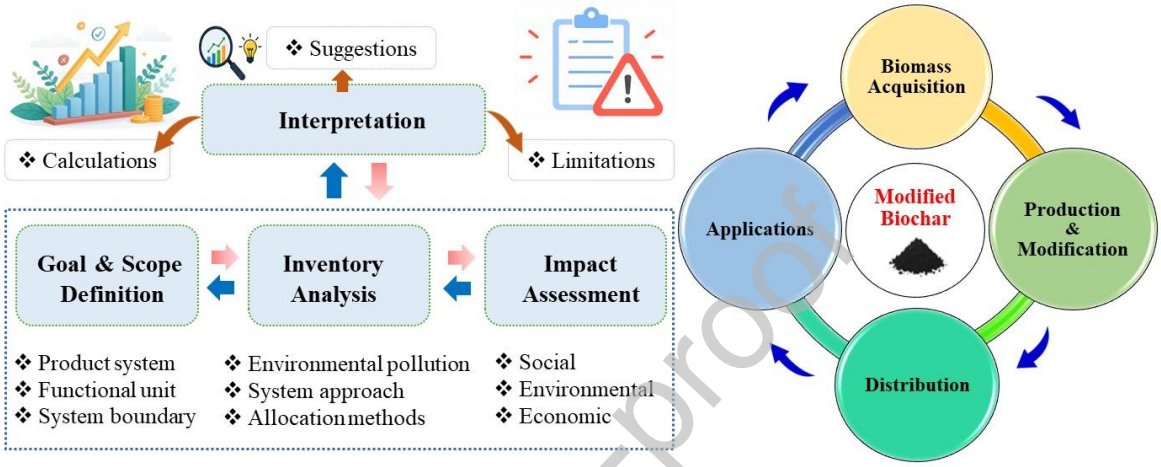

Fig. 18. Life cycle assessment of the modified biochar

LCA evaluates every parameter that can affect environmental outcomes, such as greenhouse gas emissions and global warming potential (GWP) [272]. Fawzy et al. [273] found that for every tonne of biochar produced from olive tree pruning residue, approximately 268 kg CO_2e could be permanently removed from the atmosphere. Rajabi Hamedani et al. [274] found that willow biochar (80% stable carbon) had a lower environmental impact than pig manure biochar (33.7% stable carbon).

A critical gap in many modified biochar studies is the lack of a closed-loop analysis encompassing material preparation, application, regeneration, and final disposal [275]. For example, Norberto et al. [276] investigate the environmental impact of canola straw biochar modified with H_3PO_4 and $FeCl_3$ using microwave activation. for adsorbing arsenic. The system boundary considered subsystems such as the collection, transportation, treatment, and preparation of rapeseed straw biochar, but did not include the disposal of adsorbents after use.

The results indicated that modified rapeseed straw biochar offers higher environmental efficiency, as LCA showed that the modified biochar production is environmentally friendly with -0.298 kg CO_2 eq/kg.

The LCA of potassium ferrate-modified biochar, made from tea leaf stalks, for heavy metal wastewater treatment was assessed by Zhang et al. [277] using a cradle-to-grave approach, covering raw material collection, biochar preparation, and biochar application. Prepared at 650°C and 120 minutes of pyrolysis, the modified biochar reduced carbon emissions by 38,346 kg CO_2e/day compared to potassium pertechnetate treatment. Key factors influencing emissions and costs include modifier dosage, price, and pyrolysis method, demonstrating the environmental advantages of modified biochar.

However, LCA of the modified biochar faces challenges due to numerous environmental indicators (e.g., climate change, ecotoxicity) that are not equally significant, and no consensus exists on prioritization. Future research should therefore adopt a multidimensional evaluation method that considers both environmental and social factors to provide a more reliable basis for policies and decisions regarding engineered biochar. These integrated assessments will be crucial for the purpose of facilitating the sustainable commercialization of modified biochar technologies and guiding policy decisions.

5.3.2 Economic feasibility

The literature indicates a significant disconnect between laboratory studies and industrial-scale economic forecasts regarding modified biochar. Amalina et al. [278] highlight its promise as a cost-effective alternative to traditional adsorbents, while Mirzaei et al. [279] point out production costs, infrastructure, and lack of awareness as key barriers to its larger adoption. The total production costs include four main elements: raw biomass feedstock, chemical modification reagents, energy for pyrolysis and modification, and post-treatment costs.

Raw material expenses are the main cost in biochar production, with feedstock costs accounting for 47.30%, 57.2%, and 59.98% of total production costs across small, medium, and large-scale facilities, respectively [280]. Lower-cost agricultural residues like sugarcane bagasse, rice husks, and straw are preferred over virgin biomass or specialized materials. Factors such as straw availability, influenced by yield and crop rotation, significantly impact production efficiency [281]. In Malaysia, biochar production from palm oil and rice residues costs between 116-197 USD ton^{-1}, with straws being the most economical option [282]. Hu et al. [283] conducted a techno-economic assessment of swine manure biochar production at an industrial scale of 8,000 tonnes annually, finding it economically viable if the selling price exceeds 116 USD ton^{-1}. With prices between 154 and 193 USD ton^{-1}, the internal rate of return (IRR) can range from 11% to 41%, with a discounted payback period (DPP) of about 4.6 years. The sourcing of feedstock involves hidden costs such as collection, transportation, and storage, often overlooked in cost analyses but crucial for project economics. Mcintyre and Li [284] highlighted that biosolid-derived biochar can mitigate production challenges, heavy metal content, and large-scale economic feasibility.

Modification reagents significantly impact costs, with common agents including KOH, H_3PO_4, and metal salts. The cost-effectiveness of modification chemistry depends on reagent pricing, dosage requirements, and removal efficiency improvements achieved. Chakma et al. [285] found KOH-modified biochar cheaper (CAD 15.47 kg^{-1}) and more efficient than HNO_3-modified biochar (CAD 41.29 kg^{-1}), achieving higher removal efficiency (100% vs. 95% for Cu^{2+} and Pb^{2+}). Phosphoric acid-modified cocopeat biochar achieved a low cost of 1.56 USD kg^{-1}, maintaining 99% removal efficiency for Cu^{2+} and Ni^{2+} over 20 cycles [286]. On the other hand, pristine rapeseed straw biochar costs USD 0.16 kg^{-1} (arsenic adsorption: 25 μg g^{-1}), but H_3PO_4-$FeCl_3$ modification raises costs to USD 5.14 kg^{-1}, enhancing adsorption to 960 μg g^{-1} [276]. Techno-economic analysis confirmed that larger production capacities

enhance profitability, reducing payback period and increasing NPV, as chemical efficiency directly impacts economic viability [287].

Energy consumption represents a critical economic variable in the production process, and understanding thermal efficiency is essential for optimizing these systems[288]. The pyrolysis process operates at elevated temperatures (typically 300-900°C depending on application requirements), consuming substantial electrical or thermal energy. Patwa et al. [289] studied biochar production from water hyacinth and sugarcane bagasse at 300-700°C, finding that lower pyrolysis temperatures require less energy and produce higher yields, with 400 °C for 60% energy efficiency compared to 700 °C, although carbon stability may require higher temperatures for specific applications. Torrefaction at 244 °C consumed 20.042 $MJ \cdot kg^{-1}$, resulting in a biochar cost of NT$ 12.21 with a yield of 85.93% energy [290].

Biochar regeneration capability is crucial for its economic viability over time, with chemical regeneration being the most studied method that can significantly lower operating costs [227]. Various strategies, including thermal, chemical, photocatalytic, and electrochemical, have different cost impacts. A study showed that phosphoric acid-modified cocopeat biochar achieved 96.0% desorption efficiency over 20 cycles at a low production cost of 1.56 USD kg^{-1} [286]. Another research found that potassium ferrate-modified biochar for heavy metal wastewater treatment saved 56,680 USD day^{-1} after three recycling cycles compared to conventional potassium pertechnetate treatment [277].

According to Ahmad et al. [291], the cost of biochar production is significantly lower than that of activated carbon, which costs USD 1,500 ton^{-1}. Depending on the modification strategy, the overall production costs range from 0.42-41.29 USD kg^{-1}, with annual returns of 12.5-18.85% and payback periods of 5.3-8.0 years [287]. Economic analysis has verified that increased production capacities improve profitability by minimizing the payback period and

increasing the net present value, as chemical efficiency directly affects economic viability [287].

A complete economic assessment must include biomass collection, equipment investment, functionalization costs, deployment, monitoring, and maintenance [292, 293]. While feedstock costs dominated expenditures across all scales, other operational costs, including labor, decreased proportionally with increased production volume [280]. With continued optimization of production processes and supportive policy frameworks, chemically modified biochar is poised to become an economically viable and sustainable solution for heavy metal remediation.

6. Challenges in industrializing chemically modified biochar for heavy metal remediation

6.1 *Variabilities in reported results*

Significant variations in reported adsorption capacities hinder the standardization of modified biochar for industrial applications. These inconsistencies arise from differences in feedstock type, pyrolysis conditions, and experimental parameters. Feedstock type critically influences biochar properties. As shown in Tables 1-4, pristine biochar SSA varies widely depending on the feedstock, and after modification, differences become more pronounced. For example, when corn straw, spent mushroom substrate (SMS), and hardwood sawdust were modified under identical conditions using K_2CO_3, their specific surface areas varied dramatically: SMS reached 184.47 $m^2\ g^{-1}$, hardwood sawdust achieved 105.29 $m^2\ g^{-1}$, while corn straw only reached 16.36 $m^2\ g^{-1}$ [73]. This feedstock-dependent variability directly translated to adsorption performance, with SMS-modified biochar showing maximum adsorption capacities of 90.58 mg g^{-1} for Pb^{2+} and 25.35 mg g^{-1} for Cd^{2+}, significantly outperforming the other feedstocks.

Environmental variables, including pH, temperature, and the presence of competing ions, will also affect the adsorption effectiveness of heavy metals. Research indicates that adsorption capacity often rises with increasing pH, attributed to less competition from H^+ ions. For example, the adsorption capacity of Pb^{2+} onto biochar improves with increasing pH, stabilizing beyond pH 3 [294]. Similarly, studies have shown that as the pH increases from 3 to 6, the adsorption capacity for Cu^{2+} ions improves [295]. For anionic heavy metals like Cr(VI), maximum adsorption occurs under strongly acidic conditions (pH 2-3). When the pH increased from 2 to 9, the Cr(VI) removal efficiency decreased from 99.97% to 52.71%, because Cr(VI) exists in anionic forms such as $Cr_2O_7^{2-}$, $HCrO_4^-$, and $HCr_2O_7^-$ in aqueous solution [173]. Additionally, high concentrations of cations such as K^+, Ca^{2+}, Na^+, and Mg^{2+} compete with target heavy metals for active sites, reducing ion exchange effectiveness. In multi-metal systems, competitive adsorption leads to distinct selectivity patterns. For example, in H_2O_2-modified hydrochar, the removal efficiency followed the order Pb^{2+} > Cu^{2+} > Cd^{2+} > Ni^{2+} [84]. Similarly, in alkali-modified biochar fixed-bed columns, Pb^{2+} and Cu^{2+} were preferentially adsorbed, while Cd^{2+}, Zn^{2+}, and Ni^{2+} showed little to no adsorption [192].

Understanding these variations and standardizing adsorption experimental conditions, including initial concentration, adsorbent dosage, pH, contact time, and temperature, would help eliminate inconsistencies in comparative studies of different adsorbents and facilitate industrial-scale adoption.

6.2 Lack of real-life and long-term studies

The impact of real wastewater conditions, including the presence of competing ions (e.g., Na^+, Ca^{2+}, Cl^-), is insufficiently investigated in numerous laboratory-scale studies. A major challenge is the lack of standardized testing protocols for modified biochar performance evaluation. Most previous studies employ synthetic wastewater with single-

metal solutions, which do not fully represent real-world wastewater complexities. Future investigations should focus on multi-metal adsorption experiments and field-scale validation to establish reliable performance metrics.

Another limitation is the degradation of modified biochar effectiveness over repeated adsorption cycles. Over time, modified biochar undergoes aging processes, including oxidation, microbial colonization, and surface functionalization changes, which can alter its adsorption performance [296]. While some modification strategies, such as functionalization with iron oxides, enhance reusability, biochar often suffers from structural deterioration and reduced adsorption capacity after multiple regeneration cycles. Additionally, the regeneration of biochar is often limited by the potential to cause secondary pollution and high chemical or energy demands. Improper disposal or incomplete regeneration may lead to environmental risks, such as heavy metal leaching or toxic byproduct formation. Investigating sustainable regeneration methods remains a critical research gap.

The long-term stability of modified biochar itself remains a critical challenge that determines its practical lifespan. While metal oxide modifications substantially enhance initial performance, their long-term stability presents challenges. Metal oxides can undergo dissolution at extreme pH values (particularly acidic conditions) or through competitive ion exchange with abundant cations in natural waters. Silica-enhanced Fe/Mn decorated biochar composites showed improved stability compared to metal oxide biochar alone, with silica providing a protective coating preventing metal oxide leaching and degradation [225]. The redox cycling of transition metals (Fe^{2+}/Fe^{3+}, $Mn^{2+}/Mn^{3+}/Mn^{4+}$) during repeated adsorption-desorption cycles can accelerate structural degradation through valence changes that alter chemical bonding. However, incorporation of stabilizing elements such as phosphorus, silica, or organic matter can substantially slow these degradation processes.

Capacity loss during cycling results from multiple cumulative mechanisms: (1) incomplete desorption of strongly bound metals, (2) permanent coating of surface sites by partially desorbed organic matter or colloids, (3) gradual oxidation during cycling involving contact with aqueous solution and air, (4) mechanical damage to biochar structure during handling, and (5) in some cases, active site poisoning by byproducts or residual contaminants.

Oxidative aging causes significant losses in surface functional groups, particularly carboxylic acid (-COOH) groups that provide critical coordination sites for metal binding. Research on acid-modified biochars demonstrates severe capacity decline, with HNO_3-modified biochar showing -COOH content reduction from 18.5 mmol g^{-1} initially to 4.3 mmol g^{-1} after 90 wet-dry aging cycles [297]. This functional group loss directly correlated with Cd(II) adsorption capacity decline from 18.15 mg g^{-1} to 4.86 mg g^{-1}, representing 73.3% capacity loss. These findings confirm that long-term stability considerations must be integrated into the design of modified biochars for sustainable environmental applications.

6.3 Scaling from laboratory to field applications

The shift from laboratory experiments to field applications poses a significant challenge in developing modified biochar technology, as reported high adsorption capacities in controlled conditions often do not translate effectively to field settings. This is attributed to complex heterogeneous conditions, variable environmental factors, and the interference of competing ions and organic matter [275]. Real water validation studies have revealed significant performance gaps. For instance, phosphoric acid-modified cocopeat biochar achieved 99% removal efficiency for Cu^{2+} and Ni^{2+} in real wastewater systems, with reusability for up to 20 cycles and a 96.0% desorption rate, demonstrating that modified biochar can perform effectively under practical conditions [286]. Similarly, Mn-Zn ferrite/biochar composite demonstrated removal efficiencies of 97.4-98.5% for Pb^{2+} and 97.3-97.8% for Cd^{2+} in authentic electroplating wastewater, complying with China's battery

industry emission standards [155]. Banana waste biochar showed higher adsorption capacities for real electroplating wastewater compared to chemically modified biochar, indicating that chemical modifications may not be essential for handling complex real wastewaters [298]. This finding highlights the importance of site-specific optimization and the potential limitations of laboratory-derived conclusions.

Pilot-scale and fixed-bed column studies are essential for transitioning from batch experiments to full-scale applications. Seaweed-derived biochar demonstrated removal rates of 90.38% for Cr, 91.23% for Ni, and 89.92% for Zn [299]. Moreover, phosphoric acid-modified cocopeat biochar achieved column adsorption capacities of 794.5 mg g^{-1} for Cu^{2+} and 691.4 mg g^{-1} for Ni^{2+}, significantly outperforming batch capacities, which were 566.6 and 551.7 mg g^{-1}, respectively [286]. This suggests that continuous flow systems improve performance. For practical implementation, the distribution mode of modified biochar within treatment systems significantly affects performance. Mixed distribution ensures more uniform dispersion, optimizes water flow, improves contact efficiency, and minimizes clogging risks. These operational considerations must be addressed when scaling up from laboratory to field-scale applications. For in-situ groundwater remediation, extensive pre-studies on contaminated site properties, hydro-geochemistry, contaminant profiles, aquifer materials, and dispersion of remediation agents are required [275, 300].

Despite promising results, critical challenges remain: most real water studies are at small scales (liters), long-term stability under continuous operation is inadequately understood, economic feasibility lacks systematic evaluation, and no standardized protocols exist for real water testing. Addressing these gaps needs collaborative efforts to establish realistic benchmarks, develop cost-effective production, and conduct long-term field trials. Until then, the industrial-scale application of chemically modified biochar remains limited.

7. Conclusions and future perspectives

The current review comprehensive examination of the critical role of chemical modification in enhancing the performance of pristine biochar for the adsorption of cationic and anionic heavy metal(loid)s from aqueous solutions. Chemical modification techniques, including acid, alkali, oxidation, and metal impregnation, significantly modify the physicochemical properties of pristine biochar. These modifications, such as enhanced specific surface area, improved porosity, and the introduction of functional groups (e.g., carboxyl, hydroxyl, and phosphate), markedly improve the adsorption capacity. Alkali modification (KOH, NaOH) achieved the highest specific surface area enhancement, followed by acid modification and metal impregnation. Oxidant modification showed the smallest SSA increase but effectively introduced oxygen-containing functional groups. Modified biochar demonstrates superior adsorption capacity for both cationic and anionic heavy metals, with maximum reported capacities of 1625.5 mg g^{-1} for Cd(II) ($KHCO_3$/MgO-modified peanut shell), 532.3 mg g^{-1} for Pb(II) ($MgCl_2$-modified coconut shell), 265.3 mg g^{-1} for As(III) (Fe-modified bamboo biochar), and 209.7 mg g^{-1} for Cr(VI) (KOH-modified digestion residue). Metal oxide modification consistently outperformed other methods for Cd, Pb, and Cu (effect sizes: 63.8%, 66.7%, and 58.1%, respectively). The primary adsorption mechanisms vary according to ion type. Cationic heavy metals (e.g., Pb^{2+}, Cd^{2+}, Cu^{2+}, Ni^{2+}, and Hg^0) are mainly adsorbed via precipitation, ion exchange, surface complexation, and cation-π interactions, while anionic species (e.g., Cr(VI), As(V), and Sb(III)) are mainly adsorbed through redox reactions, electrostatic attraction, and co-precipitation dominate. The Fe^{3+}/Fe^{2+} redox cycle plays a key role in iron-modified biochar for metals with variable valences. Chemical regeneration using HCl, NaOH, and EDTA-2Na achieved 80-100% recovery over multiple cycles, though performance declined gradually due to active site loss and pore blockage. However, technical bottlenecks remain for industrial applications, including significant variability in reported adsorption capacities due to non-standardized

testing conditions, lack of long-term stability studies under real wastewater conditions, insufficient life cycle and economic assessments, and limited field-scale validation. Addressing these gaps requires standardized protocols, cost-effective green modification strategies, advanced in-situ characterization, and integrated techno-economic analysis to translate laboratory research into sustainable field applications.

Despite the enormous amount of research and extensive data on the capability of chemically modified biochar for heavy metal adsorption, several significant drawbacks hinder modified biochar from being used practically and economically to remove heavy metals from real wastewater systems. Consequently, the present systematic review offers the following insights and perspectives for future research by conducting a comprehensive and reliable evaluation of relevant literature on the removal of heavy metals using chemically modified biochar, as outlined in **Fig. 19**.

(1) Standardization and field validation: Currently, reported adsorption capacities vary considerably due to inconsistent experimental conditions. Future research must determine minimum reporting standards of biochar characterization such as specific surface area, pore volume, and functional groups density. Reference heavy metal solutions should be adopted for inter-laboratory comparison. Pilot-scale fixed-bed column studies using real industrial wastewater should be conducted for extended continuous operation. Standardized accelerated aging protocols are required to predict long-term field performance. Comprehensive life cycle assessment should be conducted to quantify net environmental benefits.

(2) Green and cost effective modification strategies: The existing chemical modification using KOH, H_3PO_4 and metal salts may produce hazardous wastes and increase the production costs. Future studies should emphasize low-cost agricultural residues for reducing feedstock costs. Closed-loop chemical recovery systems must be established to recycle modification reagents. Bio-assisted synthesis utilizing plant extracts presents a promising

pathway for minimising hazardous chemical usage. These approaches are critical to improve the economic feasibility of modified biochar for industrial applications.

(3) Advanced characterization, modeling, and machine learning: Conventional ex-situ characterization provides only static snapshots. Future research should routinely apply advanced in-situ characterization to monitor real-time adsorption dynamics. Machine learning algorithms should be applied for predicting adsorption efficiency from feedstock properties, pyrolysis conditions, and modification parameters using existing literature data. Open-access databases of modified biochar properties are required to facilitate model development.

(4) Circular economy and multifunctional biochars: Improper disposal of spent modified biochar might lead to secondary pollution concerns. Future research should focus on developing low-cost regeneration methods to maintain high performance over multiple cycles. Safe disposal pathways for non-regenerable spent biochar, including cement production and supercapacitor electrode fabrication, should be investigated. Bifunctional biochars with both adsorption and catalytic degradation capabilities should be developed for complex wastewater containing multiple contaminants. Modified biochars should be evaluated in membrane bioreactors or hybrid treatment systems for continuous operation.

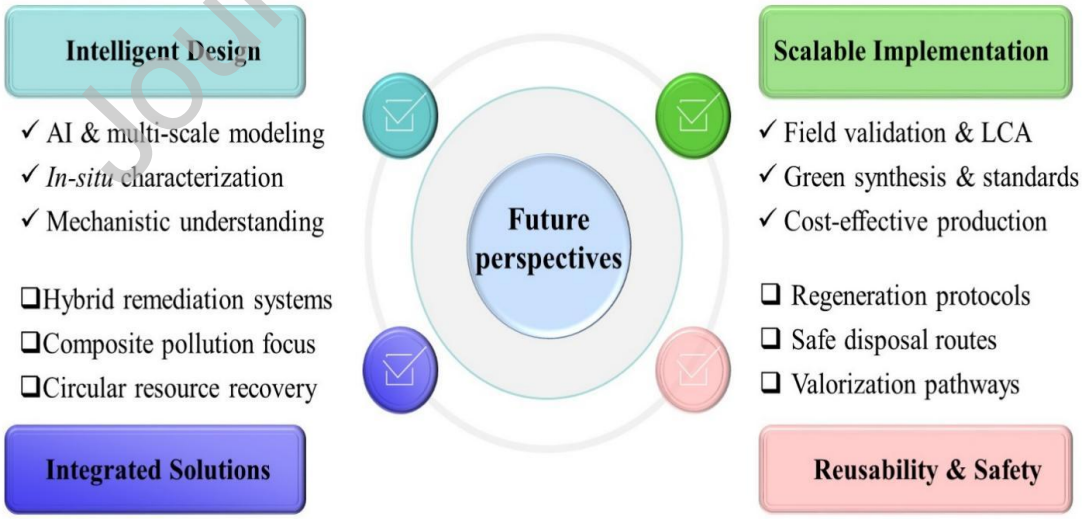

Fig. 19. Summary of the future perspective for the current review article.

CRediT authorship contribution statement

Fatma Abdelrhman: Conceptualization, Writing-original draft, Visualization. **Shri Ram:** Writing – review & editing, Visualization. **Jingmo Zhou:** Writing – review & editing, Visualization. **Ziad Ahmed:** Writing – review & editing, Visualization. **Ehab Mostafa:** Conceptualization, Writing – review & editing, Validation. **Yaning Zhang:** Conceptualization, Supervision, Writing – review & editing, Validation, Funding acquisition.

Declaration of competing interest

The authors declare that they have no known competing financial interests or personal relationships that could have appeared to influence the work reported in this paper.

Acknowledgments

Financial support was provided by Heilongjiang Provincial Key R&D Program "Unveiling the Leader" Project (Grant No. 2023ZXJ02C04), National Natural Science Foundation of China (52476005), Heilongjiang Province "Double First-class" Discipline Collaborative Innovation Achievement Project (Grant No. LJGXCG2023-080), and Heilongjiang Provincial Key R&D Program (Grant No. 2023ZX02C05).

References

[1] X. Mao, Y. Liu, S. Long, Research progress on adsorption mechanisms and regeneration applications of modified biochar for heavy metals in wastewater, Desalin. Water. Treat. 324 (2025) 101399. https://doi.org/10.1016/j.dwt.2025.101399

[2] A. Tomczyk, B. Kondracki, K. Szewczuk-Karpisz, Chemical modification of biochars as a method to improve its surface properties and efficiency in removing xenobiotics from aqueous media, Chemosphere 312 (2023) 137238. https://doi.org/10.1016/j.chemosphere.2022.137238

[3] S. Ray, R. Vashishth, From water to plate: Reviewing the bioaccumulation of heavy metals in fish and unraveling human health risks in the food chain, Emerg. Contam. 10 (2024) 100358. https://doi.org/10.1016/j.emcon.2024.100358

[4] B. Glingasorn, S. Ummartyotin, Synthesis and characterization of carbonaceous materials for lead adsorption, Resour. Chem. Mater. 4 (2025) 100103. https://doi.org/10.1016/j.recm.2025.100103

[5] J.W. Zhang, N.D. Hai, M.A. Kholif, H.P. Chao, Adsorption of heavy metals from water using teak-based carbon material through graft copolymerization, Carbon Resour. Convers. 8 (2025) 100332. https://doi.org/10.1016/j.crcon.2025.100332

[6] H. Elbasiouny, M. Darwesh, H. Elbeltagy, F.G. Abo-Alhamd, A.A. Amer, M.A. Elsegaiy, I.A. Khattab, E.A. Elsharawy, F. Ebehiry, H. El-Ramady, E.C. Brevik, Ecofriendly remediation technologies for wastewater contaminated with heavy metals with special focus on using water hyacinth and black tea wastes: a review, Environ. Monit. Assess. 193 (2021) 449. https://doi:10.1007/s10661-021-09236-2

[7] P. Grenni, A. Barra Caracciolo, L. Mariani, M. Cardoni, C. Riccucci, H. Elhaes, M.A. Ibrahim, Effectiveness of a new green technology for metal removal from contaminated water, Microchem. J. 147 (2019) 1010-1020. https://doi.org/10.1016/j.microc.2019.04.026

[8] L. Lin, G. Zhang, X. Liu, Z.H. Khan, W. Qiu, Z. Song, Synthesis and adsorption of FeMnLa-impregnated biochar composite as an adsorbent for As(III) removal from aqueous solutions, Environ. Pollut. 247 (2019) 128-135. https://doi.org/10.1016/j.envpol.2019.01.044

[9] C.S. Patil, D.B. Gunjal, V.M. Naik, N.S. Harale, S.D. Jagadale, A.N. Kadam, P.S. Patil, G.B. Kolekar, A.H. Gore, Waste tea residue as a low cost adsorbent for removal of hydralazine hydrochloride pharmaceutical pollutant from aqueous media: An environmental remediation, J. Clean. Prod. 206 (2019) 407-418. https://doi.org/10.1016/j.jclepro.2018.09.140

[10] B. Yuan, Q. An, Z. Xiao, J. Hao, K. Zhu, S. Zhai, C.S. Ha, Polyethyleneimine-integrated composite sorbents for emerging pollutants remediation in water: Cross-linking strategy and tailored affinity, Resour. Chem. Mater. 2 (2023) 231-244. https://doi.org/10.1016/j.recm.2023.05.002

[11] M. Tokarčíková, P. Peikertová, K. Čech Barabaszová, O. Životský, R. Gabor, J. Seidlerová, Regeneration possibilities and application of magnetically modified biochar for heavy metals elimination in real conditions, Water. Resour. Ind. 30 (2023). 100219 https://doi.org/10.1016/j.wri.2023.100219

[12] Y. Zheng, P. Cheng, Z. Li, C. Fan, J. Wen, Y. Yu, L. Jia, Efficient removal of gaseous elemental mercury by Fe-UiO-66@BC composite adsorbent: performance evaluation and mechanistic elucidation, Sep. Purif. Technol. 372 (2025) 133463. https://doi.org/10.1016/j.seppur.2025.133463

[13] T.Y.A. Fahmy, Y. Fahmy, F. Mobarak, M. El-Sakhawy, R.E. Abou-Zeid, Biomass pyrolysis: past, present, and future, Environ. Dev. Sustain. 22 (2020) 17-32. https://doi.org/10.1007/s10668-018-0200-5

[14] A.C.A. Zahra, A.M.Y.W. Alahakoon, L. Zhu, T. Prakoso, A. Abudula, G. Guan, Biochar-assisted gasification of raw biomass: a review on the reactivity and synergistic effect on tar reforming, Resour. Chem. Mater. 4 (2025) 100115. https://doi.org/10.1016/j.recm.2025.100115

[15] K. Karin, S. Kuboon, B. Panyapinyopol, S. Youngjan, W. Wanmolee, N. Viriya-empikul, N. Laosiripojana, K. Nakason, Efficient corn stover-derived metal-supported biochar catalyst for hydrogenation of xylose to xylitol, Resour. Chem. Mater. 4 (2025) 100083. https://doi.org/10.1016/j.recm.2024.10.002

[16] Q. Zhou, W. Yang, L. Wang, H. Lu, S. Nie, L. Xu, W. Yang, C. Wei, Biomass carbon materials for high-performance secondary battery electrodes: A review, Resour. Chem. Mater. 3 (2024) 123-145. https://doi.org/10.1016/j.recm.2023.12.002

[17] C. Yao, H. Fan, A. Adogwa, H. Xiong, M. Yang, F. Liu, Z. Chen, Y. Lou, Recent advances in carbon dioxide selective hydrogenation and biomass valorization via single-atom catalysts, Resour. Chem. Mater. 2 (2023) 189-207. https://doi.org/10.1016/j.recm.2023.05.003

[18] R. Janu, V. Mrlik, D. Ribitsch, J. Hofman, P. Sedláček, L. Bielská, G. Soja, Biochar surface functional groups as affected by biomass feedstock, biochar composition and pyrolysis temperature, Carbon Resour. Convers. 4 (2021) 36-46. https://doi.org/10.1016/j.crcon.2021.01.003

[19] M.C. Enebe, R.L. Ray, R.W. Griffin, The impacts of biochar on carbon sequestration, soil processes, and microbial communities: a review, Biochar 7 (2025) 107. https://doi.org/10.1007/s42773-025-00499-3

[20] J. Hylton, A. Hugen, S.M. Rowland, M. Griffin, L.E. Tunstall, Relevant biochar characteristics influencing compressive strength of biochar-cement mortars, Biochar 6 (2024) 87. https://doi.org/10.1007/s42773-024-00375-6

[21] Z. Chen, R. Zheng, W. Wei, W. Wei, W. Zou, J. Li, B.J. Ni, H. Chen, Recycling spent water treatment adsorbents for efficient electrocatalytic water oxidation reaction, Resour. Conserv. Recycl. 178 (2022) 106037. https://doi.org/10.1016/j.resconrec.2021.106037

[22] H.S. Lee, H.S. Shin, Competitive adsorption of heavy metals onto modified biochars: Comparison of biochar properties and modification methods, J. Environ. Manag. 299 (2021) 113651. https://doi.org/10.1016/j.jenvman.2021.113651

[23] Y.A.Y. Abdellah, H.Y. Chen, S.W. Deng, W.T. Li, R.J. Ren, X. Yang, M.S. Rana, S.S. Sun, J.J. Liu, R.L. Wang, Mikania micrantha Kunth and its derived biochar impacts on heavy metal bioavailability and siderophore-related genes during chicken manure composting, Biochar 6 (2024) 56. https://doi.org/10.1007/s42773-024-00347-w

[24] M.H. Eldesouki, U.N. Eldemerdash, M.M. Mohamed, A.A. El-Moneim, Semi-industrial CO and CO_2 conversion with biochar-supported Fe-based catalysts, Carbon Resour. Convers. 9 (2026) 100358. https://doi.org/10.1016/j.crcon.2025.100358

[25] H. Tan, R.A. Wahab, P.Y. Ong, P.S. Goh, K.Y. Wong, J.J. Klemeš, C.T. Lee, Functionalisation of biowaste-derived biochar via accelerated hydrothermal-assisted pre-treatment for enhanced sodium ion adsorption, Biomass. Conv. Bioref. 28 (2022) 1-8. https://doi.org/10.1007/s13399-023-04635-6

[26] Y. Ma, F. Zhang, L. Cheng, D. Zhang, X. Wu, Y. Ma, X. Liu, B. Xing, Remediation potential of biochar for As and Cd by modifying soil physicochemical properties: a conceptual model elucidating stabilization mechanism based on conditional probability theory, Biochar 7 (2025) 63. https://doi.org/10.1007/s42773-025-00455-1

[27] Q. Wang, C. Xu, K. Pan, X. Wu, Y. Pan, C. Duan, Z. Geng, P-modified biochar alters the microbial community in heavy metal-contaminated soils by regulating nutrient supply balance, Biochar 7 (2025) 93. https://doi.org/10.1007/s42773-025-00495-7

[28] J. Wu, T. Wang, J. Wang, Y. Zhang, W.P. Pan, A novel modified method for the efficient removal of Pb and Cd from wastewater by biochar: Enhanced the ion exchange and precipitation capacity, Sci. Total. Environ. 754 (2021) 142150. https://doi.org/10.1016/j.scitotenv.2020.142150

[29] K. Ramesh, V. Raghavan, Agricultural waste-derived biochar-based nitrogenous fertilizer for slow-release applications, ACS Omega 9 (2024) 4377-4385. https://doi.org/10.1021/acsomega.3c06687

[30] S. Teli, S. Soni, P. Teli, S. Agarwal, Recent insights into modified biochars: A half-decade study, J. Mater. Sci. 59 (2024) 18357-18394. https://doi.org/10.1007/s10853-024-10272-9

[31] Y. Hamid, L. Liu, M. Usman, R. Naidu, M. Haris, Q. Lin, Z. Ulhassan, M.I. Hussain, X. Yang, Functionalized biochars: Synthesis, characterization, and applications for removing trace elements from water, J. Hazard. Mater. 437 (2022) 129337. https://doi.org/10.1016/j.jhazmat.2022.129337

[32] W.H. Huang, D.J. Lee, C. Huang, Modification on biochars for applications: A research update, Bioresour. Technol. 319 (2021) 124100. https://doi.org/10.1016/j.biortech.2020.124100

[33] A. Kumari, M. Yadav, A. Bhatia, M. Sharma, R. Bhateria, A review and bibliometric analysis on recent modification of biochar for effective and sustainable remediation of heavy metals in aqueous medium, Discov. Chem. Eng. 5 (2025) 21. https://doi.org/10.1007/s43938-025-00088-7

[34] G. Ravindiran, S. Rajamanickam, G. Janardhan, G. Hayder, A. Alagumalai, O. Mahian, S.S. Lam, C. Sonne, Production and modifications of biochar to engineered materials and its application for environmental sustainability: a review, Biochar 6 (2024) 62. https://doi.org/10.1007/s42773-024-00350-1

[35] R. Kumar Mishra, B. Singh, B. Acharya, A comprehensive review on activated carbon from pyrolysis of lignocellulosic biomass: An application for energy and the environment, Carbon Resour. Convers. 7 (2024) 100228. https://doi.org/10.1016/j.crcon.2024.100228

[36] D. Gurtner, J.O. Back, D. Bosch, A. Hofmann, C. Pfeifer, Renewable activated carbon from wood-based gasification char: A comprehensive study on physical activation, Carbon Resour. Convers. 8 (2025) 100310. https://doi.org/10.1016/j.crcon.2025.100310

[37] K. Vijayaraghavan, Recent advancements in biochar preparation, feedstocks, modification, characterization and future applications, Environ. Technol. Rev. 8 (2019) 47-64. https://doi.org/10.1080/21622515.2019.1631393

[38] P.M. Godwin, Y. Pan, H. Xiao, M.T. Afzal, Progress in Preparation and Application of Modified Biochar for Improving Heavy Metal Ion Removal From Wastewater, J. Bioresour. Bioprod. 4 (2019) 31-42. https://doi.org/10.21967/jbb.v4i1.180

[39] T. Qiu, W. Cao, K. Xie, F. Ahmad, W. Zhao, E. Mostafa, Y. Zhang, CO_2 capture performances of H_3PO_4/KOH activated microwave pyrolyzed porous biochar, Sustain. Carbon. Mater. 1 (2025). https://doi.org/10.48130/scm-0025-0004

[40] K.L. Sefatlhi, V.U. Ultra, S. Majoni, Chemical and Structural characteristics of biochars from phytoremediation biomass of cymbopogon citratus, cymbopogon nardus, and chrysopogon zizanioides, Waste. Biomass. Valor. 15 (2024) 283-300. https://doi.org/10.1007/s12649-023-02164-x

[41] R.K. Sharma, T. Singh, S. Mandal, D. Azad, S. Kumar, Chemical treatments for biochar modification: opportunities, limitations and advantages, In: S. Ramola, D. Mohan, O. Masek, A. Méndez, T. Tsubota (Eds.), Engineered biochar: fundamentals, preparation, characterization and applications, Springer, 2022, pp. 65-84.

[42] Z. Liu, Z. Xu, L. Xu, F. Buyong, T.C. Chay, Z. Li, Y. Cai, B. Hu, Y. Zhu, X. Wang, Modified biochar: synthesis and mechanism for removal of environmental heavy metals, Carbon Res. 1 (2022) 1. https://doi:10.1007/s44246-022-00007-3

[43] V. Dodevski, M. Marinović-Cincović, B. Janković, Tailoring textural properties of activated carbon produced from Plane tree (Platanus) seeds using alkali (NaOH) activation with improved post-activation treatment procedure for environmental and energy applications, Carbon Resour. Convers. (2025) 100377. https://doi.org/10.1016/j.crcon.2025.100377

[44] G. Chu, J. Zhao, Y. Huang, D. Zhou, Y. Liu, M. Wu, H. Peng, Q. Zhao, B. Pan, C.E.W. Steinberg, Phosphoric acid pretreatment enhances the specific surface areas of biochars by generation of micropores, Environ. Pollu. 240 (2018) 1-9. https://doi.org/10.1016/j.envpol.2018.04.003

[45] N. Zhao, C. Zhao, Y. Lv, W. Zhang, Y. Du, Z. Hao, J. Zhang, Adsorption and coadsorption mechanisms of Cr(VI) and organic contaminants on H_3PO_4 treated biochar, Chemosphere 186 (2017) 422-429. https://doi.org/10.1016/j.chemosphere.2017.08.016

[46] H. Xu, Q. Zhou, T. Yan, X. Jia, D. Lu, Y. Ren, J. He, Enhanced removal efficiency of Cd^{2+} and Pb^{2+} from aqueous solution by H_3PO_4–modified tea branch biochar: Characterization, adsorption performance and mechanism, J. Environ. Chem. Eng. 12 (2024) 112183. https:// doi.org/10.1016/j.jece.2024.112183

[47] K. Szewczuk-Karpisz, P. Nowicki, Z. Sokołowska, R. Pietrzak, Hay-based activated biochars obtained using two different heating methods as effective low-cost sorbents: Solid surface characteristics, adsorptive properties and aggregation in the mixed Cu(II)/PAM system, Chemosphere 250 (2020) 126312. https://doi.org/10.1016/j.chemosphere.2020.126312

[48] Y. Nie, C. Zhao, Z. Zhou, Y. Kong, J. Ma, Hydrochloric acid-modified fungi-microalgae biochar for adsorption of tetracycline hydrochloride: Performance and mechanism, Bioresour. Technol. 383 (2023) 129224. https://doi:10.1016/j.biortech.2023.129224

[49] T. Wang, J. Wu, Y. Zhang, J. Liu, Z. Sui, H. Zhang, W.Y. Chen, P. Norris, W.P. Pan, Increasing the chlorine active sites in the micropores of biochar for improved mercury adsorption, Fuel 229 (2018) 60-67. https://doi.org/10.1016/j.fuel.2018.05.028

[50] C. Liu, W. Wang, R. Wu, Y. Liu, X. Lin, H. Kan, Y. Zheng, Preparation of Acid- and Alkali-Modified Biochar for Removal of Methylene Blue Pigment, ACS Omega 5 (2020) 30906-30922. https://doi.org/10.1021/acsomega.0c03688

[51] T. Chen, L. Luo, S. Deng, G. Shi, S. Zhang, Y. Zhang, O. Deng, L. Wang, J. Zhang, L. Wei, Sorption of tetracycline on H_3PO_4 modified biochar derived from rice straw and swine manure, Bioresour. Technol. 267 (2018) 431-437. https://doi.org/10.1016/j.biortech.2018.07.074

[52] C. Peiris, O. Nayanathara, C.M. Navarathna, Y. Jayawardhana, S. Nawalage, G. Burk, et al, The influence of three acid modifications on the physicochemical characteristics of tea-waste biochar pyrolyzed at different temperatures: a comparative study, RSC. Adv. 9 (2019) 17612-17622. https://doi.org/10.1039/C9RA02729G

[53] Y. Tang, Y. Li, L. Zhan, D. Wu, S. Zhang, R. Pang, B. Xie, Removal of emerging contaminants (bisphenol A and antibiotics) from kitchen wastewater by alkali-modified biochar, Sci. Total. Environ. 805 (2022) 150158. https://doi.org/10.1016/j.scitotenv.2021.150158

[54] S.M. Yakout, Monitoring the Changes of Chemical Properties of Rice Straw–Derived Biochars Modified by Different Oxidizing Agents and Their Adsorptive Performance for Organics, Bioremediat. J. 19 (2015) 171-182. https://doi.org/10.1080/10889868.2015.1029115

[55] L. Zhao, W. Zheng, O. Mašek, X. Chen, B. Gu, B.K. Sharma, X. Cao, Roles of phosphoric acid in biochar formation: synchronously improving carbon retention and sorption capacity, J. Environ. Qual. 46 (2017) 393-401. https://doi.org/10.2134/jeq2016.09.0344

[56] S.M. Taha, M.E. Amer, A.E. Elmarsafy, M.Y. Elkady, Adsorption of 15 different pesticides on untreated and phosphoric acid treated biochar and charcoal from water, J. Environ. Chem. Eng. 2 (2014) 2013-2025. https://doi.org/10.1016/j.jece.2014.09.001

[57] S. Rungrodnimitchai, S. Hiranphinyophat, The functionalization of activated carbon by oxidation, Key. Eng. Mater. 846 (2020) 251-256. https://doi.org/10.4028/www.scientific.net/kem.846.251

[58] X. Rong, Q. Cao, Y. Gao, X. Du, H. Dou, M. Yan, S. Li, Q. Wang, Z. Zhang, B. Chen, Performance optimization and kinetic analysis of HNO_3 coupled with microwave rapidly modified coconut shell activated carbon for VOCs adsorption, Front. Environ. Res. 10 (2023) 1047254. https://doi.org/10.3389/fenrg.2022.1047254

[59] B. Sajjadi, T. Zubatiuk, D. Leszczynska, J. Leszczynski, W.Y. Chen, Chemical activation of biochar for energy and environmental applications: a comprehensive review, Rev. Chem. Eng. 35 (2019) 777-815. https://doi.org/10.1515/revce-2018-0003

[60] Y. Wang, J. Miao, M. Saleem, Y. Yang, Q. Zhang, Enhanced adsorptive removal of carbendazim from water by $FeCl_3$-modified corn straw biochar as compared with pristine, HCl and NaOH modification, J. Environ. Chem. Eng. 10 (2022) 107024. https://doi.org/10.1016/j.jece.2021.107024

[61] G. Murtaza, Z. Ahmed, M. Valipour, I. Ali, M. Usman, R. Iqbal, U. Zulfiqar, M. Rizwan, S. Mahmood, A. Ullah, Recent trends and economic significance of modified/functionalized biochars for remediation of environmental pollutants. Sci. Rep. 14 (2024): 217,. https://doi.org/10.1038/s41598-023-50623-1

[62] K. Chin, C. Lee, P. H'ng, U. Rashid, M. Paridah, P. Khoo, M. Maminski, Refining micropore capacity of activated carbon derived from coconut shell via deashing post-treatment, BioRes. 15 (2020) 7749-7769. https://doi.org/10.15376/biores.15.4.7749-7769

[63] M.S. Hafizuddin, C.L. Lee, K.L. Chin, S. H'Ng P, P.S. Khoo, U. Rashid, Fabrication of Highly Microporous Structure Activated Carbon via Surface Modification with Sodium Hydroxide, Polymers 13 (2021) 3954. https://doi.org/10.3390/polym13223954

[64] H. Chen, X. Yang, Y. Liu, X. Lin, J. Wang, Z. Zhang, N. Li, Y. Li, Y. Zhang, KOH modification effectively enhances the Cd and Pb adsorption performance of N-enriched biochar derived from waste chicken feathers, Waste Manag. 130 (2021) 82-92. https:// doi.org/10.1016/j.wasman.2021.05.015

[65] Z. Liu, F. Zhen, Q. Zhang, X. Qian, W. Li, Y. Sun, L. Zhang, B. Qu, Nanoporous biochar with high specific surface area based on rice straw digestion residue for efficient adsorption of mercury ion from water, Bioresour. Technol. 359 (2022) 127471. https://doi.org/10.1016/j.biortech.2022.127471

[66] R. Rostamian, M. Heidarpour, S.F. Mousavi, M. Afyuni, Characterization and sodium sorption capacity of biochar and activated carbon prepared from rice hus, J Agr Sci Tech 17 (2018) 1057-1069.

[67] J.J. Lado, R.L. Zornitta, F.A. Calvi, M. Martins, M.A. Anderson, F.G. Nogueira, L.A Ruotolo, Enhanced capacitive deionization desalination provided by chemical activation of sugar cane bagasse fly ash electrodes, J. Anal. Appl. Pyrolysis. 126 (2017) 143-153. https://doi.org/10.1016/j.jaap.2017.06.014

[68] H. Wang, X. Wang, H. Teng, J. Xu, L. Sheng, Purification mechanism of city tail water by constructed wetland substrate with NaOH-modified corn straw biochar, Ecotoxicol. Environ. Saf. 238 (2022) 113597. https://doi.org/10.1016/j.ecoenv.2022.113597

[69] M. Arif, G. Liu, M. Zia-ur-Rehman, Q. Abbas, A. Ashraf, M.S. Rashid, K. Pikon, B. Yousaf, High-performance clay and K_2CO_3-Modified sludge biochar for efficient reactive black-5 Removal: Mechanistic insights and alleviation of phytotoxicity, Biomass Bioenergy 202 (2025) 108235. https://doi.org/10.1016/j.biombioe.2025.108235

[70] P. Liu, W.J. Liu, H. Jiang, J.J. Chen, W.W. Li, H.Q. Yu, Modification of bio-char derived from fast pyrolysis of biomass and its application in removal of tetracycline from aqueous solution, Bioresourc. Technology 121 (2012) 235-240. https://doi.org/10.1016/j.biortech.2012.06.085

[71] A. Herath, C.A. Layne, F. Perez, E.I.B. Hassan, C.U. Pittman, T.E. Mlsna, KOH-activated high surface area Douglas Fir biochar for adsorbing aqueous Cr(VI), Pb(II) and Cd(II), Chemosphere 269 (2021) 128409. https://doi.org/10.1016/j.chemosphere.2020.128409

[72] Z. Bao, C. Shi, W. Tu, L. Li, Q.J.E.P. Li, Recent developments in modification of biochar and its application in soil pollution control and ecoregulation, Environ. Pollut. 313 (2022) 120184. https://doi.org/10.1016/j.envpol.2022.120184

[73] X. Xu, G. Fan, X. Zhu, Y. Huang, X. Chen, The Removal of Lead and Cadmium from Solution by K_2CO_3 activated biochar derived from corn straw/spent mushroom substrate/hardwood sawdust, Water Air Soil Pollu. 236 (2024) 10. https://doi.org/10.1007/s11270-024-07653-w

[74] M. Irfan, Q. Chen, Y. Yue, R. Pang, Q. Lin, X. Zhao, H. Chen, Co-production of biochar, bio-oil and syngas from halophyte grass (Achnatherum splendens L.) under three different pyrolysis temperatures, Bioresour. Technol. 211 (2016) 457-463. https://doi.org/10.1016/j.biortech.2016.03.077

[75] A.R.A. Usman, A. Abduljabbar, M. Vithanage, Y.S. Ok, M. Ahmad, M. Ahmad, J. Elfaki, S.S. Abdulazeem, M.I. Al-Wabel, Biochar production from date palm waste:

Charring temperature induced changes in composition and surface chemistry, J. Anal. Appl. Pyrolysis 115 (2015) 392-400. https://doi.org/10.1016/j.jaap.2015.08.016

[76] X. Zhu, Y. Liu, C. Zhou, G. Luo, S. Zhang, J. Chen, A novel porous carbon derived from hydrothermal carbon for efficient adsorption of tetracycline, Carbon 77 (2014) 627-636. https://doi.org/10.1016/j.carbon.2014.05.067

[77] M. Chen, F. He, D. Hu, C. Bao, Q. Huang, Broadened operating pH range for adsorption/reduction of aqueous Cr(VI) using biochar from directly treated jute (Corchorus capsularis L.) fibers by H_3PO_4, Chem. Eng. J. 381 (2020) 122739. https://doi.org/10.1016/j.cej.2019.122739

[78] Q. Huang, D. Hu, M. Chen, C. Bao, X. Jin, Sequential removal of aniline and heavy metal ions by jute fiber biosorbents: A practical design of modifying adsorbent with reactive adsorbate, J. Mol. Liq. 285 (2019) 288-298. https://doi.org/10.1016/j.molliq.2019.04.115

[79] J.H. Khan, F. Marpaung, C. Young, J. Lin, M.T. Islam, S.M. Alsheri, T. Ahamad, N. Alhokbany, K. Ariga, L.K. Shrestha, Y. Yamauchi, K.C.W. Wu, M.S.A. Hossain, J. Kim, Jute-derived microporous/mesoporous carbon with ultra-high surface area using a chemical activation process, Microporous Mesoporous Mater. 274 (2019) 251-256. https://doi.org/10.1016/j.micromeso.2018.07.050

[80] J. Qu, Y. Wang, X. Tian, Z. Jiang, F. Deng, Y. Tao, Q. Jiang, L. Wang, Y. Zhang, KOH-activated porous biochar with high specific surface area for adsorptive removal of chromium (VI) and naphthalene from water: Affecting factors, mechanisms and reusability exploration, J. Hazard. Mater. 401 (2021) 123292. https://doi.org/10.1016/j.jhazmat.2020.123292

[81] M.J. Valero-Romero, F.J. García-Mateos, J. Rodríguez-Mirasol, T. Cordero, Role of surface phosphorus complexes on the oxidation of porous carbons, Fuel Process. Technol. 157 (2017) 116-126. https://doi.org/10.1016/j.fuproc.2016.11.014

[82] M.D. Huff, J.W. Lee, Biochar-surface oxygenation with hydrogen peroxide, J. Environ. Manag. 165 (2016) 17-21. https://doi.org/10.1016/j.jenvman.2015.08.046

[83] D. Zhang, B. Wu, T. Wang, M. Yılmaz, G. Sharma, A. Kumar, H. Shi, Multi-mechanism synergistic adsorption of lead and cadmium in water by structure-functionally adapted modified biochar: A review, Desalin. Water Treat. 322 (2025) 101156. https://doi.org/10.1016/j.dwt.2025.101156

[84] Y. Xue, B. Gao, Y. Yao, M. Inyang, M. Zhang, A.R. Zimmerman, K.S. Ro, Hydrogen peroxide modification enhances the ability of biochar (hydrochar) produced from hydrothermal carbonization of peanut hull to remove aqueous heavy metals: Batch and column tests, Chem. Eng. J. 200-202 (2012) 673-680. https://doi.org/10.1016/j.cej.2012.06.116

[85] S.H. Wang, P.R. Griffiths, Resolution enhancement of diffuse reflectance ir spectra of coals by Fourier self-deconvolution: 1. CH stretching and bending modes, Fuel 64 (1985) 229-236. https://doi.org/10.1016/0016-2361(85)90223-6

[86] J. Shin, M. Choi, C.Y. Go, S. Bae, K.C. Kim, K. Chon, NaOH-assisted H_2O_2 post-modification as a novel approach to enhance adsorption capacity of residual coffee waste biochars toward radioactive strontium: Experimental and theoretical studies, J. Hazard. Mater. 435 (2022) 129081. https://doi.org/10.1016/j.jhazmat.2022.129081

[87] H. Wang, B. Gao, S. Wang, J. Fang, Y. Xue, K. Yang, Removal of Pb (II), Cu (II), and Cd (II) from aqueous solutions by biochar derived from $KMnO_4$ treated hickory wood, Bioresour. Technol. 197 (2015) 356-362. https://doi.org/10.1016/j.biortech.2015.08.132

[88] S. Bian, S. Xu, Z. Yin, S. Liu, J. Li, S. Xu, Y. Zhang, An efficient strategy for enhancing the adsorption capabilities of biochar via sequential $KMnO_4$-promoted oxidative pyrolysis and H_2O_2 oxidation, Sustain. 13 (2021) 2641. https://doi.org/10.3390/su13052641

[89] A. Cibati, B. Foereid, A. Bissessur, S. Hapca, Assessment of Miscanthus × giganteus derived biochar as copper and zinc adsorbent: Study of the effect of pyrolysis temperature, pH and hydrogen peroxide modification, J. Clean. Prod. 162 (2017) 1285-1296. https://doi.org/10.1016/j.jclepro.2017.06.114

[90] S. Mia, F.A. Dijkstra, B. Singh, Aging induced changes in biochar's functionality and adsorption behavior for phosphate and ammonium, Environ. Sci. Technol. 51 (2017) 8359-8367. https://doi:10.1021/acs.est.7b00647

[91] K. Yin, J. Wang, S. Zhai, X. Xu, T. Li, S. Sun, S. Xu, X. Zhang, C. Wang, Y. Hao, Adsorption mechanisms for cadmium from aqueous solutions by oxidant-modified biochar derived from *Platanus orientalis* Linn leaves, J. Hazard. Mater. 428 (2022) 128261. https://doi.org/10.1016/j.jhazmat.2022.128261

[92] I. Ali, A. El-Hamed, H. Salem, A. Hallawa, Removal efficiency of Cd from aqueous solution by H_2O_2 and $KMnO_4$ modified biochar derived from orange and pea shells, Ann. Agri. Sci. Moshtohor 62 (2024). https://doi.org/10.21608/assjm.2024.279299.1272

[93] M.A. El-Nemr, N.M. Abdelmonem, I.M.A. Ismail, S. Ragab, A. El Nemr, Ozone and ammonium hydroxide modification of biochar prepared from *pisum sativum* peels improves the adsorption of copper (II) from an aqueous medium, Environ. Process. 7 (2020) 973-1007. https://doi:10.1007/s40710-020-00455-2

[94] Y. Li, H. Yin, Y. Cai, H. Luo, C. Yan, Z. Dang, Regulating the exposed crystal facets of α-Fe_2O_3 to promote Fe_2O_3-modified biochar performance in heavy metals adsorption, Chemosphere 311 (2023) 136976. https://doi.org/10.1016/j.chemosphere.2022.136976

[95] C. Liu, H.X. Zhang, Modified-biochar adsorbents (MBAs) for heavy-metal ions adsorption: A critical review, Jo. Environ. Chem. Eng. 10 (2022) 107393. https://doi.org/10.1016/j.jece.2022.107393

[96] G. Zhao, K. Ning, M. Wei, L. Zhang, L. Han, G. Zhu, J. Yang, H. Wang, F. Huang, Fabrication and Enhanced Supercapacitive Performance of Fe_2N@Cotton-based Porous Carbon fibers as Electrode Material, Resour. Chem. Mater. 2 (2023) 277-287. https://doi.org/10.1016/j.recm.2023.07.005

[97] Y. Wang, Y. Wen, W. Su, W. Fu, C.H. Wang, Carbon deposition behavior on biochar during chemical vapor deposition process, Chem. Eng. J. 485 (2024) 149726. https://doi.org/10.1016/j.cej.2024.149726

[98] J. Wang, S. Wang, Preparation, modification and environmental application of biochar: A review, J. Clean. Prod. 227 (2019) 1002-1022. https://doi.org/10.1016/j.jclepro.2019.04.282

[99] T. Sizmur, T. Fresno, G. Akgül, H. Frost, E. Moreno-Jiménez, Biochar modification to enhance sorption of inorganics from water, Bioresour. Technol 246 (2017) 34-47. https://doi.org/10.1016/j.biortech.2017.07.082

[100] M. Haris, Z. Amjad, M. Usman, A. Saleem, A. Dyussenova, Z. Mahmood, K. Dina, J. Guo, W. Wang, A review of crop residue-based biochar as an efficient adsorbent to remove trace elements from aquatic systems, Biochar 6 (2024) 47. https://doi.org/10.1007/s42773-024-00341-2

[101] C. Li, L. Zhang, Y. Gao, A. Li, Facile synthesis of nano ZnO/ZnS modified biochar by directly pyrolyzing of zinc contaminated corn stover for Pb(II), Cu(II) and Cr(VI) removals, Waste Manag. 79 (2018) 625-637. https://doi.org/10.1016/j.wasman.2018.08.035

[102] S.M. Shaheen, A. Mosa, A. El-Naggar, M.F. Hossain, H. Abdelrahman, N.K. Niazi, M. Shahid, T. Zhang, Y.F. Tsang, et al, Manganese oxide-modified biochar: production, characterization and applications for the removal of pollutants from aqueous environments-a review, Bioresour. Technol. 346 (2022) 126581. https://doi.org/10.1007/s42773-024-00407-1

[103] A.Y. Li, H. Deng, Y.H. Jiang, C.H. Ye, B.G. Yu, X.L. Zhou, A.Y. Ma, Superefficient Removal of heavy metals from wastewater by Mg-loaded biochars: Adsorption characteristics and removal Mechanisms, Langmuir 36 (2020) 9160-9174. https://doi.org/10.1021/acs.langmuir.0c01454

[104] X. Xu, T. Yang, F. Li, S. Ji, J. Zhao, Y. Huo, J. Liu, Recent advances in zinc-based chalcogenides for potassium ion batteries, Resour. Chem. Mater. 3 (2024) 279-293. https://doi.org/10.1016/j.recm.2023.08.002

[105] J. Nandhini, E. Karthikeyan, S. Rajeshkumar, Green synthesis of zinc oxide nanoparticles: Eco-friendly advancements for biomedical marvels, Resour. Chem. Mater. 3 (2024) 294-316. https://doi.org/10.1016/j.recm.2024.05.001

[106] D. Bosch, J.O. Back, D. Gurtner, S. Giberti, A. Hofmann, A. Bockreis, Alternative feedstock for the production of activated carbon with $ZnCl_2$: Forestry residue biomass and waste wood, Carbon Resour. Convers. 5 (2022) 299-309. https://doi.org/10.1016/j.crcon.2022.09.001

[107] H. Chen, G. Yurong, J. Li, Z. Fang, N. Bolan, A. Bhatnagar, B. Gao, D. Hou, S. Wang, H. Song, X. Yang, S. Shaheen, J. Meng, W. Chen, J. Rinklebe, H. Wang, Engineered biochar for environmental decontamination in aquatic and soil systems: a review, Carbon Res. 1 (2022) 4. https://doi.org/10.1007/s44246-022-00005-5

[108] Q. Huang, S. Song, Z. Chen, B. Hu, J. Chen, X.J.B. Wang, Biochar-based materials and their applications in removal of organic contaminants from wastewater: state-of-the-art review, Biochar 1 (2019) 45-73. https://doi.org/10.1007/s42773-019-00006-5

[109] E. Wen, X. Yang, H. Chen, S.M. Shaheen, B. Sarkar, S. Xu, H. Song, Y. Liang, J. Rinklebe, et al, Iron-modified biochar and water management regime-induced changes in plant growth, enzyme activities, and phytoavailability of arsenic, cadmium and lead in a paddy soil, J. Hazard. Mater. 407 (2021) 124344. https://doi.org/10.1016/j.jhazmat.2020.124344

[110] H. Lyu, J. Tang, M. Cui, B. Gao, B. Shen, Biochar/iron (BC/Fe) composites for soil and groundwater remediation: synthesis, applications, and mechanisms, Chemosphere 246 (2020) 125609. https://doi.org/10.1016/j.chemosphere.2019.125609

[111] X. Li, X. Zhang, P. Zhang, X. Wang, H. Sun, Y. Lu, L. Jiao, C. Liu, Incorporation of N-doped biochar into zero-valent iron for efficient reductive degradation of neonicotinoids: mechanism and performance, Biochar 5 (2023) 78. https://doi.org/10.1007/s42773-023-00280-4

[112] L. Luo, J. Li, A. James, C. Hu, G. Zhang, J. Pan, Effective removal of nitrate nitrogen from water and soil using biochar-loaded nano zero-valent iron: performance and mechanisms, Biochar 7 (2025) 117. https://doi.org/10.1007/s42773-025-00516-5

[113] P. Cheng, Z.K. Li, Y.L. Zheng, Q. Meng, Y. Yu, Y. Jin, X.F. Gao, X.M. Guo, L. Jia, Study on the regulation of performance and Hg0 removal mechanism of MIL-101(Fe)-derived carbon materials, Sep. Purif. Technol.379 (2025) 134939. https://doi.org/10.1016/j.seppur.2025.134939

[114] S. Zhu, T. Qu, M.K. Irshad, J.J.B. Shang, Simultaneous removal of Cd (II) and As (III) from co-contaminated aqueous solution by α-FeOOH modified biochar, 2 (2020) 81-92. https://doi.org/10.1007/s42773-020-00040-8

[115] Z.H. Khan, M. Gao, W. Qiu, M.S. Islam, Z. Song, Mechanisms for cadmium adsorption by magnetic biochar composites in an aqueous solution, Chemosphere 246 (2020) 125701. https://doi.org/10.1016/j.chemosphere.2019.125701

[116] J. Zhou, J. He, G. Li, T. Wang, D. Sun, X. Ding, J. Zhao, S.J. Wu, Direct incorporation of magnetic constituents within ordered mesoporous carbon−silica nanocomposites for highly efficient electromagnetic wave absorbers, J. Phys. Chem. 114 (2010) 7611-7617. https://doi.org/10.1021/jp911030n

[117] X. Jia, J. Zhou, J. Liu, P. Liu, L. Yu, B. Wen, Y. Feng, The antimony sorption and transport mechanisms in removal experiment by Mn-coated biochar, Sci. Total. Environ. 724 (2020) 138158. https://doi.org/10.1016/j.scitotenv.2020.138158

[118] S. Wang, B. Gao, Y. Li, A. Mosa, A.R. Zimmerman, L.Q. Ma, W.G. Harris, K.W. Migliaccio, Manganese oxide-modified biochars: Preparation, characterization, and sorption of arsenate and lead, Bioresour. Technol. 181 (2015) 13-17. https://doi.org/10.1016/j.biortech.2015.01.044

[119] Q. Zheng, L. Yang, D. Song, S. Zhang, H. Wu, S. Li, X. Wang, High adsorption capacity of Mg–Al-modified biochar for phosphate and its potential for phosphate interception in soil, Chemosphere 259 (2020) 127469. https://doi:10.1016/j.chemosphere.2020.127469

[120] H. Pan, X. Yang, H. Chen, B. Sarkar, N. Bolan, S.M. Shaheen, F. Wu, L. Che, Y. Ma, J. Rinklebe, H. Wang, Pristine and iron-engineered animal- and plant-derived biochars enhanced bacterial abundance and immobilized arsenic and lead in a contaminated soil, Sci. Total. Environ. 763 (2021) 144218. https://doi.org/10.1016/j.scitotenv.2020.144218

[121] X. Yang, S.M. Shaheen, J. Wang, D. Hou, Y.S. Ok, S.L. Wang, H. Wang, J. Rinklebe, Elucidating the redox-driven dynamic interactions between arsenic and iron-impregnated

biochar in a paddy soil using geochemical and spectroscopic techniques, J. Hazard. Mater. 422 (2022) 126808. https://doi.org/10.1016/j.jhazmat.2021.126808

[122] L. Lin, Z. Li, X. Liu, W. Qiu, Z. Song, Effects of Fe-Mn modified biochar composite treatment on the properties of As-polluted paddy soil, Environ. Pollut. 244 (2019) 600-607. https://doi:10.1016/j.envpol.2018.10.011

[123] V. Nguyen Van, M. Zafar, S. Behera, H.s. Park, Arsenic(III) removal from aqueous solution by raw and Zinc-loaded pine cone biochar: Equilibrium, kinetics and thermodynamics studies, Int. J. Environ. Sci. Technol. 12 (2014). https://doi:10.1007/s13762-014-0507-1

[124] R. Li, W. Liang, J.J. Wang, L.A. Gaston, D. Huang, H. Huang, S. Lei, M.K. Awasthi, B. Zhou, R. Xiao, Z. Zhang, Facilitative capture of As(V), Pb(II) and methylene blue from aqueous solutions with MgO hybrid sponge-like carbonaceous composite derived from sugarcane leafy trash, J. Environ. Manag. 212 (2018) 77-87. https://doi.org/10.1016/j.jenvman.2017.12.034

[125] M. Hawryluk-Sidoruk, M. Raczkiewicz, P. Krasucka, W. Duan, O. Mašek, R. Zarzycki, R. Kobyłecki, B. Pan, P. Oleszczuk, Effect of biochar chemical modification (acid, base and hydrogen peroxide) on contaminants content depending on feedstock and pyrolysis conditions, Chem. Eng. J. 481 (2024) 148329. https://doi.org/10.1016/j.cej.2023.148329

[126] J. Zuo, W. Li, Z. Xia, T. Zhao, C. Tan, et al, Preparation of modified biochar and its adsorption of Cr(VI) in aqueous solution, Coatings 11 (2023), 1884. https://doi.org/10.3390/coatings13111884

[127] B. Wang, B. Gao, J. Fang, Recent advances in engineered biochar productions and applications, Crit. Rev. Environ. Sci. Technol. 47 (2018) 1-50. https//doi.org/10.1080/10643389.2017.1418580

[128] S. Ambika, M. Kumar, L. Pisharody, M. Malhotra, G. Kumar, V. Sreedharan et al, Modified biochar as a green adsorbent for removal of hexavalent chromium from various environmental matrices: mechanisms, methods, and prospects, Chem. Eng. J. 439 (2022) 135716. https://doi.org/10.1016/j.cej.2022.135716

[129] A. Hafeez, T. Pan, J. Tian, K. Cai, Modified Biochars and Their Effects on Soil Quality: A Review, Environ. Sci. Pollut. Res. 9 (2022) 60. https://doi.org/10.1007/s11356-021-17645-2

[130] M. Chen, F. Wang, D.L. Zhang, W.M. Yi, Y. Liu, Effects of acid modification on the structure and adsorption $NH4^{+}$-N properties of biochar, Renew. Energy 169 (2021) 1343-1350. https://doi.org/10.1016/j.renene.2021.01.098

[131] S. Zhou, H. Li, Z. Wu, S. Li, Z. Cao, B. B. Ma, Y. Zou, N. Zhang, Z. Liu, Y. Wang, X. Liao, Y. Wu, The addition of nano zero-valent iron during compost maturation effectively removes intracellular and extracellular antibiotic resistance genes by reducing the abundance of potential host bacteria, Bioresour. Technol. 384 (2023) 129350. https://doi.org/10.1016/j.biortech.2023.129350

[132] T. Xu, R. Gao, Y. Yan, J. Fang, S. Ding, Application of modified biochar in constructed wetlands for efficient livestock wastewater treatment, Environ. Res. 286 (2025) 122917. https://doi.org/10.1016/j.envres.2025.122917

[133] Y. Yi, Z. Huang, B. Lu, J. Xian, E.P. Tsang, W. Cheng, J. Fang, Z. Fang, Magnetic biochar for environmental remediation: A review, Bioresour. Technol. 298 (2020) 122468. https://doi.org/10.1016/j.biortech.2019.122468

[134] K. Yin, J. Wang, X. Tian, N. Yu, X. Zhang, Y. Zhao, Y. Liu, S. Sui, C. Wang, F. Lian, S. Zhai, X. Li, B. Xing, Effect of biochar-derived dissolved organic matter on tetracycline sorption by $KMnO_4$-modified biochar, Chem. Eng. J. 474 (2023) 145872. https://doi.org/10.1016/j.cej.2023.145872

[135] Q. Jin, J. Cui, Fungi-enabled hierarchical porous magnetic carbon derived from biomass for efficient remediation of As(iii)-contaminated water and soil: performance and mechanism, Environ. Sci. Nano 10 (2023) 1297-1312. https://doi.org/10.1039/d2en01027e

[136] Y. Mei, S. Zhuang, J. Wang, Adsorption of heavy metals by biochar in aqueous solution: A review, Sci. Total Environ. 968 (2025) 178898. https://doi:10.1016/j.scitotenv.2025.178898

[137] S. Chen, M. Zhong, H. Wang, S. Zhou, W. Li, T. Wang, J. Li, Study on adsorption of Cu^{2+}, Pb^{2+}, Cd^{2+}, and Zn^{2+} by the $KMnO_4$ modified biochar derived from walnut shell, Int. J. Environ. Sci. Technol. 20 (2023) 1551-1568. https://doi.org/10.1007/s13762-022-04002-4

[138] K. Iamsaard, C.H. Weng, J.H. Tzeng, J. Anotai, A.R. Jacobson, Y.T. Lin, Systematic optimization of biochars derived from corn wastes, pineapple leaf, and sugarcane bagasse for Cu(II) adsorption through response surface methodology, Bioresour. Technol. 382 (2023) 129131. https://doi.org/10.1016/j.biortech.2023.129131

[139] P. Premchand, F. Demichelis, C. Galletti, D. Chiaramonti, S. Bensaid, E. Antunes, D. Fino, Enhancing biochar production: A technical analysis of the combined influence of chemical activation (KOH and NaOH) and pyrolysis atmospheres (N_2/CO_2) on yields and properties of rice husk-derived biochar, J. Environ. Manag. 370 (2024) 123034. https://doi.org/10.1016/j.jenvman.2024.123034

[140] T. Sun, P. Pei, Y. Sun, Y. Xu, H. Jia, Performance and mechanism of As(III/V) removal from aqueous solution by novel positively charged animal-derived biochar, Sep. Purif. Technol. 290 (2022) 120836. https://doi.org/10.1016/j.seppur.2022.120836

[141] Y. He, X. Jia, S. Zhou, J. Chen, S. Zhang, X. Li, Y. Huang, T. Wågberg, G. Hu, Separatable MoS_2 loaded biochar/$CaCO_3$/Alginate gel beads for selective and efficient

removal of Pb(II) from aqueous solution, Sep. Purif. Technol. 303 (2022) 122212. https://doi.org/10.1016/j.seppur.2022.122212

[142] H. Lin, D. Yang, C. Zhang, W. Liu, L. Zhang, Y. Dong, Selective removal behavior of lead and cadmium from calcium-rich solution by MgO loaded soybean straw biochars and mechanism analysis, Chemosphere 319 (2023) 138010. https://doi.org/10.1016/j.chemosphere.2023.138010

[143] L. Sun, P. Gong, Y. Sun, Q. Qin, K. Song, J. Ye, H. Zhang, B. Zhou, Y. Xue, Modified chicken manure biochar enhanced the adsorption for Cd^{2+} in aqueous and immobilization of Cd in contaminated agricultural soil, Sci. Total. Environ. 851 (2022) 158252. https://doi.org/10.1016/j.scitotenv.2022.158252

[144] H. Roh, M.R. Yu, K. Yakkala, J.R. Koduru, J.K. Yang, Y.Y. Chang, Removal studies of Cd(II) and explosive compounds using buffalo weed biochar-alginate beads, J. Ind. Eng. Chem. 26 (2015) 226-233. https://doi.org/10.1016/j.jiec.2014.11.034

[145] Z. Feng, N. Chen, T. Liu, C. Feng, $KHCO_3$ activated biochar supporting MgO for Pb(II) and Cd(II) adsorption from water: Experimental study and DFT calculation analysis, J. Hazard. Mater. 426 (2022) 128059. https://doi.org/10.1016/j.jhazmat.2021.128059

[146] Y. Ke, F. Zhang, Z. Zhang, R. Hough, Q. Fu, Y.F. Li, S. Cui, Effect of combined aging treatment on biochar adsorption and speciation distribution for Cd(II), Sci. Total Environ. 867 (2023) 161593. https://doi.org/10.1016/j.scitotenv.2023.161593

[147] Q. Shi, H. Zhang, A. Shahab, H. Zeng, H. Zeng, A.U.R. Bacha, I. Nabi, J. Siddique, H. Ullah, Efficient performance of magnesium oxide loaded biochar for the significant removal of Pb^{2+} and Cd^{2+} from aqueous solution, Ecotoxicol. Environ. Saf. 221 (2021) 112426. https://doi.org/10.1016/j.ecoenv.2021.112426

[148] Y. Gao, W. Gao, H. Zhu, H. Chen, S. Yan, M. Zhao, H. Sun, J. Zhang, S. Zhang, A review on N-doped biochar for oxidative degradation of organic contaminants in wastewater by persulfate activation, Int. J. Environ. Res. Public Health 19 (2022) 14805. https://doi.org/10.3390/ijerph192214805

[149] K. Yoon, D.-W. Cho, A. Bhatnagar, H. Song, Adsorption of As(V) and Ni(II) by Fe-Biochar composite fabricated by co-pyrolysis of orange peel and red mud, Environ. Res. 188 (2020) 109809. https://doi.org/10.1016/j.envres.2020.109809

[150] Q. An, Y.Q. Jiang, H.Y. Nan, Y. Yu, J.N. Jiang, Unraveling sorption of nickel from aqueous solution by $KMnO_4$ and KOH-modified peanut shell biochar: Implicit mechanism, Chemosphere 214 (2019) 846-854. https://doi.org/10.1016/j.chemosphere.2018.10.007

[151] A. Li, Y. Zhang, W. Ge, Y. Zhang, L. Liu, G. Qiu, Removal of heavy metals from wastewaters with biochar pyrolyzed from MgAl-layered double hydroxide-coated rice husk: Mechanism and application, Bioresour. Technol. 347 (2022) 126425. https://doi.org/10.1016/j.biortech.2021.126425

[152] D.B. Salem, A. Ouakouak, F. Touahra, N. Hamdi, A.S. Eltaweil, A. Syed, R. Boopathy, H.N. Tran, Easy separable, floatable, and recyclable magnetic-biochar/alginate bead as super-adsorbent for adsorbing copper ions in water media, Bioresour. Technol. 383 (2023) 129225. https://doi.org/10.1016/j.biortech.2023.129225

[153] X. Qian, R. Wang, Q. Zhang, Y. Sun, W. Li, L. Zhang, B. Qu, A delicate method for the synthesis of high-efficiency Hg (II) The adsorbents based on biochar from corn straw biogas residue, J. Clean. Prod. 355 (2022) 131819. https://doi.org/10.1016/j.jclepro.2022.131819

[154] S. Wan, J. Wu, S. Zhou, R. Wang, B. Gao, F. He, Enhanced lead and cadmium removal using biochar-supported hydrated manganese oxide (HMO) nanoparticles: Behavior and

mechanism, Sci. Total Environ. 616-617 (2018) 1298-1306. https://doi.org/10.1016/j.scitotenv.2017.10.188

[155] Z. Niu, W. Feng, H. Huang, B. Wang, L. Chen, Y. Miao, S.J.C. Su, Green synthesis of a novel Mn–Zn ferrite/biochar composite from waste batteries and pine sawdust for Pb^{2+} removal, Chemosphere 252 (2020) 126529. https://doi.org/10.1016/j.chemosphere.2020.126529

[156] T.M.A. Babeker, M.N. Khalil, E. Fayad, D.S. Alshaya, F.G. Elsaid, I.A. Elhassan, Superior Cu (II) purification using carrageenan biochar-olivine composite: Synergistic effects of K (I), Mg (II), Fe (II/ III), and Si (IV), Environ. Res. 285 (2025) 122282. https://doi.org/10.1016/j.envres.2025.122282

[157] M. Ghorbani, E. Amirahmadi, Optimizing biochar for heavy metal remediation: A meta-analysis of modification methods and pyrolysis conditions, Environ. 12 (2025) 399. https://doi.org/10.3390/environments12110399

[158] B. Cao, J. Qu, Y. Yuan, W. Zhang, X. Miao, X. Zhang, Y. Xu, T. Han, H. Song, S. Ma, X. Tian, Y. Zhang, Efficient scavenging of aqueous Pb(II)/Cd(II) by sulfide-iron decorated biochar: Performance, mechanisms and reusability exploration, J. Environ. Chem. Eng. 10 (2022) 107531. https://doi.org/10.1016/j.jece.2022.107531

[159] Y. Li, S.M. Shaheen, M. Azeem, L. Zhang, C. Feng, J. Peng, W. Qi, J. Liu, Y. Luo, Y. Peng, E.F. Ali, K. Smith, J. Rinklebe, Z. Zhang, R. Li, Removal of lead (Pb^{+2}) from contaminated water using a novel MoO3-biochar composite: Performance and mechanism, Environ. Pollut. 308 (2022) 119693. https://doi.org/10.1016/j.envpol.2022.119693

[160] Q. Wang, C.J. Duan, C.Y. Xu, Z.C. Geng, Efficient removal of Cd(II) by phosphate-modified biochars derived from apple tree branches: Processes, mechanisms, and application, Sci. Total Environ. 819 (2022) 152876. https://doi.org/10.1016/j.scitotenv.2021.152876

[161] D. Sun, F. Li, J. Jin, S. Khan, K.M. Eltohamy, M. He, X. Liang, Qualitative and quantitative investigation on adsorption mechanisms of Cd(II) on modified biochar derived from co-pyrolysis of straw and sodium phytate, Sci. Total Environ. 829 (2022) 154599. https://doi.org/10.1016/j.scitotenv.2022.154599

[162] B. Liu, Z. Zhang, D.X. Guan, B. Wang, S. Zhou, T. Chen, J. Wang, Y. Li, B. Gao, Qualitative and quantitative analysis for Cd^{2+} removal mechanisms by biochar composites from co-pyrolysis of corn straw and fly ash, Chemosphere 330 (2023) 138701. https://doi.org/10.1016/j.chemosphere.2023.138701

[163] W. Ahmed, T. Xu, M. Mahmood, A. Núñez-Delgado, S. Ali, A. Shakoor, M. Qaswar, H. Zhao, W. Liu, W. Li, S. Mehmood, Nano-hydroxyapatite modified biochar: Insights into the dynamic adsorption and performance of lead (II) removal from aqueous solution, Environ. Res. 214 (2022) 113827. https://doi.org/10.1016/j.envres.2022.113827

[164] T. Chen, X. Wen, X. Li, J. He, B. Yan, Z. Fang, L. Zhao, Z. Liu, L. Han, Single/co-adsorption and mechanism of methylene blue and lead by β-cyclodextrin modified magnetic alginate/biochar, Bioresour. Technol. 381 (2023) 129130. https://doi.org/10.1016/j.biortech.2018.07.074

[165] X. Jiang, X. Yin, Y. Tian, S. Zhang, Y. Liu, Z. Deng, Y. Lin, L. Wang, Study on the mechanism of biochar loaded typical microalgae Chlorella removal of cadmium, Sci. Total Environ. 813 (2022) 152488. https://doi.org/10.1016/j.scitotenv.2021.152488

[166] S. Wei, Y. Tao, M. Ma, W. Tong, F. Bi, L. Wang, J. Qu, Y. Zhang, One-step microwave-assisted synthesis of MgO-modified magnetic biochar for enhanced removal of lead and phosphate from wastewater: Performance and mechanisms, Sep. Purif. Technol. 354 (2025) 128936. https://doi.org/10.1016/j.seppur.2024.128936

[167] I. Ahmad, U. Farwa, Z.U.H. Khan, M. Imran, M.S. Khalid, B. Zhu, A. Rasool, G.M. Shah, M. Tahir, M. Ahmed, S. Rezapour, L. Bulgariu, Biosorption and health risk

assessment of arsenic contaminated water through cotton stalk biochar, Surf. Interfaces 29 (2022) 101806. https://doi.org/10.1016/j.surfin.2022.101806

[168] G. Yan, Y. Gao, K. Xue, Y. Qi, Y. Fan, X. Tian, J. Wang, R. Zhao, P. Zhang, Y. Liu, J. Liu, Toxicity mechanisms and remediation strategies for chromium exposure in the environment, Fron. Environ. Sci. 11 (2023) 113120. https://doi.org/10.3389/fenvs.2023.1131204

[169] S.S. Raut, D. Kumari, S. Singh, D. Pandey, A. Daverey, K. Dutta, Fabrication of different magnetic biochar from Citrus limetta peels for Cr (VI) adsorption: Characterisation, and performance, Resour. Chem. Mater. 4 (2025) 100118. https://doi.org/10.1016/j.recm.2025.100118

[170] X. Zhang, S. Wu, Y. Liu, Z. Wang, H. Zhang, R. Xiao, Removal of Cr(VI) from aqueous solution by Rice-husk-based activated carbon prepared by Dual-mode heating method, Carbon Resour. Convers. 6 (2023) 76-84. https://doi.org/10.1016/j.crcon.2023.01.003

[171] S.M. Shaheen, H. Ullah, Y. Wu, A. Mosa, Y. Fang, et al, Remediation of emerging inorganic contaminants in soils and water using pristine and engineered biochar: a review, Biochar 7 (2025) 34. https://doi.org/10.1007/s42773-024-00407-1

[172] H. Jin, S. Capareda, Z. Chang, J. Gao, Y. Xu, J. Zhang, Biochar pyrolytically produced from municipal solid wastes for aqueous As(V) removal: Adsorption property and its improvement with KOH activation, Bioresour. Technol. 169 (2014) 622-629. https://doi.org/10.1016/j.biortech.2014.06.103

[173] A. Nawaz, B. Singh, P. Kumar, H_3PO_4-modified Lagerstroemia speciosa seed hull biochar for toxic Cr(VI) removal: isotherm, kinetics, and thermodynamic study, Biomass Conv. Bioref. 13 (2023) 7027-7041. https://doi:10.1007/s13399-021-01780-8

[174] V.K. Jaiswal, A.D. Gupta, R. Kushwaha, R. Kumar, K. Singh, H. Singh, D. Mohan, R.S. Singh, Arsenic removal from water using an acid-modified biochar, J. Mol. Struct. 1324 (2025) 140904. https://doi.org/10.1016/j.molstruc.2024.140904

[175] R. Kushwaha, R.S. Singh, D. Mohan, Comparative study for sorption of arsenic on peanut shell biochar and modified peanut shell biochar, Bioresour. Technol. 375 (2023) 128831. https://doi.org/10.1016/j.biortech.2023.128831

[176] Y. Peng, M. Azeem, R. Li, L. Xing, Y. Li, Y. Zhang, Z. Guo, Q. Wang, H.H. Ngo, G. Qu, Z. Zhang, Zirconium hydroxide nanoparticle encapsulated magnetic biochar composite derived from rice residue: Application for As(III) and As(V) polluted water purification, J. Hazard. Mater. 423 (2022) 127081. https://doi.org/10.1016/j.jhazmat.2021.127081

[177] P. Lyu, L. Li, X. Huang, G. Wang, C. Zhu, Pre-magnetic bamboo biochar cross-linked CaMgAl layered double-hydroxide composite: High-efficiency removal of As(III) and Cd(II) from aqueous solutions and insight into the mechanism of simultaneous purification, Sci. Total Environ. 823 (2022) 153743. https://doi.org/10.1016/j.scitotenv.2022.153743

[178] S. Wang, B. Gao, Y. Li, A.E. Creamer, F. He, Adsorptive removal of arsenate from aqueous solutions by biochar supported zero-valent iron nanocomposite: Batch and continuous flow tests, J. Hazard. Mater. 322 (2017) 172-181. https://doi.org/10.1016/j.jhazmat.2016.01.052

[179] L. Lin, Z. Song, Y. Huang, Z.H. Khan, W. Qiu, Removal and Oxidation of Arsenic from Aqueous Solution by Biochar Impregnated with Fe-Mn Oxides, Water Air Soil Pollut. 230 (2019) 105. https://doi.org/10.1007/s11270-019-4146-5

[180] N. Zhu, T. Yan, J. Qiao, H. Cao, Adsorption of arsenic, phosphorus and chromium by bismuth impregnated biochar: Adsorption mechanism and depleted adsorbent utilization, Chemosphere 164 (2016) 32-40. https://doi.org/10.1016/j.chemosphere.2016.08.036

[181] M. Masuku, J.F. Nure, H.I. Atagana, N. Hlongwa, T.T.I. Nkambule, Advancing the development of nanocomposite adsorbent through zinc-doped nickel ferrite-pinecone biochar for removal of chromium (VI) from wastewater, Sci. Total Environ. 908 (2024) 168136. https://doi.org/10.1016/j.scitotenv.2023.168136

[182] H. Zhou, M. Ye, Y. Zhao, S.A. Baig, N. Huang, M. Ma, Sodium citrate and biochar synergistic improvement of nanoscale zero-valent iron composite for the removal of chromium (VI) in aqueous solutions, J. Environ. Sci. 115 (2022) 227-239. https://doi.org/10.1016/j.jes.2021.05.044

[183] K.Z. Benis, J. Soltan, K.N. McPhedran, A novel method for fabrication of a binary oxide biochar composite for oxidative adsorption of arsenite: characterization, adsorption mechanism and mass transfer modeling, J. Clean. Prod. 356 (2022) 131832. https://doi.org/10.1016/j.jclepro.2022.131832

[184] M. Vithanage, I. Herath, S. Joseph, J. Bundschuh, N. Bolan, Y.S. Ok, M.B. Kirkham, J. Rinklebe, Interaction of arsenic with biochar in soil and water: A critical review, Carbon 113 (2017) 219-230. https://doi.org/10.1016/j.carbon.2016.11.032

[185] I. Herath, M. Vithanage, J. Bundschuh, J.P. Maity, P. Bhattacharya, Natural Arsenic in Global Groundwaters: Distribution and Geochemical Triggers for Mobilization, Curr. Pollut. Rep. 2 (2016) 68-89. https://doi.org/10.1007/s40726-016-0028-2

[186] X. Guo, A. Liu, J. Lu, X. Niu, M. Jiang, Y. Ma, X. Liu, M. Li, Adsorption Mechanism of Hexavalent Chromium on Biochar: Kinetic, Thermodynamic, and Characterization Studies, ACS Omega 5 (2020) 27323-27331. https://doi:10.1021/acsomega.0c03652

[187] Y.P. Wang, Y.L. Liu, S.Q. Tian, J.J. Yang, L. Wang, J. Ma, Straw biochar enhanced removal of heavy metal by ferrate, J. Hazard. Mater. 416 (2021) 126128. https://doi.org/10.1016/j.jhazmat.2021.126128

[188] I.M. Kenawy, M.A.H. Hafez, M.A. Ismail, M.A. Hashem, Adsorption of Cu(II), Cd(II), Hg(II), Pb(II) and Zn(II) from aqueous single metal solutions by guanyl-modified cellulose, Int. J. Biol. Macromol. 107 (2018) 1538-1549. https://doi.org/10.1016/j.ijbiomac.2017.10.017

[189] J. Zhao, X.J. Shen, X. Domene, J.M. Alcañiz, X. Liao, C. Palet, Comparison of biochars derived from different types of feedstock and their potential for heavy metal removal in multiple-metal solutions, Sci. Rep. 9 (2019) 9869. https://doi.org/10.1038/s41598-019-46234-4

[190] M. Zahedifar, N. Seyedi, S. Shafiei, M. Basij, Surface-modified magnetic biochar: Highly efficient adsorbents for removal of Pb(II) and Cd(II), Mater. Chem. Phys. 271 (2021) 124860. https://doi.org/10.1016/j.matchemphys.2021.124860

[191] J. Liang, X. Li, Z. Yu, G. Zeng, Y. Luo, L. Jiang, Z. Yang, Y. Qian, H. Wu, Amorphous MnO_2 modified biochar derived from aerobically composted swine manure for adsorption of Pb(II) and Cd(II), ACS Sustain. Chem. Eng. 5 (2017) 5049-5058. https://doi.org/10.1021/acssuschemeng.7b00434

[192] Z. Ding, X. Hu, Y. Wan, S. Wang, B. Gao, Removal of lead, copper, cadmium, zinc, and nickel from aqueous solutions by alkali-modified biochar: Batch and column tests, J. Ind. Eng. Chem. 33 (2016) 239-245. https://doi.org/10.1016/j.jiec.2015.10.007

[193] Y. Yu, X. Chen, L. Zhao, S. He, L. Feng, W. Zhao, H. Mu, Q. Zhao, L. Wei, Effects of metal oxides loaded with biochar on adsorption of cationic and anionic metals: A meta-analysis, J. Environ. Manag. 392 (2025) 126771. https://doi.org/10.1016/j.jenvman.2025.126771

[194] Z.A. Ganie, N. Khandelwal, A. Choudhary, G.K. Darbha, Clean water production from plastic and heavy metal contaminated waters using redox-sensitive iron nanoparticle-loaded biochar, Environ. Res. 235 (2023) 116605. https://doi.org/10.1016/j.envres.2023.116605

[195] Y. Li, S. Wang, X.F. Ouyang, Z. Dang, H. Yin, Acetate anions intercalated Fe/Mg-layered double hydroxides modified biochar for efficient adsorption of anionic and cationic heavy metal ions from polluted water, Chemosphere 362 (2024) 142652. https://doi.org/10.1016/j.chemosphere.2024.142652

[196] J. Wu, D. Huang, X. Liu, J. Meng, C. Tang, J. Xu, Remediation of As(III) and Cd(II) co-contamination and its mechanism in aqueous systems by a novel calcium-based magnetic biochar, J. Hazard. Mater. 348 (2018) 10-19. https://doi.org/10.1016/j.jhazmat.2018.01.011

[197] M. Yu, Y. Sun, W. Shi, C. Zhang, X. Wang, Preparation of Fe-doped Biochar and Its Adsorption Performance for Ni^{2+} and Co^{2+} Metal Ions, Chin. J. Mater. Res. 38 (2024) 849-860. https://doi.org/10.11901/1005.3093.2023.571

[198] J. Wu, T. Wang, Y. Zhang, W.P. Pan, The distribution of Pb (II)/Cd (II) adsorption mechanisms on biochars from aqueous solution: Considering the increased oxygen functional groups by HCl treatment, Bioresour. Technol. 291 (2019) 121859. https://doi.org/10.1016/j.biortech.2019.121859

[199] R. Wang, M.L. Klein, V. Carnevale, E. Borguet, Investigations of water/oxide interfaces by molecular dynamics simulations, WIREs Comput. Mol. Sci. 11 (2021) e1537. https://doi.org/10.1002/wcms.1537

[200] L. Ramrakhiani, S. Ghosh, S. Sarkar, S. Majumdar, Heavy metal biosorption in multi component system on dried activated sludge: investigation of adsorption mechanism by

surface characterization, Mater. Today Proc. 3 (2016) 3538-3552. https://doi.org/10.1016/j.matpr.2016.10.036

[201] Q. Fan, J. Sun, L. Chu, L. Cui, G. Quan, et al, Effects of chemical oxidation on surface oxygen-containing functional groups and adsorption behavior of biochar, Chemosphere 207 (2018) 33-40. https://doi.org/10.1016/j.chemosphere.2018.05.044

[202] X. Jing, X. Chen, M. Zhang, X. Xu, Preparation of polypyrrole/titanium nitride composite modified biochar and its application research in microbial fuel cells, RSC Adv. 15 (2025) 6089-6099. https://doi.org/10.1039/D4RA08808E

[203] H. Xiong, L. Han, H. Zhang, K. Song, Z. Yang, A Micro-CT Approach for 3D In-Situ Visualizing the Cu (II) adsorption in corn cob biochar, Water Air Soil Pollut. 234 (2022) 2. https://doi.org/10.1007/s11270-022-06014-9

[204] D. Yang, W. Fang, H. Chen, H. Sun, X. Liu, J. Luo, Acid rain triggers chromium re-mobilization in iron-biochar remediated industrial soils: Microscale insights from in situ imaging, Environ. Pollut. 397 (2026) 127937. https://doi.org/10.1016/j.envpol.2026.127937

[205] H. Zhang, W. Zhong, R. Qiu, L. Han, Kinetics and modeling of Pb (II) adsorption in pellet biochar based on micro-computed tomography characterization, Bioresour. Technol. 387 (2023) 129645. https://doi.org/10.1016/j.biortech.2023.129645

[206] A.M. Egorin, S.A. Novikova, I.D. Priymak, Y.O. Privar, A.V. Brikmans, et al, Valorization of birch biochar: An efficient and sustainable solution for lead decontamination of water, Biomass 5 (2025) 75. https://doi.org/10.3390/biomass5040075

[207] D. Luo, Z. Tang, X. Yu, T. Zhang, C.R. Chang, Z. Hu, Revealing the ZrO_2 crystal effect of Pd/ZrO_2 catalyst for toluene combustion: A combined DRIFTS and DFT study, Appl. Catal. B: Environ. 339 (2023) 123117. https://doi.org/10.1016/j.apcatb.2023.123117

[208] Z. Sun, H. Zhou, J. Hou, F. Shen, X. Guo, L. Dai, In-situ DRIFTS insights into the evolution of surface functionality of biochar upon thermal air oxidation, J. Environ. Manag. 370 (2024) 122582. https://doi.org/10.1016/j.jenvman.2024.122582

[209] M. Fan, C. Li, Y. Sun, L. Zhang, S. Zhang, X. Hu, In situ characterization of functional groups of biochar in pyrolysis of cellulose, Sci. Total. Environ. 799 (2021) 149354. https://doi.org/10.1016/j.scitotenv.2021.149354

[210] N. Chen, S. Cao, L. Zhang, X. Peng, X. Wang, et al, Structural dependent Cr(VI) adsorption and reduction of biochar: hydrochar versus pyrochar, Sci. Total. Environ. 783 (2021) 147084. https://doi.org/10.1016/j.scitotenv.2021.147084

[211] D. Sasongko, D. Gunawan, A.J.H.o.A. Indarto, A.E.S.R. Technology, Biochar-based Water Treatment Systems for Clean Water Provision, Enhanced Sustain. Rem. Technol. 6 (2021) 77-101. https://doi.org/10.1002/9781119670391.ch4

[212] A.A.H. Saeed, N.Y. Harun, S. Sufian, M.R. Bilad, Z.Y. Zakaria, A.H. Jagaba et al, Pristine and magnetic kenaf fiber biochar for Cd^{2+} adsorption from aqueous solution, Environ. Res. Public Health 18 (2021) 7949. https://doi.org/10.3390/ijerph18157949

[213] X. Wang, Z. Guo, Z. Hu, J. Zhang, Recent advances in biochar application for water and wastewater treatment: a review, Peer J. 8 (2020) e9164. https://doi.org/10.7717/peerj.9164

[214] S.M. Ndirangu, Y. Liu, K. Xu, S.J.J.o.C. Song, Risk evaluation of pyrolyzed biochar from multiple wastes, J. Chem. 2019 (2019) 4506314. https://doi.org/10.1155/2019/4506314

[215] Y. Wu, Z. Wang, Y. Yan, Y. Zhou, B. Huma, Z. Tan, T. Zhou, Recovery and regeneration of water-hardened magnetic composite biochar sphere for the removal of multiple heavy metals in contaminated soils, J. Clean. Prod. 450 (2024) 141906. https://doi.org/10.1016/j.jclepro.2024.141906

[216] Y. Wu, Y. Yan, Z. Wang, Z. Tan, T. Zhou, Biochar application for the remediation of soil contaminated with potentially toxic elements: Current situation and challenges, J. Environ. Manag. 351 (2024) 119775. https://doi.org/10.1016/j.jenvman.2023.119775

[217] L. Jia, P. Cheng, Y. Yu, S.H. Chen, C.X. Wang, L. He, H.T. Nie, J.C. Wang, J.C. Zhang, B.G. Fan, Y. Jin, Regeneration mechanism of a novel high-performance biochar mercury adsorbent directionally modified by multimetal multilayer loading, J. Environ. Manag. 326 (2023) 116790. https:doi.org/10.1016/j.jenvman.2022.116790

[218] M.O. Omorogie, J.O. Babalola, E.I. Unuabonah, Regeneration strategies for spent solid matrices used in adsorption of organic pollutants from surface water: a critical review, Desalin. Water Treat. 57 (2016) 518-544. https://doi.org/10.1080/19443994.2014.967726

[219] P. Gao, Z. Tan, Y. Yan, M. Yang, S. Han, C. Yang, S. Li, Y. Zhang, Preparation of $ZnCl_{(2)}$-Activated Magnetic Biochar and Its Performance in Removing Hexavalent Chromium from Water, Nanomaterials 15 (2025). https://doi.org/10.3390/nano15201586

[220] M. Choudhary, R. Kumar, S. Neogi, Activated biochar derived from *Opuntia ficus-indica* for the efficient adsorption of malachite green dye, Cu^{+2} and Ni^{+2} from water, J. Hazard. Mater. 392 (2020) 122441. https://doi.org/10.1016/j.jhazmat.2020.122441

[221] C. Gan, Y. Liu, X. Tan, S. Wang, G. Zeng, B. Zheng, T. Li, Z. Jiang, W. Liu, Effect of porous zinc–biochar nanocomposites on Cr(vi) adsorption from aqueous solution, RSC Adv. 5 (2015) 35107-35115. https://doi.org/10.1039/c5ra04416b

[222] A.G. Karunanayake, O.A. Todd, M. Crowley, L. Ricchetti, C.U. Pittman, R. Anderson, D. Mohan, T. Mlsna, Lead and cadmium remediation using magnetized and nonmagnetized biochar from Douglas fir, Chem. Eng. J. 331 (2018) 480-491. https:doi.org/10.1016/j.cej.2017.08.124

[223] R. Gayathri, K. Gopinath, P.S.J.C. Kumar, Adsorptive separation of toxic metals from aquatic environment using agro waste biochar: Application in electroplating industrial

wastewater, Chemosphere 262 (2021) 128031. https://doi.org/10.1016/j.chemosphere.2020.128031

[224] S.Y. Wang, Y.K. Tang, C. Chen, J.T. Wu, Z. Huang, Y.Y. Mo, K.X. Zhang, J.B. Chen, Regeneration of magnetic biochar derived from eucalyptus leaf residue for lead (II) removal, Bioresour. Technol. 186 (2015) 360-364. https://doi.org/10.1016/j.biortech.2015.03.139

[225] Q. Wu, C.Y. Dong, M. Chen, Y. Zhang, M. Cai, Y. Chen, M. Jin, Z. Wei, Silica enhanced activation and stability of Fe/Mn decorated sludge biochar composite for tetracycline degradation, Chemosphere (2023) 138614. https://doi.org/10.1016/j.chemosphere.2023.138614

[226] Y. Ma, M. Li, P. Li, L. Yang, L. Wu, F. Gao, X. Qi, Z. Zhang, Hydrothermal synthesis of magnetic sludge biochar for tetracycline and ciprofloxacin adsorptive removal, Bioresour. Technol. 319 (2021) 124199. https://doi.org/10.1016/j.biortech.2020.124199

[227] T. Alsawy, E. Rashad, M. El-Qelish, R.H. Mohammed, A comprehensive review on the chemical regeneration of biochar adsorbent for sustainable wastewater treatment, npj Clean Water 5 (2022) 29. https://doi.org/10.1038/s41545-022-00172-3

[228] Q. Miao, G. Li, Potassium phosphate/magnesium oxide modified biochars: Interfacial chemical behaviours and Pb binding performance, Sci. Total. Environ. 759 (2021) 143452. https://doi.org/10.1016/j.scitotenv.2020.143452

[229] L. Gao, Z. Li, W. Yi, Y. Li, P. Zhang, A. Zhang, L. Wang, Impacts of pyrolysis temperature on lead adsorption by cotton stalk-derived biochar and related mechanisms, J. Environ. Chem. Eng. 9 (2021) 105602. https://doi.org/10.1016/j.jece.2021.105602

[230] J. Liu, H. Liu, X. Yang, X. Jia, M. Cai, Y. Bao, Preparation of Si–Mn/biochar composite and discussions about characterizations, advances in application and adsorption

mechanisms, Chemosphere 281 (2021) 130946. https://doi.org/10.1016/j.chemosphere.2021.130946

[231] M. Imran, M.M. Iqbal, J. Iqbal, N.S. Shah, Z.U.H. Khan, B. Murtaza, M. Amjad, S. Ali, M. Rizwan, Synthesis, characterization and application of novel MnO and CuO impregnated biochar composites to sequester arsenic (As) from water: Modeling, thermodynamics and reusability, J. Hazard. Mater. 401 (2021) 123338. https://doi.org/10.1016/j.jhazmat.2020.123338

[232] J. Hu, G. Chen, I.M. Lo, Removal and recovery of Cr(VI) from wastewater by maghemite nanoparticles, Water Res. 39 (2005) 4528-4536. https://doi.org/10.1016/j.watres.2005.05.051

[233] C.A. Odega, O.O. Ayodele, S.O. Ogutuga, G.T. Anguruwa, A.E. Adekunle, C.O. Fakorede, Potential application and regeneration of bamboo biochar for wastewater treatment: A review, Adv. Bamboo Sci. 2 (2023) 100012. https://doi:10.1016/j.bamboo.2022.100012

[243] D. Xu, M. Zhang, W. Yang, T. Liu, Q. Yao, Y.J.C.I. Hong, E. Progress, Preparation of alumina modified sludge biocharcoal particles and their adsorption characteristics for Pb (II), Chem. Ind. Eng. Pro. 39 (2020) 1153. https://doi.org/10.16085/j.issn.1000-6613.2019-1003

[235] X. Cui, J. Wang, X. Wang, G. Du, K.Y. Khan, B. Yan, Z. Cheng, G. Chen, Pyrolysis of exhausted hydrochar sorbent for cadmium separation and biochar regeneration, Chemosphere 306 (2022) 135546. https://doi.org/10.1016/j.chemosphere.2022.135546

[236] A.R. Altaf, H. Teng, L. Gang, Y.G. Adewuyi, M. Zheng, Effect of Sonochemical Treatment on Thermal Stability, Elemental Mercury (Hg^0) Removal, and Regenerable Performance of Magnetic Tea Biochar, ACS Omega 6 (2021) 23913-23923. https://doi.org/10.1021/acsomega.1c02925

[237] Renu, T. Sithole, A review on regeneration of adsorbent and recovery of metals: Adsorbent disposal and regeneration mechanism, S. Afr. J. Chem. Eng. 50 (2024) 39-50. https://doi.org/10.1016/j.sajce.2024.07.0064.07.006

[238] S. Liu, M. Li, Y. Liu, N. Liu, X. Tan, L. Jiang, J. Wen, X. Hu, Z. Yin, Removal of 17β-estradiol from aqueous solution by graphene oxide supported activated magnetic biochar: Adsorption behavior and mechanism, J. Taiwan Inst. Chem. Eng. 102 (2019) 330-339. https://doi.org/10.1016/j.jtice.2019.05.002

[239] X. Chen, S. Jiang, J. Wu, X. Yi, G. Dai, Y. Shu, Three-year field experiments revealed the immobilization effect of natural aging biochar on typical heavy metals (Pb, Cu, Cd), Sci. Total Environ. 912 (2024) 169384. https://doi.org/10.1016/j.scitotenv.2023.169384

[240] H. Xia, H. Wang, Y. Zhang, Fabrication and application of magnetic $MgFe_2O_4$-OH@biochar composites decorated with β-ketoenamine for Pb(II) and Cd(II) adsorption and immobilization from aqueous solution, Sep. Purif. Technol. 354 (2025) 129320. https://doi.org/10.1016/j.seppur.2024.129320

[241] A.A. Oladipo, E.O. Ahaka, M. Gazi, High adsorptive potential of calcined magnetic biochar derived from banana peels for Cu^{2+}, Hg^{2+}, and Zn^{2+} ions removal in single and ternary systems, Environ. Sci. Pollut. Res. 26 (2019) 31887-31899. https://doi.org/10.1007/s11356-019-06321-5

[242] I.S. Bădescu, D. Bulgariu, I. Ahmad, L. Bulgariu, Valorisation possibilities of exhausted biosorbents loaded with metal ions – A review, J. Environ. Manag. 224 (2018) 288-297. https://doi.org/10.1016/j.jenvman.2018.07.066

[243] R. Fernández-González, M.A. Martín-Lara, J.A. Moreno, G. Blázquez, M. Calero, Effective removal of zinc from industrial plating wastewater using hydrolyzed olive cake: Scale-up and preparation of zinc-based biochar, J. Clean. Prod. 227 (2019) 634-644. https://doi.org/10.1016/j.jclepro.2019.04.195

[244] M.A. Martín-Lara, G. Blázquez, A. Ronda, M. Calero, Kinetic study of the pyrolysis of pine cone shell through non-isothermal thermogravimetry: Effect of heavy metals incorporated by biosorption, Renew. Energy 96 (2016) 613-624. https://doi.org/10.1016/j.renene.2016.05.026

[245] L.M.S. Pandey, S.K. Shukla, An insight into waste management in Australia with a focus on landfill technology and liner leak detection, J. Clean. Prod. 225 (2019) 1147-1154. https://doi.org/10.1016/j.jclepro.2019.03.320

[246] S. Gupta, S. Sireesha, I. Sreedhar, C.M. Patel, K.L. Anitha, Latest trends in heavy metal removal from wastewater by biochar based sorbents, J. Water Process Eng. 38 (2020) 101561. https://doi.org/10.1016/j.jwpe.2020.101561

[247] L. Wang, Y. Wang, F. Ma, V. Tankpa, S. Bai, X. Guo, X. Wang, Mechanisms and reutilization of modified biochar used for removal of heavy metals from wastewater: A review, Sci. Total Environ. 668 (2019) 1298-1309. https://doi.org/10.1016/j.scitotenv.2019.03.011

[248] Y. Shan, B. Song, G. Ku, L. Wang, Z. Wang, C. Chen, N.A. Oladoja, J. Ali, E.M. Glebov, X. Zhuang, Dual-pathway catalysis: Nano Fe-modified *Platanus* Fluff biochar mediates peroxymonosulfate activation for enhanced tetracycline hydrochloride degradation through radical and non-radical synergies, J. Environ. Chem. Eng. (2026) 122541. https://doi.org/10.1016/j.jece.2026.122541

[249] N. Jin, Q. Liu, J. Song, Y. Hou, A. Ding, D. Zhang, A bioreporter-toxicity-characteristic-leaching-procedure (Bio-TCLP) test battery approach for risk assessment and Cr-remediation performance optimization, Bioresour. Technol. 442 (2026) 133740. https://doi.org/10.1016/j.biortech.2025.133740

[250] K. Zhao, C. Mao, R. Ding, C. Wong, L. Ge, G. Lisak, Rapid on-site determination of heavy metals and metalloids in contaminated biochar samples by accelerated leaching

process coupled with voltammetric sensors, Talanta 287 (2025) 127572. https://doi.org/10.1016/j.talanta.2025.127572

[251] Y. Fan, S. Sun, X. Gu, M. Zhang, Y. Peng, P. Yan, S. He, Boosting the denitrification efficiency of iron-based constructed wetlands in-situ via plant biomass-derived biochar: Intensified iron redox cycle and microbial responses, Water Res. 253 (2024) 121285. https://doi.org/10.1016/j.watres.2024.121285

[252] P. Ma, B. Yin, M. Wu, M. Han, L. Lv, W. Li, G. Zhang, Z. Ren, Synergistic enhancement of microbes-to-pollutants and inter-microbes electron transfer by Fe, N modified ordered mesoporous biochar in anaerobic digestion, J. Hazard. Mater. 476 (2024) 135030. https://doi.org/10.1016/j.jhazmat.2024.135030

[253] W. Jia, Y. Yang, L. Yang, Y. Gao, High-efficient nitrogen removal and its microbiological mechanism of a novel carbon self-sufficient constructed wetland, Sci. Total Environ. 775 (2021) 145901. https://doi.org/10.1016/j.scitotenv.2021.145901

[254] Y. Qi, Y. Zhong, L. Luo, J. He, B. Feng, Q. Wei, K. Zhang, H. Ren, Subsurface constructed wetlands with modified biochar added for advanced treatment of tailwater: Performance and microbial communities, Sci. Total Environ. 906 (2024) 167533. https://doi.org/10.1016/j.scitotenv.2023.167533

[255] H. Wang, L. Sheng, S. Zang, Study on H_2SO_4-modified corn straw biochar as substrate material of constructed wetland, Environ. Sci. Pollut. Res. 30 (2023) 115556-115570. https://doi.org/10.1007/s11356-023-30569-7

[256] X. Deng, G. Chen, C. Zhang, X. Gao, B. Sun, B. Shan, Manganese-modified biochar for sediment remediation: Effect, microbial community response, and mechanism, Environ. Pollut. 363 (2024) 125175. https://doi.org/10.1016/j.envpol.2024.125175

[257] S. Tang, J. Gong, B. Song, W. Cao, J. Li, Remediation of biochar-supported effective microorganisms and microplastics on multiple forms of heavy metals in eutrophic lake, J. Hazard. Mater. 465 (2024) 133098. https://doi.org/10.1016/j.jhazmat.2023.133098

[258] E. Besseling, P. Redondo-Hasselerharm, E.M. Foekema, A.A. Koelmans, Quantifying ecological risks of aquatic micro- and nanoplastic, Crit. Rev. Environ. Sci. Technol. 49 (2019) 32-80. https://doi.org/10.1080/10643389.2018.1531688

[259] Y. Wu, S. Song, X. Chen, Y. Shi, H. Cui, Y. Liu, S. Yang, Source-specific ecological risks and critical source identification of PPCPs in surface water: Comparing urban and rural areas, Sci. Total Environ. 854 (2023) 158792. https://doi.org/10.1016/j.scitotenv.2022.158792

[260] Y. Zong, H. Chen, Z. Malik, Q. Xiao, S. Lu, Comparative study on the potential risk of contaminated-rice straw, its derived biochar and phosphorus modified biochar as an amendment and their implication for environment, Environ. Pollut. 293 (2022) 118515. https://doi.org/10.1016/j.envpol.2021.118515

[261] Y.Y. Yang, G.S. Toor, P.C. Wilson, C.F. Williams, Micropollutants in groundwater from septic systems: Transformations, transport mechanisms, and human health risk assessment, Water Res. 123 (2017) 258-267. https://doi.org/10.1016/j.watres.2017.06.054

[262] R. Mahmud, S.M. Moni, K. High, M. Carbajales-Dale, Integration of techno-economic analysis and life cycle assessment for sustainable process design – A review, J. Clean. Prod. 317 (2021) 128247. https://doi.org/10.1016/j.jclepro.2021.128247

[263] G. Li, R. Hu, N. Wang, T. Yang, F. Xu, J. Li, J. Wu, Z. Huang, M. Pan, T. Lyu, Cultivation of microalgae in adjusted wastewater to enhance biofuel production and reduce environmental impact: Pyrolysis performances and life cycle assessment, J. Clean. Prod. 355 (2022) 131768. https://doi.org/10.1016/j.jclepro.2022.131768

[264] D. Gahane, D. Biswal, S.A. Mandavgane, Life cycle assessment of biomass pyrolysis, BioEnerg. Res. 15 (2022) 1387-1406. https://doi.org/10.1007/s12155-022-10390-9

[265] D.C. Makepa, C.H. Chihobo, T.T. Manhongo, D. Musademba, Life-cycle assessment of microwave-assisted pyrolysis of pine sawdust as an emerging technology for biodiesel production, Results Eng. 20 (2023) 101480. https://doi.org/10.1016/j.rineng.2023.101480

[266] J. Zhu, C. Yang, M. Qiao, T. Zhao, K.S. Emmanuel, K.H.D. Tang, H. Wang, Z. Zhang, J. Pan, et al, Potential and benefits of biochar production: crop straw management and carbon emission mitigation in Shaanxi Province, China, Environ. Sci. Pollut. Res. 32 (2025) 21879-21893. https://doi.org/10.1007/s11356-024-31936-8

[267] F.A.S. Azarakhsh, M. Madadi, Á. Galán-Martín, J.F.M. Denayer, D. Liu, K. Karimi, Sustainable conversion of furfural residues to bioenergy: supporting environmental management via life cycle assessment, Energy Convers. Manag. 348 (2026) 120751. https://doi.org/10.1016/j.enconman.2025.120751

[268] S. Adhikari, M.A.P. Mahmud, E. Moon, W. Timms, Comprehensive life cycle assessment of garden organic waste valorisation: A case study in regional Australia, J. Clean. Prod. 472 (2024) 143496. https://doi.org/10.1016/j.jclepro.2024.143496

[269] A. Hosseinian, P. Brancoli, N. Vali, J. Ylä-Mella, A. Pettersson, E. Pongrácz, Life cycle assessment of sewage sludge treatment: Comparison of pyrolysis with traditional methods in two Swedish municipalities, J. Clean. Prod. 455 (2024) 142375. https://doi.org/10.1016/j.jclepro.2024.142375

[270] M.U. Ozturk, A. Ayol, O. Tezer, Life cycle assessment of olive pomace gasification for an up-draft fixed bed gasifier system, Int. J. Hydrog. Energy 48 (2023) 23339-23347. https://doi.org/10.1016/j.ijhydene.2023.01.206

[271] B.F. Admas, L.C. de Araújo Silva Moura, T.G. Tarkegn, D.V. Silva, R.L.F. Melo, F.R. do Carmo, Life Cycle Assessment of Biochar: A Bibliometric Analysis of Trends and Future Perspectives, Bioenerg. Res. 19 (2026) 39. https://doi.org/10.1007/s12155-026-10959-8

[272] A. James, A. Sánchez, J. Prens, W. Yuan, Biochar from agricultural residues for soil conditioning: Technological status and life cycle assessment, Curr. Opin. Environ. Sci. 25 (2022) 100314. https://doi.org/10.1016/j.coesh.2021.100314

[273] S. Fawzy, A.I. Osman, N. Mehta, D. Moran, A.a.H. Al-Muhtaseb, D.W. Rooney, Atmospheric carbon removal via industrial biochar systems: A techno-economic-environmental study, J. Clean Prod. 371 (2022) 133660. https://doi.org/10.1016/j.jclepro.2022.133660

[274] S. Rajabi Hamedani, T. Kuppens, R. Malina, E. Bocci, A. Colantoni, M. Villarini, Life Cycle assessment and environmental valuation of biochar production: Two case studies in belgium, Energies 12 (2019) 2166. https://doi.org/10.3390/en12112166

[275] M. Hassan, B. Wang, P. Wu, S. Wang, Engineered biochar for in-situ and ex-situ remediation of contaminants from soil and water, Sci. Total Environ. 957 (2024) 177384. https://doi.org/10.1016/j.scitotenv.2024.177384

[276] J. Norberto, K. Zoroufchi Benis, K.N. McPhedran, J. Soltan, Microwave activated and iron engineered biochar for arsenic adsorption: Life cycle assessment and cost analysis, J. Environ. Chem. Eng.11 (2023) 109904. https://doi.org/10.1016/j.jece.2023.109904

[277] M. Zhang, R. Liu, J. Huang, W. Si, G. Wang, G. Liu, Life cycle assessment and environmental benefit analysis of a modified biochar system for heavy metal wastewater treatment, J. Water Process Eng. 76 (2025) 108072. https://doi.org/10.1016/j.jwpe.2025.108072

[278] F. Amalina, S. Krishnan, A.W. Zularisam, M. Nasrullah, Pristine and modified biochar applications as a multifunctional component towards a sustainable future: Recent advances

and new insights, Sci. Total. Environ. (2023) 169608. https://doi.org/10.1016/j.scitotenv.2023.169608

[279] N. Mirzaei, A. Hajinezhad, H. Yousefi, S.F. Moosavian, R. Fattahi, Biochar at the Core of Nature-Based Carbon Management: A Comparative Review Bridging Environmental Sustainability and Economic Feasibility, Energy Sci. Eng. 14 (2026) 611-624. https://doi.org/10.1002/ese3.70350.

[280] R.I. Rubel, L. Wei, Economic assessment of biochar-based controlled-release nitrogen fertilizer production at different industrial scales, Waste Biomass Valor. 16 (2025) 6833-6849. https://doi.org/10.1007/s12649-025-03096-4

[281] Y. Tang, J.S. Ford, T.T. Cockerill, Environmental and economic assessment of biochar production systems from agricultural residues, Biochar 8 (2026) 24. https://doi.org/10.1007/s42773-025-00527-2

[282] D.M. Saharudin, H.K. Jeswani, A. Azapagic, Biochar from agricultural wastes: Environmental sustainability, economic viability and the potential as a negative emissions technology in Malaysia, Sci. Total Environ. 919 (2024) 170266. https://doi.org/10.1016/j.scitotenv.2024.170266

[283] M. Hu, K. Guo, H. Zhou, W. Zhu, L. Deng, L. Dai, Techno-economic assessment of swine manure biochar production in large-scale piggeries in China, Energy 308 (2024) 133037. https://doi.org/10.1016/j.energy.2024.133037

[284] H. Mcintyre, S.J.B. Li, From waste to resource: Evaluating the impact of biosolid-derived Biochar on agriculture and the environment, Biomass 4 (2024) 809-825. https://doi.org/10.3390/biomass4030045

[285] S. Chakma, M. Hasan, Y. Hu, S.K. Rakshit, K.J.W.m. Kang, Valorization of red mud and biomass waste via pre-pyrolysis activation for high-performance magnetic biochar in

heavy metal remediation, Waste Manag. 204 (2025) 114970. https://doi.org/10.1016/j.wasman.2025.114970

[286] S. Sireesha, I. Sreedhar, Phosphorous modified cocopeat biochar as a low cost, efficient and stable adsorbent for the removal of Cu(II) and Ni(II) from aqueous and real systems, Sci Rep. 15 (2025) 37035. https://doi.org/10.1038/s41598-025-20743-x

[287] P. Saetiao, N. Kongrit, J. Jitjamnong, Waste-derived mesoporous biochar for glycerol to glycerol carbonate upgrading: intensified process design and techno-economic analysis, RSC Adv.16 12 (2026) 10984-11004. https://doi.org/10.1039/d5ra09460g

[288] Z.B. Li, Y. Yu, L. Jia, Y.W. Wu, P. Cheng, Z. Zhang, Z.K. Li, C.H. Fan, X.M. Guo, Thermal characteristic analysis and performance optimization of a novel heating boiler based on a porous media model, Appl. Therm. Eng. 289 (2026) 130035. https://doi.org/10.1016/j.applthermaleng.2026.130035

[289] D. Patwa, U. Bordoloi, A.A. Dubey, K. Ravi, S. Sekharan, P. Kalita, Energy-efficient biochar production for thermal backfill applications, Sci. Total. Environ. (2022) 155253. https://doi.org/10.1016/j.scitotenv.2022.155253

[290] W.H. Chen, K.T. Lee, K.Y. Ho, A.B. Culaba, V. Ashokkumar, J.J. Ching, Multi-objective operation optimization of spent coffee ground torrefaction for carbon-neutral biochar production, Bioresour. Technol. 370 (2023) 128584. https://doi.org/10.1016/j.biortech.2023.128584

[291] M. Ahmad, S.S. Lee, X. Dou, D. Mohan, J.K. Sung, J.E. Yang, Y.S. Ok, Effects of pyrolysis temperature on soybean stover- and peanut shell-derived biochar properties and TCE adsorption in water, Bioresour. Technol. 118 (2012) 536-544. https://doi.org/10.1016/j.biortech.2012.05.042

[292] N. Wang, B. Wang, H. Wang, P. Wu, M. Hassan, S. Wang, X. Zhang, Engineered biochar for simultaneous removal of heavy metals and organic pollutants from wastewater:

mechanisms, efficiency, and applications, Biochar X 1 (2025) e008. https://doi.org/10.48130/bchax-0025-0008

[293] N.R. Pandit, J. Mulder, S.E. Hale, A.R. Zimmerman, B.H. Pandit, G. Cornelissen, Multi-year double cropping biochar field trials in Nepal: Finding the optimal biochar dose through agronomic trials and cost-benefit analysis, Sci. Total Environ. 637-638 (2018) 1333-1341. https://doi.org/10.1016/j.scitotenv.2018.05.107

[294] Q. Wu, Y. Xian, Z. He, Q. Zhang, J. Wu, G. Yang, X. Zhang, H. Qi, J. Ma, Y. Xiao, L. Long, Adsorption characteristics of Pb(II) using biochar derived from spent mushroom substrate, Sci. Rep. 9 (2019) 15999. https://doi.org/10.1038/s41598-019-52554-2

[295] R. Ahuja, A. Kalia, R. Sikka, C. P, Nano Modifications of Biochar to Enhance Heavy Metal Adsorption from Wastewaters: A Review, ACS Omega 7 (2022) 45825-45836. https://doi.org/10.1021/acsomega.2c05117

[296] H. Wang, L. Zheng, J. Zhang, J. Liu, Orientation-dependent fiber-optic inclinometer based on core-offset michelson interferometer, Sci. Rep. 12 (2022) 7849. https://doi.org/10.1038/s41598-022-12089-5

[297] Z. Zhu, W. Duan, Z. Chang, W. Du, F. Chen, F. Li, P.J.S. Oleszczuk, Stability of functionally modified biochar: The role of surface charges and surface homogeneity, Sustainability 15 (2023) 7745. https://doi.org/10.3390/su15107745

[298] E. Arriola-Villaseñor, A.N. Ardila A., R. Barrera Z., J. Hernández, Using banana waste biochar for simultaneous removal of heavy metals from raw real wastewater from the electroplating industry, Desalin. Water Treat. (2023). https://doi.org/10.5004/dwt.2023.30079

[299] G. Ravindiran, S. Rajamanickam, M. Ramalingam, G. Hayder, B.K. Sathaiah, M.K. Reddy, S.K. Muniasamy, P.A.J.E.r. Kumar, Conversion of seaweed waste to biochar for the removal of heavy metal ions from aqueous solution: A sustainable method to address

eutrophication problem in water bodies, Environ. Res. 241 (2023) 117551. https://doi.org/10.1016/j.envres.2023.117551

[300] R. McGregor, Six pilot-scale studies evaluating the in situ treatment of PFAS in groundwater, Remediation 30 (2020) 39-50. https://doi.org/10.1002/rem.21653

Graphical Abstract

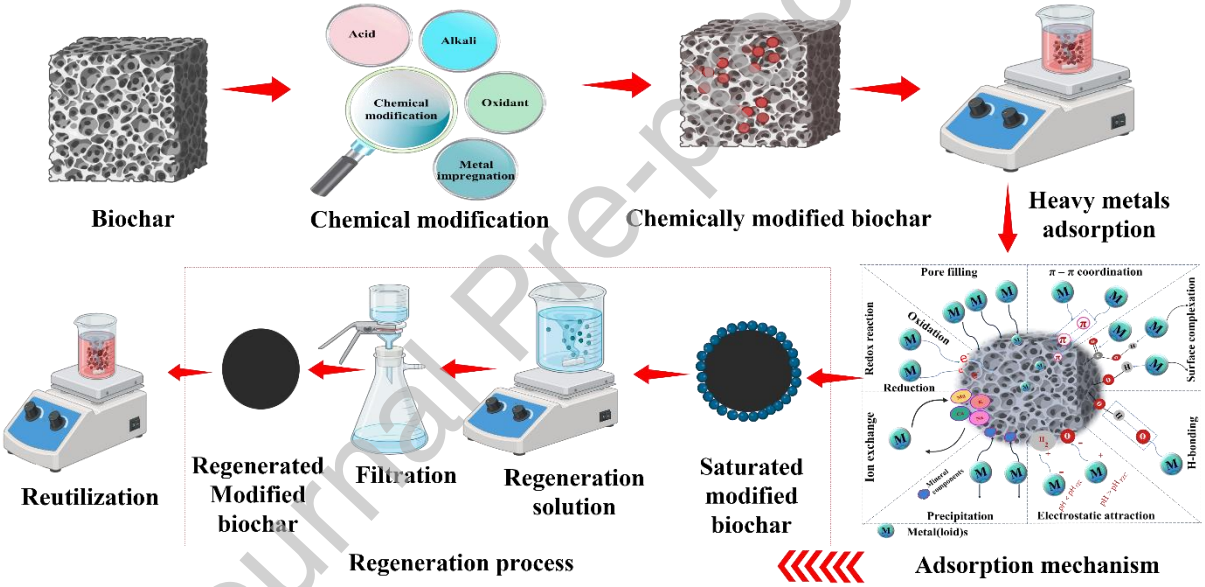

Declaration of interests

☒The authors declare that they have no known competing financial interests or personal relationships that could have appeared to influence the work reported in this paper.

☐The authors declare the following financial interests/personal relationships which may be considered as potential competing interests: